



Calhoun: The NPS Institutional Archive
DSpace Repository

Theses and Dissertations

1. Thesis and Dissertation Collection, all items

2000

Digital communications jamming.

Sen, Cem.

Monterey, California. Naval Postgraduate School

<http://hdl.handle.net/10945/32961>

Downloaded from NPS Archive: Calhoun



Calhoun is the Naval Postgraduate School's public access digital repository for research materials and institutional publications created by the NPS community. Calhoun is named for Professor of Mathematics Guy K. Calhoun, NPS's first appointed -- and published -- scholarly author.

Dudley Knox Library / Naval Postgraduate School
411 Dyer Road / 1 University Circle
Monterey, California USA 93943

<http://www.nps.edu/library>

NAVAL POSTGRADUATE SCHOOL

Monterey, California



THESIS

DIGITAL COMMUNICATIONS JAMMING

by

Cem Sen

September 2000

Thesis Advisor:
Thesis Co-Advisor:
Second Reader:

Rasler W. Smith
Jovan Lebaric
David V. Adamiak

Approved for public release; distribution is unlimited.

20001117 029

REPORT DOCUMENTATION PAGE			Form Approved OMB No. 0704-0188	
<p>Public reporting burden for this collection of information is estimated to average 1 hour per response, including the time for reviewing instruction, searching existing data sources, gathering and maintaining the data needed, and completing and reviewing the collection of information. Send comments regarding this burden estimate or any other aspect of this collection of information, including suggestions for reducing this burden, to Washington Headquarters Services, Directorate for Information Operations and Reports, 1215 Jefferson Davis Highway, Suite 1204, Arlington, VA 22202-4302, and to the Office of Management and Budget, Paperwork Reduction Project (0704-0188) Washington DC 20503.</p>				
1. AGENCY USE ONLY (Leave blank)		2. REPORT DATE September 2000	3. REPORT TYPE AND DATES COVERED Master's Thesis	
4. TITLE AND SUBTITLE Digital Communications Jamming			5. FUNDING NUMBERS	
6. AUTHOR(S) Sen, Cem				
7. PERFORMING ORGANIZATION NAME(S) AND ADDRESS(ES) Naval Postgraduate School Monterey, CA 93943-5000			8. PERFORMING ORGANIZATION REPORT NUMBER	
9. SPONSORING/MONITORING AGENCY NAME(S) AND ADDRESS(ES)			10. SPONSORING/MONITORING AGENCY REPORT NUMBER	
11. SUPPLEMENTARY NOTES The views expressed in this thesis are those of the author and do not reflect the official policy or position of the Department of Defense or the U.S. Government.				
12a. DISTRIBUTION/AVAILABILITY STATEMENT Approved for public release; distribution is unlimited.			12b. DISTRIBUTION CODE	
13. ABSTRACT (maximum 200 words) The purpose of this thesis is to model coherently detected BFSK, BPSK and QPSK, and noncoherently detected BFSK communications systems in the presence of additive white Gaussian Noise (AWGN) and different types of jamming signals by using MATLAB Communications Toolbox and Simulink. The theoretical results are available for the effect of AWGN on the performance of digital communication systems. To determine the performance of a system in the presence of AWGN and different types of jamming signals we need to use computer simulation. The results obtained by simulation are presented for bit-error rate (BER) as a function of signal-to-noise ratio (SNR) and signal-to-jamming ratio (SJR). As observed from the simulation results, different types of jamming affect each digital modulation technique differently.				
14. SUBJECT TERMS MATLAB Communications Toolbox, Simulink, Jamming, Bit-Error Rate, BFSK, BPSK, QPSK.			15. NUMBER OF PAGES 162	
			16. PRICE CODE	
17. SECURITY CLASSIFICATION OF REPORT Unclassified	18. SECURITY CLASSIFICATION OF THIS PAGE Unclassified	19. SECURITY CLASSIFICATION OF ABSTRACT Unclassified	20. LIMITATION OF ABSTRACT UL	

Approved for public release; distribution is unlimited.

DIGITAL COMMUNICATIONS JAMMING

Cem Sen
First Lieutenant, Turkish Army
B.S., Turkish Military Academy, Ankara, 1993

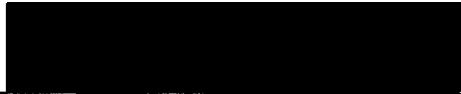
Submitted in partial fulfillment of the
requirements for the degree of

MASTER OF SCIENCE IN SYSTEMS ENGINEERING

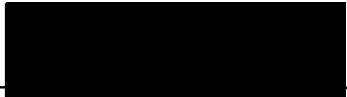
from the


NAVAL POSTGRADUATE SCHOOL
September 2000

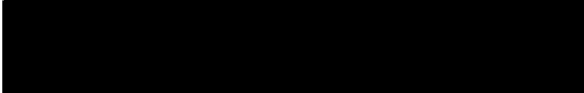
Author:


Cem Sen

Approved by:


Rasler W. Smith, Thesis Advisor


Jovan Lebaric, Thesis Co-Advisor


David V. Adamiak, Second Reader


Jeffrey B. Knorr, Chairman
Department of Electrical Engineering

ABSTRACT

The purpose of this thesis is to model coherently detected BFSK, BPSK and QPSK, and noncoherently detected BFSK communications systems in the presence of additive white Gaussian Noise (AWGN) and different types of jamming signals by using MATLAB Communications Toolbox and Simulink.

The theoretical results are available for the effect of AWGN on the performance of digital communication systems. To determine the performance of a system in the presence of AWGN and different types of jamming signals we need to use computer simulation. The results obtained by simulation are presented for bit-error rate (BER) as a function of signal-to-noise ratio (SNR) and signal-to-jamming ratio (SJR).

As observed from the simulation results, different types of jamming affect each digital modulation technique differently.

TABLE OF CONTENTS

I.	INTRODUCTION.....	1
A.	BACKGROUND.....	1
B.	OBJECTIVE.....	1
C.	RELATED WORK.....	1
D.	ORGANIZATION OF THESIS.....	1
II.	COMMUNICATIONS AND SIGNAL DEFINITION.....	3
A.	COMMUNICATIONS.....	3
B.	SIGNALS AND THEIR CLASSIFICATIONS.....	4
1.	Continuous-Time and Discrete-Time Signals.....	4
2.	Analog and Digital Signals.....	4
3.	Periodic and Nonperiodic Signals.....	4
4.	Deterministic and Random Signals.....	5
5.	Energy and Power Signals.....	5
C.	TRANSMISSION OF MESSAGE SIGNALS.....	6
D.	LIMITATIONS OF COMMUNICATION SYSTEMS.....	6
E.	RESOURCES OF COMMUNICATION SYSTEMS.....	7
F.	DIGITAL COMMUNICATIONS.....	8
1.	Digital Communications Techniques.....	8
a.	Digital Transmission.....	8
b.	Digital Radio.....	8
2.	Digital Modulation and Digital Modulation Techniques.....	9
a.	Amplitude Shift Keying (ASK).....	9
b.	Frequency Shift Keying (FSK).....	10
c.	Phase Shift Keying (PSK).....	10
d.	Quadrature Phase Shift Keying (QPSK).....	11

III.	NOISE AND ITS EFFECTS ON DIGITAL RECEIVERS	13
A.	MATCHED FILTER AND CORRELATION RECEIVERS	15
1.	Matched Filter Receiver	15
2.	Correlation Receiver.....	16
B.	COHERENT AND NONCOHERENT DETECTION.....	17
1.	Coherent Detection of Binary ASK Signals.....	17
2.	Coherent Detection of Binary FSK Signals	18
3.	Coherent Detection of Binary PSK Signals	19
4.	Coherent Detection of Quadrature PSK Signals	19
5.	Noncoherent Detection of Binary ASK Signals.....	20
6.	Noncoherent Detection of Binary FSK Signals	21
7.	Noncoherent Detection of Binary PSK Signals	21
C.	PROBABILITY OF ERROR AND ERROR PERFORMANCE	22
IV.	FUNDAMENTAL DESIGN PARAMETERS OF ANTENNAS.....	31
A.	INTRODUCTION.....	31
B.	RADIATION PATTERN	32
C.	POLARIZATION.....	36
V.	SPREAD SPECTRUM COMMUNICATIONS	39
A.	INTRODUCTION.....	39
B.	SPREAD SPECTRUM SYSTEM.....	39
C.	SPREAD SPECTRUM TECHNIQUES.....	40
1.	Direct Sequence Spread Spectrum	41
2.	Frequency-Hopping Spread Spectrum	43
VI.	THEORY OF JAMMING.....	45
A.	INTRODUCTION.....	45
B.	J/S RATIO	46

C.	THEORY OF JAMMING FOR BFSK AND BPSK	47
1.	Barrage Noise Jamming.....	49
2.	Pulsed Noise Jamming	51
3.	Tone Jamming.....	52
D.	THEORY OF JAMMING FOR SPREAD SPECTRUM.....	53
1.	Broadband Noise Jamming	53
2.	Partial-Band Noise Jamming.....	55
3.	Multiple-Tone Jamming.....	56
4.	Pulse Jamming.....	57
5.	Repeat-Back Jamming.....	58
VII.	THEORY OF ANTI-JAMMING.....	61
A.	INTRODUCTION.....	61
B.	ANTI-JAMMING TECHNIQUES	63
1.	Error Control Coding.....	63
a.	Block Codes.....	65
b.	Convolutional Codes	67
2.	Antennas	69
a.	High Gain/Narrow Beam.....	69
b.	Null Steering Antennas	69
c.	Least Mean Square Algorithm.....	70
d.	Maximum SNR Algorithm.....	70
VIII.	SIMULATION.....	71
A.	INTRODUCTION.....	71
B.	SIMULINK MODEL AND BLOCK ANALYSIS.....	72

C. PERFORMANCE OF DIGITAL COMMUNICATIONS SYSTEM WITH BARRAGE NOISE JAMMING	80
1. Performance of Coherent BFSK with Barrage Noise Jamming.....	80
a. AM by Weibull Noise	80
b. FM by Weibull Noise.....	83
2. Performance of Noncoherent BFSK with Barrage Noise Jamming.....	85
a. AM by Weibull Noise	85
b. FM by Weibull Noise.....	87
3. Performance of BPSK with Barrage Noise Jamming	89
a. AM by Weibull Noise	89
b. FM by Weibull Noise.....	91
4. Performance of QPSK with Barrage Noise Jamming	93
a. AM by Weibull Noise	93
b. FM by Weibull Noise.....	95
D. PERFORMANCE OF DIGITAL COMMUNICATIONS SYSTEM WITH PULSED NOISE JAMMING	97
1. Performance of Coherent BFSK with Pulsed Noise Jamming.....	97
a. AM-Modulated Pulsed Noise Jamming	97
b. FM-Modulated Pulsed Noise Jamming	99
2. Performance of Noncoherent BFSK with Pulsed Noise Jamming.....	101
a. AM-Modulated Pulsed Noise Jamming	101
b. FM-Modulated Pulsed Noise Jamming	103
3. Performance of BPSK with Pulsed Noise Jamming	105
a. AM-Modulated Pulsed Noise Jamming	105
b. FM-Modulated Pulsed Noise Jamming	107
4. Performance of QPSK with Pulsed Noise Jamming	109
a. AM-Modulated Pulsed Noise Jamming	109
b. FM-Modulated Pulsed Noise Jamming	111

E. PERFORMANCE OF DIGITAL COMMUNICATIONS SYSTEM WITH TONE JAMMING.....	113
1. Performance of Coherent BFSK with Tone Jamming.....	113
a. AM-Modulated Tone Jamming	113
b. FM-Modulated Tone Jamming	115
2. Performance of Noncoherent BFSK with Tone Jamming.....	117
a. AM-Modulated Tone Jamming	117
b. FM-Modulated Tone Jamming	119
3. Performance of BPSK with Tone Jamming	121
a. AM-Modulated Tone Jamming	121
b. FM-Modulated Tone Jamming	123
4. Performance of QPSK with Tone Jamming	125
a. AM-Modulated Tone Jamming	125
b. FM-Modulated Tone Jamming	127
IX. CONCLUSIONS AND RECOMMENDATIONS.....	129
APPENDIX. MATLAB COMMUNICATIONS TOOLBOX AND SIMULINK.....	135
LIST OF REFERENCES	137
BIBLIOGRAPHY	139
INITIAL DISTRIBUTION LIST	141

ACKNOWLEDGEMENT

Numerous individuals assisted me in completing this thesis. I would like to thank Dr. Rasler Smith and Dr. Jovan Lebaric for their technical support, clear explanation and supervising, and Major David Adamiak for his advice and help.

I wish to express my gratitude to my country for providing this opportunity and education, and my parents for their constant support and encouragement to accomplish this hard work.

This thesis would not have been possible without the love and support of my wife, Hulya. I am grateful for the inspiration she has been to me. Last but certainly not least, I would like to thank my newborn daughter, Doga Cansin, for bringing me different kind of enthusiasm for life.

I. INTRODUCTION

A. BACKGROUND

The acceptance of the idea that Electronic Warfare (EW) can play a major role in military conflicts dates back many years. Most of the efforts to use EW have dealt with radars and produced important results in that particular field. Recent years have brought about an increasing awareness that there are similar needs and opportunities for exploitations concerning communication systems [Ref.1].

B. OBJECTIVE

The objective of this study is to obtain a computer-based prediction of noise and jamming (barrage, pulsed and tone) effects on the probability-of-error for coherently detected BFSK, BPSK, QPSK, and noncoherently detected BFSK communication systems. To accomplish this, several models were developed using MATLAB Communications Toolbox and Simulink. The performance of the models has been verified by comparing the simulation results and the theoretical results for the bit error probability in the presence of additive white Gaussian Noise (AWGN).

C. RELATED WORK

Although there are a lot of papers about performance analysis of spread spectrum techniques under different types of jamming signals, there is no directly related work with the simulations performed in this research. While the literature has examples of simulations using Gaussian Noise sources, none has been found using other distributions.

D. ORGANIZATION OF THESIS

Chapter II introduces the overall communication system and signal definition. Signals and their classifications, transmission of message signals, limitations and

resources of communication systems, and digital communication systems are discussed. Chapter III covers noise and its effects on digital receivers. The matched filter and correlation receivers, coherent and noncoherent detection, probability of error and error performance of digital communication systems are examined. Chapter IV deals with fundamental design parameters of antennas. Chapter V covers spread spectrum communications. It deals with spread spectrum system and spread spectrum techniques. Chapter VI discusses the theory of jamming. It explores the theory of jamming for BFSK and BPSK, and the theory of jamming for spread spectrum. Chapter VII deals with the theory of anti-jamming. Chapter VIII covers the models used for the simulation and the simulation results. Chapter IX presents conclusion and recommendations.

II. COMMUNICATIONS AND SIGNAL DEFINITION

A. COMMUNICATIONS

Electronic communication is the transmission, reception and processing of information between a source and a user destination. The information can be in analog or digital form. Figure 2.1 is a block diagram of a communications system consisting of a transmitter, a channel, and a receiver.

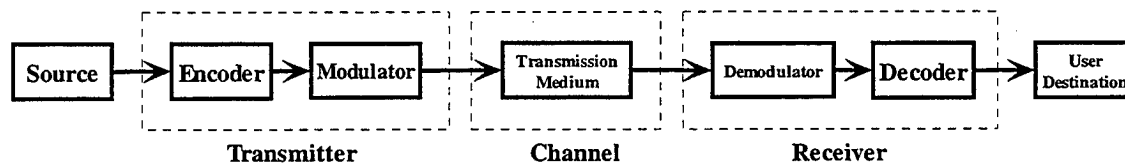


Figure 2.1 Communications System Block Diagram

The transmitter converts the source information to a form that is suitable for transmission over the channel. This process is performed by an encoder and a modulator. The encoder converts the output of either an analog or digital source into a sequence of binary digits and chooses the best form for the signal in order to optimize its demodulation. The modulator modifies the carrier by changing its amplitude, frequency, and/or phase.

The channel is the transmission medium that provides a connection between the transmitter output and the receiver input. There are two types of channels: point-to-point and broadcast. Wire lines and fiber optics are examples of point-to-point channels, and a satellite in geostationary orbit is an example of a broadcast channel.

The receiver receives the transmitted signal from the transmission medium and converts it back to a facsimile of its original form. This process is performed by a demodulator and a decoder. The demodulator provides the inverse operation of the modulator to recover the encoded signal in its original form. The decoder performs the inverse operation of encoder to detect the signal.

B. SIGNALS AND THEIR CLASSIFICATIONS

A signal is a function representing a physical quantity. Mathematically, a time-domain signal is represented as a function of an independent variable t ; thus, a signal is denoted by $s(t)$. We can identify five different methods of dividing signals into classes.

1. Continuous-Time and Discrete-Time Signals

A signal $s(t)$ is a continuous-time signal if t is a continuous variable. If t is a discrete variable then $s(t)$ is a discrete-time signal.

2. Analog and Digital Signals

An analog signal has an amplitude that is continuous for all time. Both the signal and time are comprised by an infinite number of values. A digital signal is a discrete-time signal whose amplitude can take only discrete values. An analog signal can be converted into a digital signal by sampling, quantizing and coding.

3. Periodic and Nonperiodic Signals

A periodic signal repeats itself precisely after a fixed length of time. Mathematically, $s(t)$ is periodic if there exists a constant T_0 , such that

$$s(t) = s(t+T_0). \quad (2.1)$$

The smallest positive value of T_0 which satisfies the Equation 2.1 is the period of $s(t)$. If there is no T_0 to satisfy Equation 2.1 then the signal is considered to be aperiodic.

4. Deterministic and Random Signals

Deterministic signals are signals whose values are completely specified for any given time. They are modeled by explicit mathematical expressions. Random signals are signals which take random values at any given time. They are modeled in terms of probabilities and statistical moments.

5. Energy and Power Signals

The energy E of a signal $s(t)$ absorbed by a $1-\Omega$ resistor is defined as

$$E = \int_{-\infty}^{\infty} |s(t)|^2 dt . \quad (2.2)$$

If E is finite ($0 < E < \infty$) then $s(t)$ is considered to be an energy signal. An energy signal is a pulse-like signal that exists for only a finite interval of time. Some examples of energy signals are rectangular pulse, pulsed sinusoids, and Gaussian pulse.

The average power P of a signal $s(t)$ absorbed by a $1-\Omega$ resistor is defined as

$$P = \lim_{T \rightarrow \infty} \frac{1}{T} \int_{-T/2}^{T/2} |s(t)|^2 dt . \quad (2.3)$$

If P is finite ($0 < P < \infty$) then $s(t)$ is considered to be a power signal. Random signals are usually power signals.

C. TRANSMISSION OF MESSAGE SIGNALS

Analog or digital methods can be used to transmit a message over a communication channel. Today, there is an increasing trend toward the use of digital communications [Ref. 2]. Why use digital? The primary advantages and disadvantages are as follows:

1. Advantages

- a. Digital signals can be regenerated.
- b. Digital circuits are less subject to distortion and interference than analog circuits.
- c. Digital circuits are more reliable.
- d. Digital circuits are more flexible.
- e. The combining of digital signals using time-division multiplexing (TDM) is simple.
- f. Digital messages can be handled in packets.

2. Disadvantages

- a. Digital transmission requires a greater system bandwidth and increased system complexity.
- b. Digital detection requires system synchronization.
- c. Digital communication systems are expensive.

D. LIMITATIONS OF COMMUNICATION SYSTEMS

Typically, while propagating through a channel, the transmitted signal is distorted by nonlinearities and imperfections in the frequency response of the channel. Other

sources of degradation are noise and interference picked up by the signal during the course of passage through the channel. Noise and the distortion constitute two basic limitations in the design of communication systems [Ref. 3]. There are various sources of noise that can be either internal or external. Although noise is a random signal, it may be described in terms of its statistical properties such as its average power. A discussion of noise and its effects on receivers is presented in Chapter III.

E. RESOURCES OF COMMUNICATION SYSTEMS

Received signal power is considered along with noise power to determine the signal-to-noise ratio (*SNR*) at the receiver input, to give

$$SNR = \text{Signal Power} / \text{Noise Power} = P_S / P_N , \quad (2.4)$$

or in decibels

$$SNR \text{ (dB) } = 10 \log_{10} (P_S) - 10 \log_{10} (P_N) . \quad (2.5)$$

Channel bandwidth is the range of frequencies that the channel can support while still maintaining satisfactory fidelity. Shannon's channel capacity theorem states a direct relationship between channel bandwidth and *SNR* in determination of channel capacity, i.e.,

$$C = B \log_2 (1 + SNR) \quad (2.6)$$

where C is the channel capacity, B is the channel bandwidth and SNR is the received signal-to-noise ratio.

F. DIGITAL COMMUNICATIONS

1. DIGITAL COMMUNICATIONS TECHNIQUES

a. *Digital Transmission*

Digital transmission is the transmission of digital pulses between two or more locations using electronic circuits. Digital transmission systems require a physical connection between the transmitter and receiver. These connections may be wire lines or optical fibers. Figure 2.2 is a simple block diagram of a digital transmission [Ref. 4].

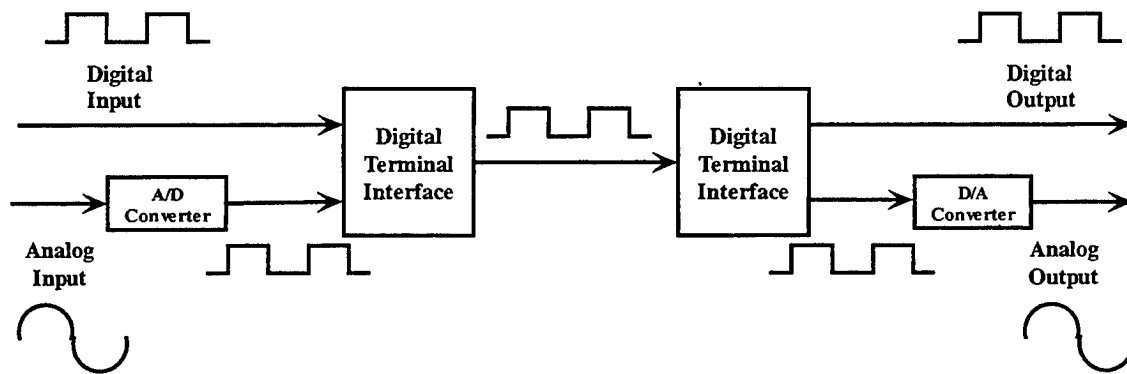


Figure 2.2 Digital Transmission [From Ref. 4]

b. *Digital Radio*

Digital radio involves transmission of digitally modulated analog carriers between two or more locations. With this technique, free space or the Earth's atmosphere is used as the transmission medium. Figure 2.3 is a simple block diagram of a digital radio [Ref. 4].

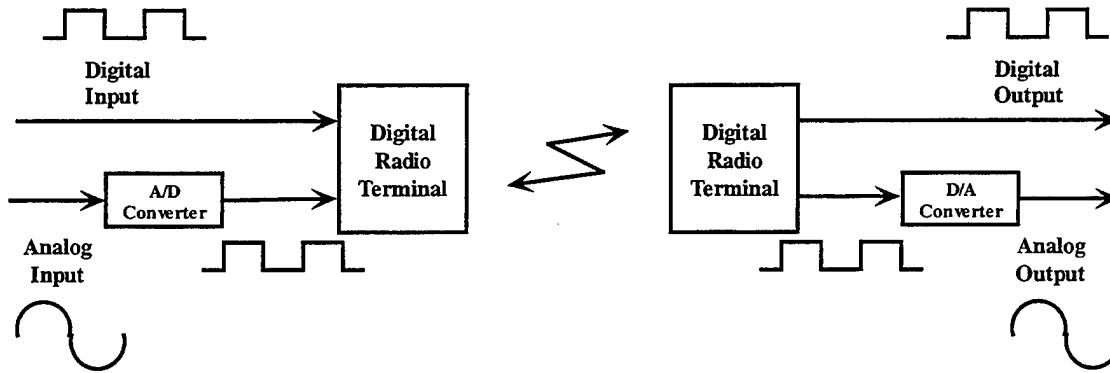


Figure 2.3 Digital Radio [From Ref. 4]

2. DIGITAL MODULATION TECHNIQUES

A continuous message signal is sampled, quantized, and encoded into a corresponding sequence of binary symbols. These binary symbols can then be used to modulate a carrier signal in amplitude, frequency, or phase, as described below.

a. *Amplitude Shift Keying (ASK)*

With ASK the amplitude of the carrier signal is switched between either of two values corresponding to binary symbols *0* and *1*. The general analytic expression is

$$s_i(t) = \sqrt{\frac{2E_i(t)}{T}} \cos(\omega_0 t + \phi), \quad i = 1, 2 \quad (2.7)$$

where the parameter *E* is symbol energy and *T* is symbol duration. Figure 2.4 (a) shows typical abrupt amplitude changes at symbol transitions. ASK is inefficient in modulation and spectrum utilization, particularly at the higher data rates.

b. Frequency Shift Keying (FSK)

In Binary FSK, the frequency of a constant amplitude carrier signal is switched between either of two values corresponding to binary symbols 0 and 1. The transmitted BFSK signal is

$$s(t) = \begin{cases} \sqrt{\frac{2E_b}{T_b}} \cos(2\pi f_1 t + \theta_c) & , 0 \leq t \leq T_b & : 1 \\ \sqrt{\frac{2E_b}{T_b}} \cos(2\pi f_2 t + \theta_c) & , 0 \leq t \leq T_b & : 0 \end{cases} \quad (2.8)$$

where $E_b = A_c^2 T_b / 2$ is the average energy per bit, T_b is the bit duration, and a rectangular pulse shape is assumed. Figure 2.4 (b) illustrates the typical frequency changes at symbol transitions.

c. Phase Shift Keying (PSK)

In BPSK, the modulating data signal shifts the phase of the waveform to one of two states, either zero or π . The transmitted BPSK signal is therefore

$$s(t) = \begin{cases} \sqrt{\frac{2E_b}{T_b}} \cos(2\pi f_c t + \theta_c) & , 0 \leq t \leq T_b & : 1 \\ \sqrt{\frac{2E_b}{T_b}} \cos(2\pi f_c t + \theta_c + \pi) = -\sqrt{\frac{2E_b}{T_b}} \cos(2\pi f_c t + \theta_c) & , 0 \leq t \leq T_b & : 0 \end{cases} \quad (2.9)$$

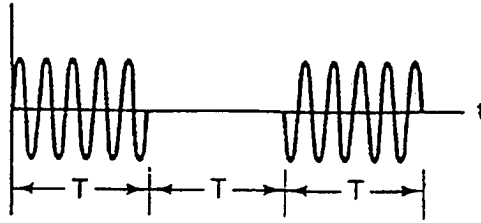
Figure 2.4 (c) shows a typical BPSK waveform with its abrupt changes at the symbol transitions.

d. Quadrature Phase Shift Keying (QPSK)

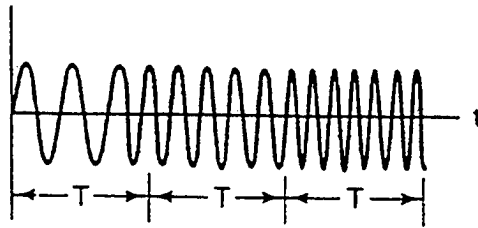
In QPSK, two bits are transmitted in a single modulation symbol. The phase of the carrier takes on one of four equally spaced values such as 0 , $\pi/2$, π and $3\pi/2$, where each value of phase corresponds to a unique pair of message bits. A QPSK signal can be defined as

$$s(t) = \sqrt{\frac{2E_s}{T_s}} \cos \left[2\pi f_c t + (i-1)\frac{\pi}{2} \right], \quad i = 1, 2, 3, 4 \quad (2.10)$$

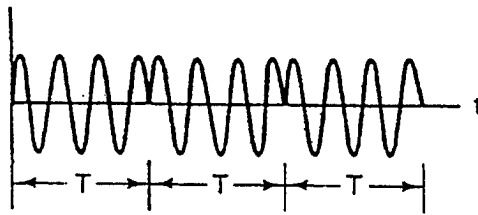
where T_s denotes symbol duration (equal to twice the bit duration T_b).



(a)



(b)



(c)

Figure 2.4 Digital Modulation Techniques (a) ASK (b) FSK (c) PSK [From Ref. 2]

III. NOISE AND ITS EFFECTS ON DIGITAL RECEIVERS

The term noise refers to unwanted electrical signals that are always present in electrical systems. The presence of noise superimposed on a signal tends to mask the signal, limits the receiver's ability to make correct symbol decisions, and thereby reduces the rate of information transmission [Ref. 2].

There are two sources of noise, man-made and natural. Spark-plug ignition noise and switching transients are examples of man-made noise. Atmospheric disturbances and galactic emanations are examples of natural noise. However, noise is not the only source of received signal degradation. Jamming and interference can be extremely detrimental to receiver performance as well. We can eliminate much of these deleterious effects through filtering, shielding, proper choice of modulation techniques and the selection of an optimum receiver detector.

The purpose of detection is to establish the presence or absence of a signal in noise. In order to enhance the strength of the signal relative to that of noise, a detection system usually consists of a predetection filter followed by a decision device. The optimum choice of a predetection filter depends on the type of noise. In an electrical circuit, noise is generated owing to various physical phenomena.

Thermal (Gaussian) noise is associated with the rapid and random movement of electrons within a conductor due to thermal agitation. Because thermal noise is equally distributed throughout the frequency spectrum, it is sometimes called a white noise. Since thermal noise is random, additive, and present in all conducting devices, it is the most significant of all noise sources.

Impulsive noise is caused by a number of sources such as man-made noise and atmospheric disturbances. It is randomly varying and is superimposed onto any signal present. Galactic and solar noise, lightning and switching noise are examples of impulsive noise. Impulsive noise may occur in bursts or discrete impulses.

Shot noise is generated in semiconductors. It is a random fluctuation that accompanies any current crossing a potential barrier. The effect occurs because the carriers (holes and electrons) do not cross the barrier simultaneously, but rather with a random distribution. It is similar to thermal noise in that its spectrum is flat.

Besides thermal, impulsive, and shot noise, transistors exhibit a low-frequency noise phenomenon known as flicker noise. Below frequencies of a few kilohertz, flicker noise appears, the spectral density of which increases as the frequency decreases. The mean-square value of flicker noise is inversely proportional to frequency; hence, it is referred to as one-over-f ($1/f$) noise [Ref. 3].

Noise is mainly of concern in receiving systems, where it sets a lower limit on the signal magnitude that can be usefully received. Even when precautions are taken to eliminate noise from faulty connections or that arising from external sources, it is found that certain fundamental sources of noise are present within electronic equipment as described above that limit the receiver sensitivity. The effects of noise on the receiver will now be discussed.

A. MATCHED FILTER AND CORRELATION RECEIVERS

1. Matched Filter Receiver

A matched filter is a linear filter designed to provide maximum output signal-to-noise (SNR) ratio for a given transmitted signal. The optimum receiver for detecting the presence of signal $s(t)$ in the received noisy waveform is as shown in Figure 3.1. It consists of a filter matched to $s(t)$, a sampler, and a decision device. At time $t=T$, the matched filter output is sampled by the sampler, and the amplitude of this sample is compared with a preset threshold V_T by the decision device. If the threshold is exceeded, the receiver decides that signal $s(t)$ is present; otherwise, it will decide that $s(t)$ is absent. Here, $h(t)$ is the impulse response of the filter, which is a time-reversed and delayed version of the input $s(t)$ and T is a constant time delay.

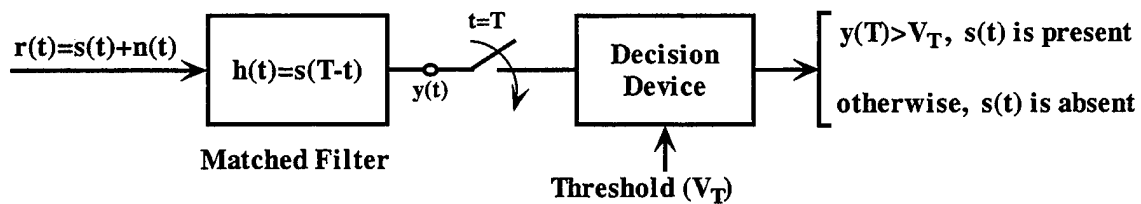


Figure 3.1 Matched Filter Receiver

The output of the matched filter of Figure 3.1 can be found as

$$y(T) = \int_0^T r(\tau) h(t - \tau) d\tau = \int_0^T r(\tau) s[t - (T - \tau)] d\tau = \int_0^T r(\tau) s(t - T + \tau) \Big|_{t=T} d\tau, \quad (3.1)$$

and then,

$$y(T) = \int_0^T r(\tau) s(\tau) d\tau. \quad (3.2)$$

2. Correlation Receiver

The block diagram of a correlation receiver is as shown in Figure 3.2. If the correlator output is larger than the predetermined threshold V_T , the receiver decides that signal $s(t)$ is present; otherwise, it will decide that $s(t)$ is absent.

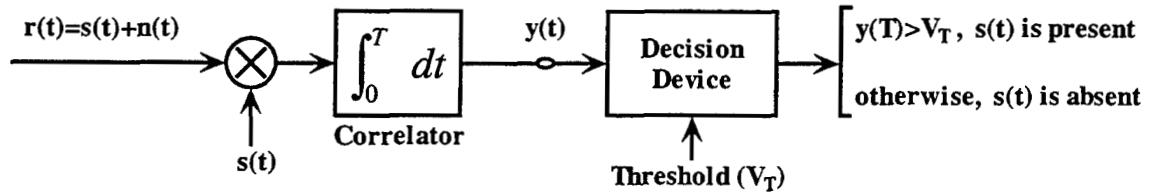


Figure 3.2 Correlation Receiver

The output of the correlator of Figure 3.2 can be found as

$$y(T) = \int_0^T r(\tau)s(\tau)d\tau . \quad (3.3)$$

Since the matched filter output Equation 3.2 and the correlator output Equation 3.3 are identical at the sampling time $t=T$, the matched filter and correlation receivers are used interchangeably.

B. COHERENT AND NONCOHERENT DETECTION

Coherent detection is the process where the receiver exploits knowledge of the carrier's phase to detect the signals; when the receiver does not exploit such phase information, the process is called noncoherent detection. Noncoherent systems are less complex than coherent systems, but the trade off is higher probability of error.

1. Coherent Detection of Binary ASK Signals

For the demodulation of binary ASK we may use a coherent detector as depicted in Figure 3.3. The detector consists of three basic components: A multiplier, supplied with a locally generated version of the sinusoidal carrier, an integrator that performs a low-pass filtering action, and a decision device that compares the integrator output with a preset threshold. The amplitude of the carrier signal is switched between either of two values corresponding to binary symbols 0 and 1. Here, $r(t)$ is received signal, $n(t)$ is noise, and $s(t)$ is equal to $\sqrt{2E_i(t)/T} \cos(\omega_0 t + \phi)$ for $0 \leq t \leq T$ and $i=1,2$.

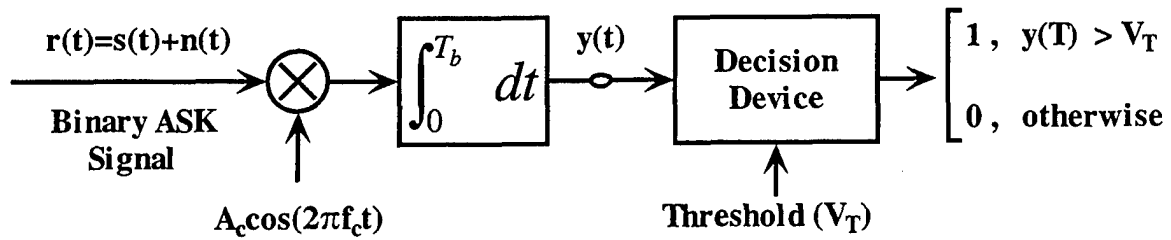


Figure 3.3 Coherent Detector for Binary ASK [From Ref. 3]

2. Coherent Detection of Binary FSK Signals

For the demodulation of binary FSK we may use a coherent detector depicted as in Figure 3.4. This detector consists of two correlators that are individually tuned to the two different carrier frequencies chosen to represent symbols 1 and 0 . The decision device compares $y(t)$ with a preset threshold. If the threshold is exceeded, the detector decides in favor of symbol 1 ; otherwise, it decides in favor of symbol 0 .

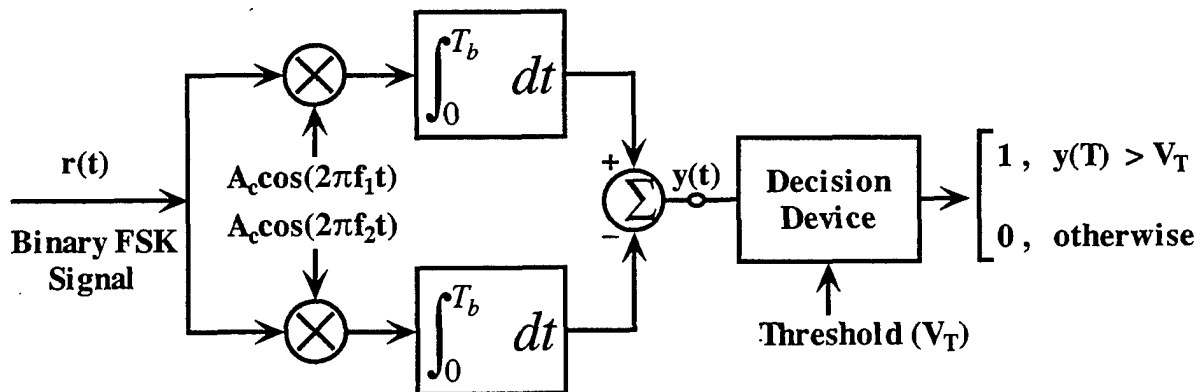


Figure 3.4 Coherent Detector for Binary FSK [From Ref. 3]

3. Coherent Detection of Binary PSK Signals

Figure 3.5 is a block diagram of a coherent detector for binary PSK. The detector consists of a multiplier, an integrator, and a decision device. The received binary PSK signal is multiplied by a locally generated version of the sinusoidal carrier. An integrator is used to perform a low-pass filtering action. Then, a decision device is used to compare the integrator output with a preset threshold.

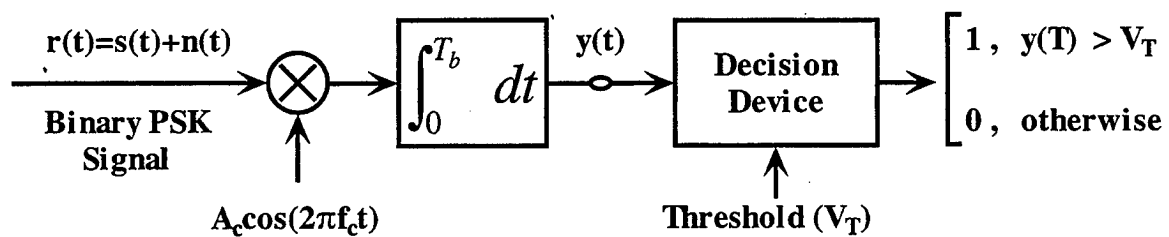


Figure 3.5 Coherent Detector for Binary PSK [From Ref. 3]

4. Coherent Detection of Quadrature PSK Signals

The QPSK detector depicted in Figure 3.6 consists of two multipliers, two correlators, a pair of decision devices, and a parallel-to-serial converter. The received QPSK signal is multiplied by an in-phase component (in-phase with carrier) and a quadrature component (90° out of phase with carrier). The integrators perform low-pass filtering. The outputs of the integrators are passed through decision devices that generate the in-phase and quadrature binary streams. The parallel to serial converter is used to reproduce the original binary sequence.

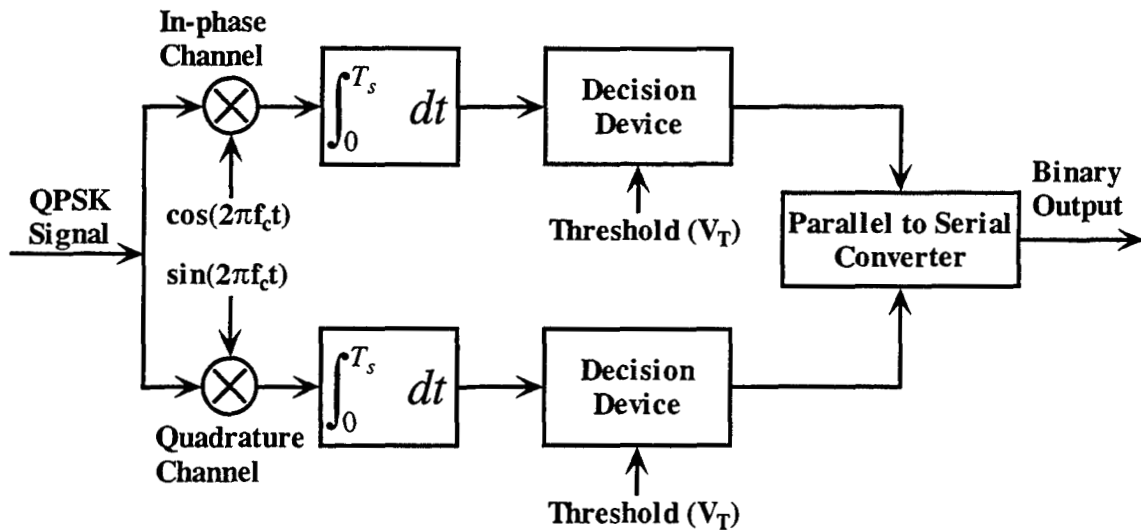


Figure 3.6 Coherent Detector for Quadrature PSK [From Ref. 3]

5. Noncoherent Detection of Binary ASK Signals

If the input noise is low, a noncoherent receiver may be the best solution considering both cost and noise performance. The noncoherent binary ASK detector is depicted in Figure 3.7. The detector consists of two basic components: an envelope detector and a decision device.

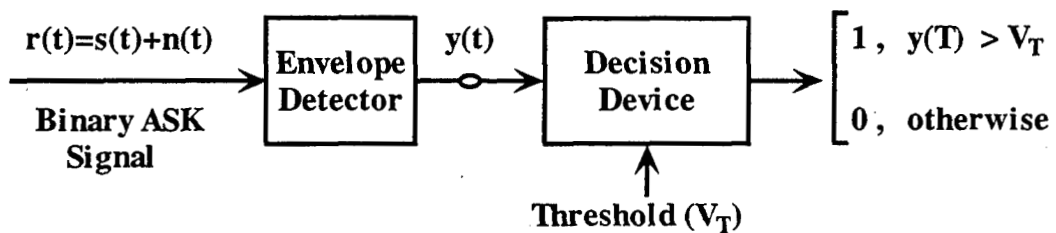


Figure 3.7 Noncoherent Detection of Binary ASK [From Ref. 3]

6. Noncoherent Detection of Binary FSK Signals

The detector is composed of pair of band pass filters (BPF) followed by envelope detectors, as in Fig. 3.8. Here R_1 and R_2 denote the envelope samples of the upper and lower paths of the receiver, respectively. The decision device compares R_1 and R_2 . If R_1 is greater than R_2 , the detector makes a decision in favor of symbol 1; otherwise, it decides in favor of symbol 0.

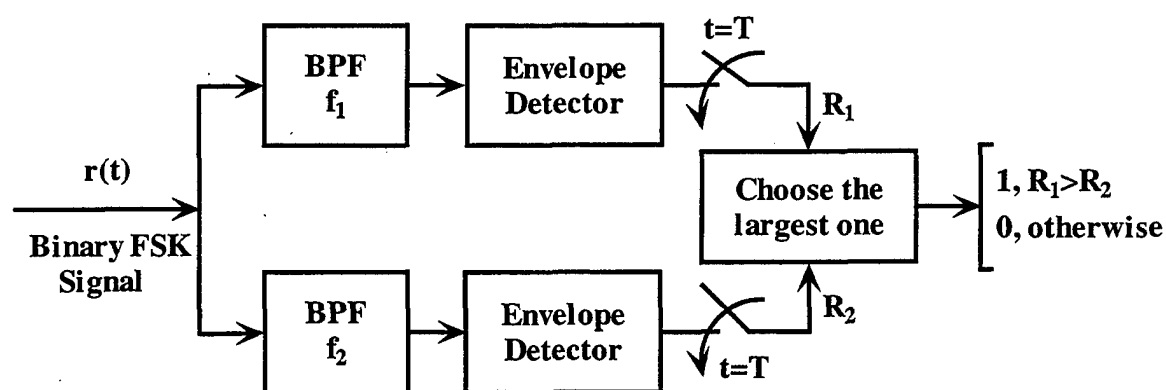


Figure 3.8 Noncoherent Detection of BFSK Using Envelope Detectors [From Ref. 3]

7. Noncoherent Detection of Binary PSK Signals

PSK signals cannot be detected noncoherently. An important form of PSK can be classified as noncoherent or differentially coherent, since it does not require a reference in-phase with the received carrier. This type of PSK is called differential PSK (DPSK). It utilizes phase information of the prior symbol as a phase reference for detecting the current symbol.

At any particular instant of time, we have the received DPSK signal as one input into the multiplier in Figure 3.9 and a delayed version of this signal, delayed by the bit duration T , as the other input. The integrator output is compared with a preset threshold by the decision device.

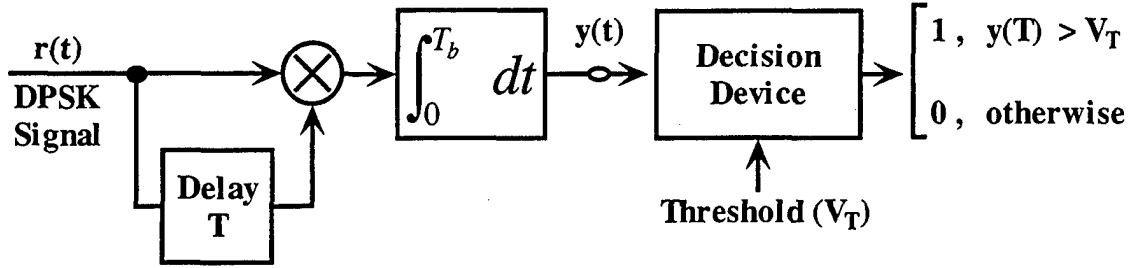


Figure 3.9 Noncoherent Detection of BPSK Signals [From Ref. 3]

C. PROBABILITY OF ERROR AND ERROR PERFORMANCE

An important measure of performance used for digital modulation is probability of symbol error, P_e . It is often convenient to specify system performance by the probability of bit error P_b , even when decisions are made on the bases of symbols rather than bits. The relationship between P_e and P_b is

$$P_b = \frac{P_e}{\log_2 M} \quad (3.4)$$

where M represents the number of possible output conditions. For binary modulation ($M=2$), the symbol error probability is equal to the bit error probability.

The probability of error is a function of the signal energy per bit (E_b) to noise power density (N_0) ratio. We can write the following identities, showing the relationship between E_b/N_0 and SNR for binary signals,

$$\frac{E_b}{N_0} = \frac{ST}{N_0} = \frac{S}{RN_0} = \frac{SW}{RN_0W} = \frac{S}{N} \left(\frac{W}{R} \right) \quad (3.5)$$

where E_b is the signal energy per binary symbol, N_0 is the noise power density ($N = N_0W$), S is the modulating signal power, T is bit time duration, R is bit rate ($1/T$), and W is the signal bandwidth.

For the binary detector depicted in Figure 3.10, in the presence of additive white Gaussian noise (AWGN), the received signal by the receiver can be represented by

$$r(t) = s_i(t) + n(t), \quad i = 1, 2. \quad (3.6)$$

Good engineering design can eliminate much of the noise. The thermal noise, caused by the thermal motion of electrons in all dissipative components, cannot be eliminated. We can describe the thermal noise as a Gaussian random process, because its instant values have the Gaussian distribution. It is “white” because of its uniform power spectral density for all frequencies, and “additive” because it is simply added to the signal.

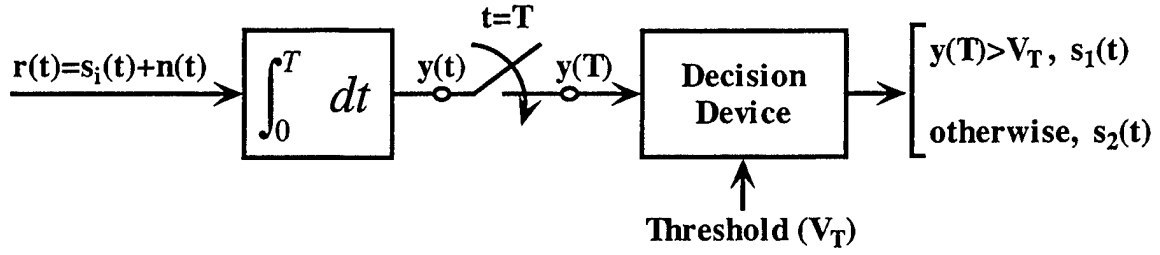


Figure 3.10 Digital Signal Detection by a Binary Detector

The output of the filter, sampled at $t=T$, yields

$$y(T) = a_i(T) + n_o(T), \quad i = 1, 2 \quad (3.7)$$

where $a_i(T)$ is the signal component of $y(T)$, and $n_o(T)$ is the noise component. Note that the noise component is a zero-mean Gaussian random variable, and thus y is a Gaussian random variable with a mean of either a_1 or a_2 depending on whether $s_1(t)$ or $s_2(t)$ was sent. The decision device compares the filter output y with threshold V_T , $s_1(t)$ is decided if $y > V_T$ or $s_2(t)$ is decided if $y < V_T$.

For binary signal detection systems, there are two ways in which errors can occur. That is, given that signal $s_1(t)$ was transmitted, an error results if $s_2(t)$ is received; or given that signal $s_2(t)$ was transmitted, an error results if $s_1(t)$ is received. Thus, the probability of error P_e is expressed as

$$P_e = P(s_2|s_1)P(s_1) + P(s_1|s_2)P(s_2) \quad (3.8)$$

where $P(s_1)$ and $P(s_2)$ are the a priori probabilities that $s_1(t)$ and $s_2(t)$, are transmitted, and $P(s_1|s_2)$ and $P(s_2|s_1)$ are the conditional probabilities. $P(s_1|s_2)$ is the probability of receiving $s_1(t)$, given that $s_2(t)$ is sent. When symbol 1 or 0 occurs with equal probability, that is, $P(s_1) = P(s_2) = 1/2$, then

$$P_e = \frac{1}{2} [P(s_2|s_1) + P(s_1|s_2)]. \quad (3.9)$$

The probability density function (pdf) of the zero-mean Gaussian random noise n_0 in Equation 3.7 is

$$f_{n_0}(\xi) = \frac{1}{\sqrt{2\pi}\sigma_{n_0}} e^{\frac{-\xi^2}{2\sigma_{n_0}^2}} \quad (3.10)$$

where $\sigma_{n_0}^2$ is the noise variance. It follows from Equations 3.7 and 3.10 that

$$f(y|s_1) = \frac{1}{\sqrt{2\pi}\sigma_{n_0}} e^{\frac{-(y-a_1)^2}{2\sigma_{n_0}^2}}, \quad (3.11)$$

and

$$f(y|s_2) = \frac{1}{\sqrt{2\pi}\sigma_{n_0}} e^{\frac{-(y-a_2)^2}{2\sigma_{n_0}^2}} \quad (3.12)$$

which are illustrated in Figure 3.11.

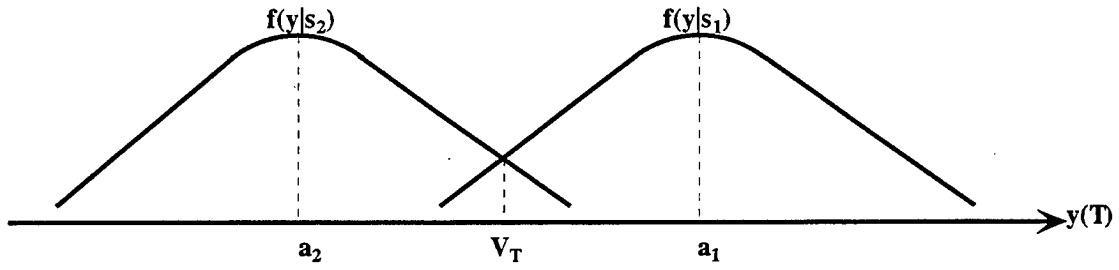


Figure 3.11 The Conditional Pdfs of Binary Signal

By using Figure 3.11 we can find that

$$P(s_2 | s_1) = \int_{-\infty}^{V_T} f(y | s_1) dy, \quad (3.13)$$

and

$$P(s_1 | s_2) = \int_{V_T}^{\infty} f(y | s_2) dy. \quad (3.14)$$

Because of the symmetry of $f(y | s_i)$ Equation 3.9 reduces to

$$P_e = P(s_2 | s_1) = P(s_1 | s_2). \quad (3.15)$$

Thus, the probability of error P_e is numerically equal to the area under the tail of either likelihood function $f(y|s_1)$ or $f(y|s_2)$ on the incorrect side of the threshold, e.g.,

$$P_e = \int_{V_T}^{\infty} f(y | s_2) dy \quad (3.16)$$

where $V_T = (a_1 + a_2)/2$ is the optimum threshold. Using Equation 3.12, we can obtain

$$P_e = \int_{V_T}^{\infty} \frac{1}{\sqrt{2\pi}\sigma_{n_0}} e^{\frac{-(y-a_2)^2}{2\sigma_{n_0}^2}} dy. \quad (3.17)$$

If we introduce $u = (y - a_2)/\sigma_{n_0}$ and $\sigma_{n_0} du = dy$, the integral simplifies to

$$P_e = \int_{\frac{(a_1-a_2)}{2\sigma_{n_0}}}^{\infty} \frac{1}{\sqrt{2\pi}} e^{\frac{-u^2}{2}} du = Q\left(\frac{a_1 - a_2}{2\sigma_{n_0}}\right) \quad (3.18)$$

where $Q(x)$ is defined as

$$Q(x) = \frac{1}{\sqrt{2\pi}} \int_x^{\infty} e^{-\frac{u^2}{2}} du. \quad (3.19)$$

As an example, for coherently detected BPSK $a_1 = \sqrt{E_b}$ when $s_1(t)$ is sent and $a_2 = -\sqrt{E_b}$ when $s_2(t)$ is sent, where E_b is the signal energy per binary symbol. For AWGN, we can replace the noise variance with $N_0/2$, so Equation 3.18 can be written as

$$P_e = \int_{\sqrt{\frac{2E_b}{N_0}}}^{\infty} \frac{1}{\sqrt{2\pi}} e^{-\frac{u^2}{2}} du, \quad (3.20)$$

or

$$P_e = Q\left(\sqrt{\frac{2E_b}{N_0}}\right). \quad (3.21)$$

We can obtain the probability of error for the other digital modulation techniques by applying the same procedure explained above. Assuming AWGN, error performance of digital modulation techniques in terms of probability of error is tabulated in Table 3.1.

Digital Modulation Technique	Coherent	Noncoherent
Binary ASK	$P_e = Q\left(\sqrt{\frac{E_b}{N_0}}\right)$	$P_e = \frac{1}{2}e^{\frac{-E_b}{2N_0}}$
BPSK	$P_e = Q\left(\sqrt{\frac{2E_b}{N_0}}\right)$	—
BFSK	$P_e = Q\left(\sqrt{\frac{E_b}{N_0}}\right)$	$P_e = \frac{1}{2}e^{\frac{-E_b}{2N_0}}$
QPSK	$P_e = Q\left(\sqrt{\frac{2E_b}{N_0}}\right)$	—

Table 3.1 Probability of Error of Digital Modulation Techniques in Terms of Bit Energy and Noise Power Spectral Density.

THIS PAGE INTENTIONALLY LEFT BLANK

IV. FUNDAMENTAL DESIGN PARAMETERS OF ANTENNAS

A. INTRODUCTION

An antenna is a device that provides a means for radiating or receiving radio waves. Using this definition, an antenna can be thought as a coupling device that connects the transmitting or receiving device to the transmission medium. An antenna may be designed for only transmitting or only receiving or both transmitting and receiving purposes.

An antenna can be any conducting structure that can carry an electrical current. If it carries a time-varying electrical current, it will radiate an electromagnetic wave (maybe not efficiently or in a desired direction, but it will radiate). Usually one designs a structure to radiate efficiently with certain desired characteristics. If improperly designed or utilized, adjacent or peripheral components (including the transmission line, the power supply line, nearby structures or even a person touching the equipment to which the antenna is connected) may also radiate.

By matching the antenna impedance to its connecting transmission line, the power can be transferred efficiently. The transmission line ideally should transfer all of its power to the antenna and not radiate energy itself.

It is normally desired that an antenna radiate in a specified direction or directions. This is achieved by designing it to have the proper radiation pattern.

Antennas can aid anti-jamming using their spatial filtering ability. In the microwave frequency region, highly directive antennas can be designed that are useful for point-to-point communication systems. These systems coupled with low-sidelobe

technology can provide a high degree of protection against jammers located at angles displaced from the axis of the main antenna beams. Sidelobe cancellation systems are also used with directive antennas to provide additional attenuation of sidelobe jamming signals. These systems utilize auxiliary or guard antennas to adaptively generate antenna patterns that provide nulls in the directions of jammers. In theory, the number of sidelobe jamming signals that can be nulled is equal to the number of auxiliary antennas. The potential for sidelobe cancellation is increased when a phased array antenna is used. For arrays, the number of independent nulls that can be formed is equal to the number of elements minus one [Ref. 5].

B. RADIATION PATTERN

The radiation pattern of the antenna represents the relative distribution of radiated power as a function of direction in space. The radiation pattern depicts the transmitted signal strength graphically for a constant input power.

Various parts of a radiation pattern are referred to as lobes, which may be subclassified into major (main), minor, side, and back lobes.

A radiation lobe is a portion of the radiation pattern bounded by regions of relatively weak radiation intensity [Ref. 6]. Figure 4.1 (a) demonstrates a symmetrical three-dimensional polar pattern with a number of radiation lobes. Figure 4.1 (b) illustrates a linear two-dimensional pattern where the same pattern characteristics are indicated.

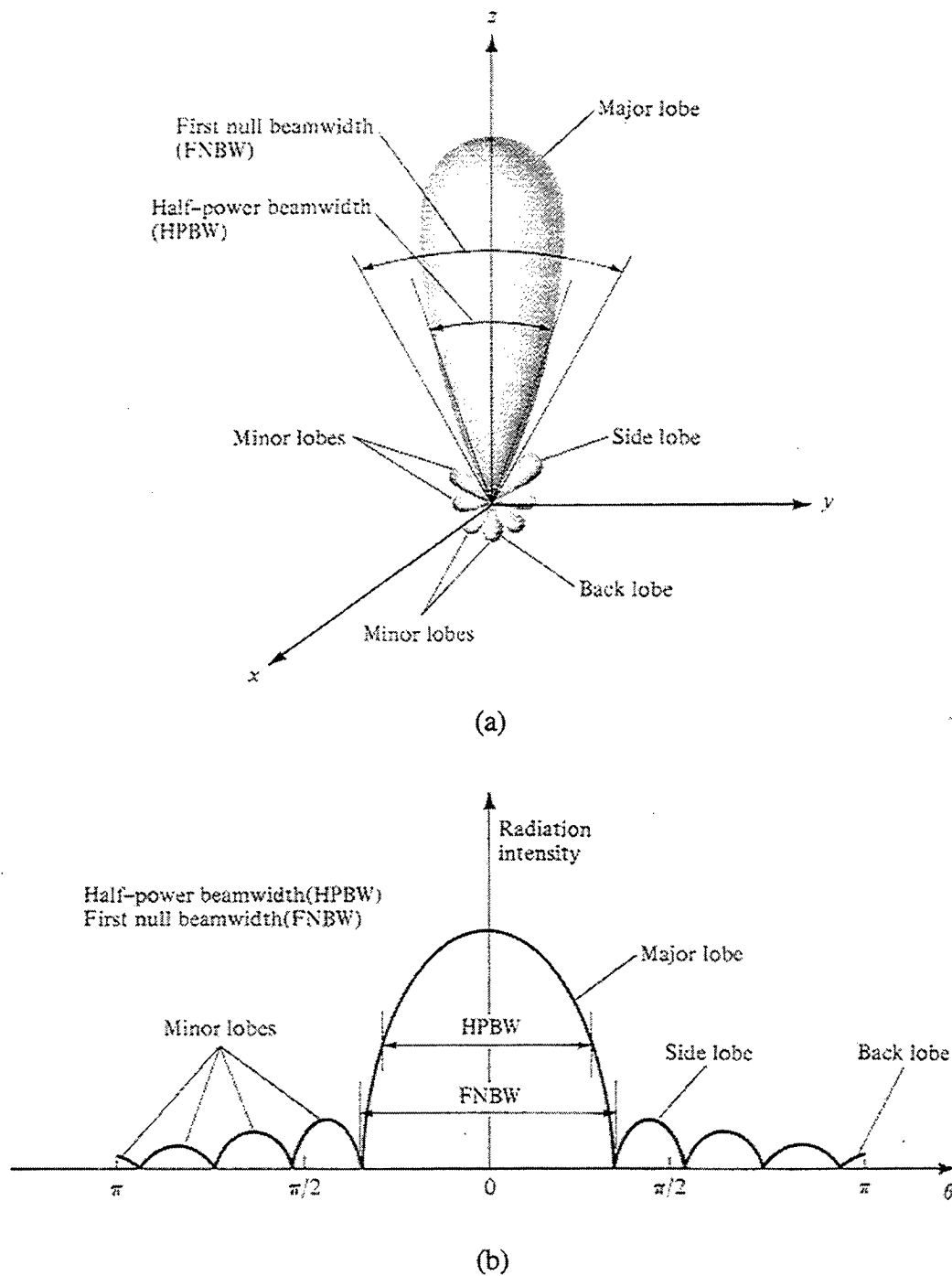


Figure 4.1 (a) Radiation Lobes and Beamwidths of an Antenna Pattern (b) Linear Plot of Power Pattern and its Associated Lobes and Beamwidths [From Ref. 6]

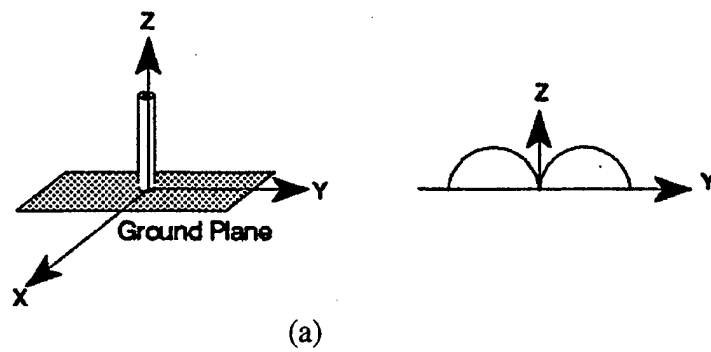
A major lobe (main beam) is defined as the radiation lobe containing the direction of maximum radiation. A minor lobe is any lobe except a major lobe. A side lobe is a radiation lobe in any direction other than the intended lobe. Usually a side lobe is adjacent to the main lobe and occupies the hemisphere in the direction of the main beam. A back lobe is a radiation lobe whose axis makes an angle of approximately 180° with respect to the main beam of an antenna [Ref. 6].

Minor lobes usually represent radiation in undesired directions, and they should be minimized. Side lobes are normally the largest of the minor lobes. The level of minor lobes is usually expressed as a ratio of the power density in the lobe in question to that of the major lobe. This ratio is often termed the side lobe ratio or side lobe level [Ref. 6].

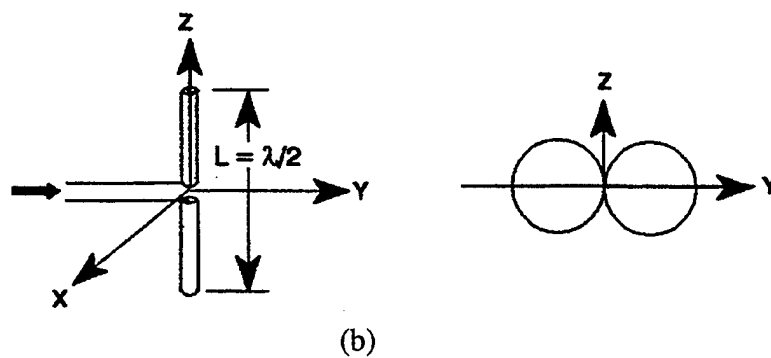
A measure of the width of the main beam is given by the beamwidth between first nulls (FNBW). The half-power beamwidth (HPBW) is the angular separation of the points where the main beam of the power pattern equals one-half that of maximum.

Radiation patterns of some important antennas are shown in Figure 4.2 and Figure 4.3 [Ref. 7].

MONOPOLE



$\lambda/2$ DIPOLE



LINEAR DIPOLE ARRAY

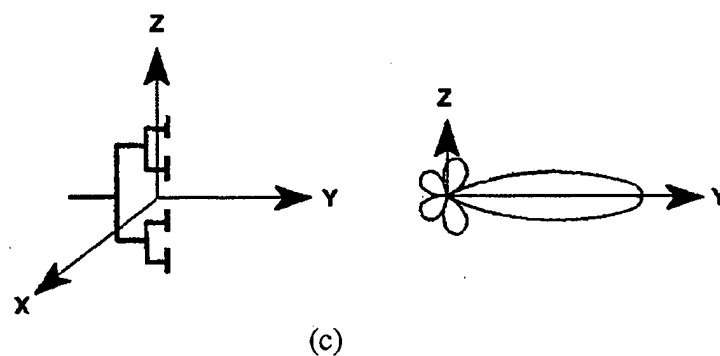


Figure 4.2 Radiation Pattern of a (a) Monopole (b) Dipole (c) Linear Dipole Array
[From Ref. 7]

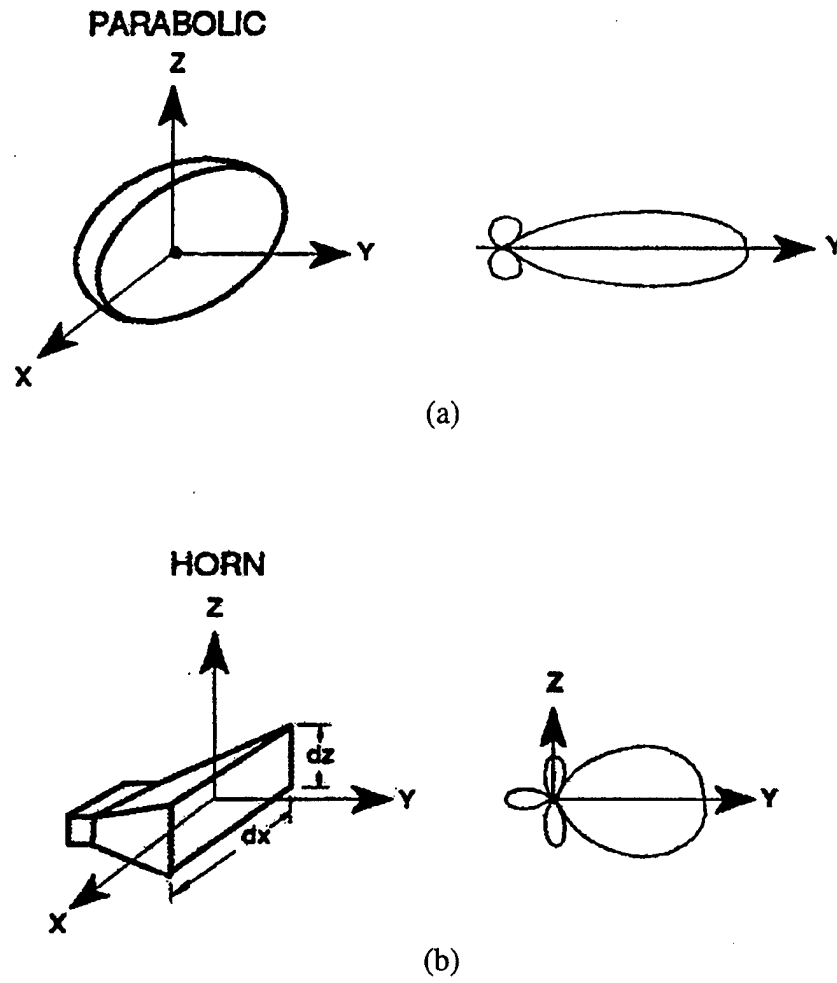


Figure 4.3 Radiation Pattern of a (a) Parabolic Antenna (b) Horn Antenna [From Ref.7]

C. POLARIZATION

All transverse electromagnetic (*TEM*) waves traveling in free space have an electric field component, \vec{E} , and a magnetic field component, \vec{H} , which are mutually perpendicular to each other and to the direction of propagation. The orientation of

the \vec{E} vector is used to define the polarization of the wave: if \vec{E} is orientated vertically with respect to the ground, the wave is said to be vertically polarized; conversely, if \vec{E} is parallel to the ground, the wave is said to be horizontally polarized. Sometimes the \vec{E} field vector rotates with time and it is said to either be circularly or elliptically polarized. Polarization of the wave radiating from an antenna is an important concept when one is concerned with the coupling between two antennas or the propagation of a radio wave.

THIS PAGE INTENTIONALLY LEFT BLANK

V. SPREAD SPECTRUM COMMUNICATIONS

A. INTRODUCTION

All of the modulation techniques discussed in Chapter II have been designed to communicate digital information from one place to another as effectively as possible in an AWGN environment. Although many real world communication channels are accurately modeled as AWGN channels, there are other important channels that do not fit this model. For example, a military communication system that might be jammed by a continuous wave tone near the modem's (an acronym for modulator-demodulator) center frequency or by a distorted retransmission of the modem's own signal. We cannot model either of this interference as AWGN. But, we can use spread spectrum techniques to eliminate the effects of these types of interference.

Spread spectrum techniques can be very useful in solving a wide range of communications problems. The amount of performance improvement that is achieved through the use of spread spectrum is defined as the "processing gain" of a spread spectrum system. Processing gain is the difference between system performance using spread spectrum techniques and system performance not using spread spectrum techniques. An often-used approximation for processing gain is the ratio of spread bandwidth (W_{ss}) to the information rate (R).

B. SPREAD SPECTRUM SYSTEM

A system is defined to be spread spectrum system if it fulfills the following requirements:

1. The transmitted signal occupies a bandwidth much in excess of the minimum bandwidth necessary to send the information.
2. Spreading is accomplished by means of spreading signal, often called a code signal, which is independent of the data.
3. At the receiver, despreading (recovering the original data) is accomplished by the correlation of the received spread signal with a synchronized replica of the spreading signal used to spread the information [Ref. 2].

Spread spectrum signals are used for:

1. Combating or suppressing the detrimental effect of interference due to jamming, interference arising from other users of the channel, and self interference due to multipath propagation.
2. Hiding a signal by transmitting it at a low power and, thus, making it difficult for an unintended listener to detect in the presence of background noise.
3. Achieving message privacy in the presence of other listeners.

C. SPREAD SPECTRUM TECHNIQUES

There are five types of spread spectrum techniques, which are:

- Direct sequence
- Frequency hopping
- Time hopping
- Hybrid
- Chirp

The two types of spread spectrum techniques most commonly employed are direct sequence (DS) spread spectrum and frequency hopping (FH) spread spectrum, described below.

1. Direct Sequence Spread Spectrum

Direct sequence systems are the best known and most widely used spread spectrum systems. This is because of their relative simplicity from the standpoint that they do not require a high-speed frequency synthesizer (A frequency synthesizer is a device which converts a stable frequency into the various hopping frequencies.)

In a direct sequence spread spectrum system, the signal is multiplied by a high rate pseudo-random binary sequence, with the result that the transmitted signal's power spectrum is spread over a significantly larger bandwidth. This lowers the magnitude of the transmitted signal's spectrum and makes it appear more noise-like to an observer [Ref. 8]. By making the transmitted signal's spectrum appear more noise-like, it is more difficult for a hostile observer to detect (successful determination of signal presence or absence) and intercept (to convert the transmitted signal back to its original form) the signal as compared to a conventional signal. Therefore, a direct sequence spread spectrum system may be considered to be both a low probability of detection (LPD) and a low probability of intercept (LPI) system as compared to conventional communication systems. Figure 5.1 is a basic block diagram of a direct sequence spread spectrum system [Ref. 9].

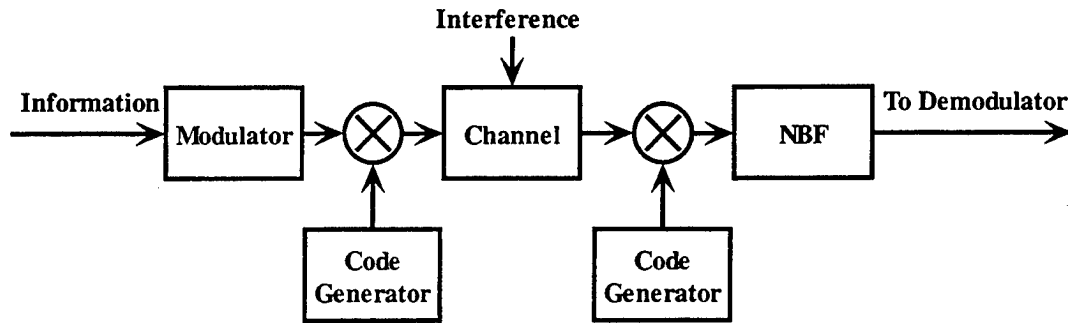


Figure 5.1 Basic Block Diagram of a Direct Sequence Spread Spectrum System
[From Ref. 9]

This technique can be defined in terms of a code sequence $c(t)$ in the form of positive and negative pulses of unit amplitude (representing a binary code sequence of ones and zeros.) These symbols occur at a rate R_C , the chip rate, where a chip is one symbol and T_C is the chip time. Usually R_C is much larger than R_I , the rate at which information symbols occur.

The spreading is accomplished by multiplying the information-modulated carrier by the code. The despreading is accomplished by multiplying the received waveform by the same code synchronized to the incoming code.

As can be seen from Figure 5.1, there is an interference term added to the channel. When the received signal is multiplied by the code sequence, the interference bandwidth increases greatly above that of the information-modulated carrier. The narrow band filter (NBF) rejects almost all the power of the undesired signal. The reduction is approximately by the factor of R_I/R_C , which in effect causes a corresponding processing gain (P_G) of R_C/R_I .

2. Frequency Hopping Spread Spectrum

In a frequency-hopped (FH) spread spectrum system, the carrier frequency of the signal is changed (hopped) in a pseudo-random fashion over a large band of frequencies. Although a potential adversary may be able to detect the signal, an FH signal will be more difficult to intercept than conventional signals, because how the carrier frequency is varied is not known by the adversary. Therefore, a FH spread spectrum system may be considered to be a LPI system as compared to conventional communication systems. If in a FH spread spectrum system more than one symbol is transmitted per frequency hop, then it is called slow FH spread spectrum system. If one symbol is transmitted by one or more consecutive hops, then it is called fast FH spread spectrum system. Figure 5.2 is a basic block diagram of a frequency hopping spread spectrum system [Ref. 9].

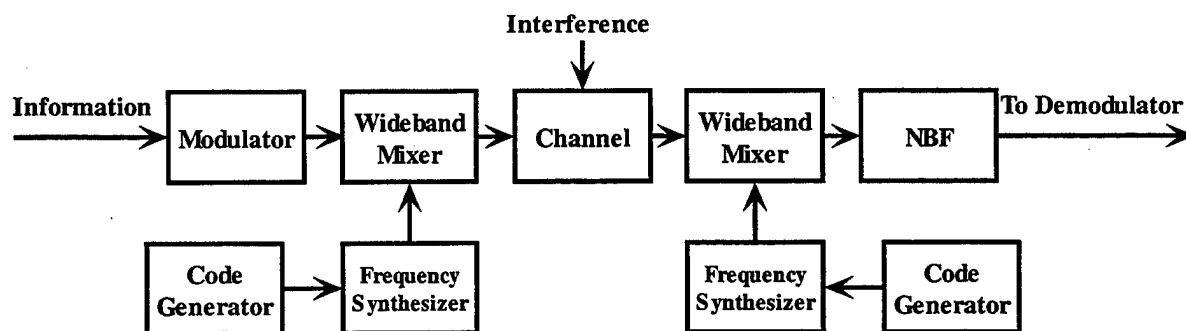


Figure 5.2 Basic Block Diagram of a Frequency Hopping Spread Spectrum System
[From Ref. 9]

A frequency hopping system consists basically of a wideband mixer, a code generator and frequency synthesizer capable of responding to the coded output from the

code generator. A great deal of effort has been expended in developing rapid-response frequency synthesizers for spread spectrum systems.

The objective of a frequency hopping system is to produce a transmitted signal (which has a frequency spectrum of bandwidth W_l associated with it) such that the center frequency f_i is changed in discrete steps in an apparently random manner. That is, the frequency seems to hop at a hopping rate of R , over a total allocated bandwidth W_{ss} . The ratio W_{ss}/W_l is called processing gain.

VI. THEORY OF JAMMING

A. INTRODUCTION

Electronic warfare (EW) is the use of electromagnetic energy to determine, exploit, reduce, or prevent hostile use of the electromagnetic spectrum and action, which retains friendly use of the electromagnetic spectrum [Ref. 1].

The acceptance of the idea that EW can play a major role in military conflicts dates back many years. Most of the efforts to use EW have dealt with radars and produced important results in that particular field. Recent years have brought about an increasing awareness that there are similar needs and opportunities for exploitations concerning communication systems [Ref. 1].

Electronic Warfare has three main categories, which are:

- Electronic Support (ES)
- Electronic Attack (EA)
- Electronic Protection (EP)

ES involves detecting enemy signal activity, classifying signals and extracting intelligence, and determining emitter locations. EA includes the use of directed energy weapons (lasers, microwave, particle beams), antiradiation missiles (missiles which are guided to their targets by following the radiations of critical sensors or communications links back to their source) and electromagnetic pulses to destroy enemy electronic equipment. EP involves the use of counter techniques for reducing the effectiveness of an enemy's EA activities.

B. J/S RATIO

A basic communications system in a jamming environment is as shown in Figure 6.1. Here, the source of unwanted electrical signals is the noise power of a jammer in addition to thermal (Gaussian), impulsive, shot and flicker noise. Therefore, extending Equation 3.5, the bit energy per noise power spectral density of interest is $E_b/(N_0 + J_0)$, where J_0 is the noise power spectral density due to the jammer.

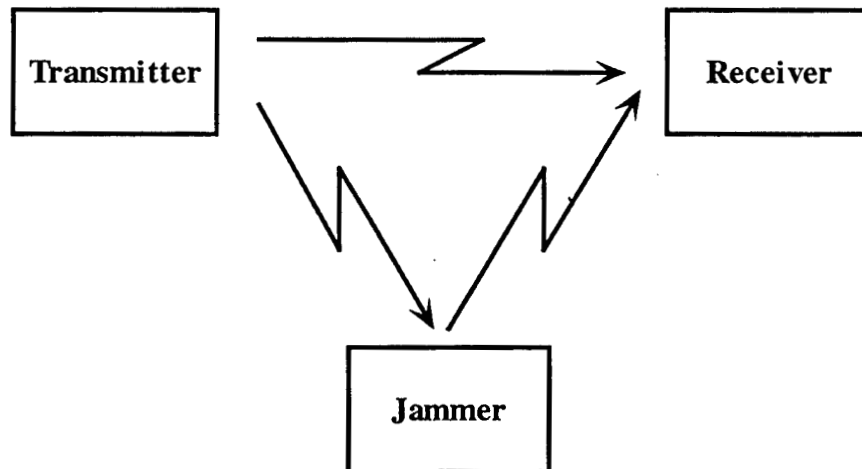


Figure 6.1 Basic Communications System in a Jamming Environment

We can define $(E_b/J_0)_{\text{required}}$ as the bit energy per jammer noise power spectral density required for maintaining the link at a specified error probability. The parameter E_b can be written as

$$E_b = ST_b = \frac{S}{R} \quad (5.1)$$

where S is the received signal power, T_b the bit duration, and R the data rate in bits/s.

Then we can express $(E_b/J_0)_{required}$ as

$$\left(\frac{E_b}{J_0}\right)_{required} = \left(\frac{S/R}{J/W}\right)_{required} = \frac{W/R}{(J/S)_{required}} \quad (5.2)$$

where W is the bandwidth of the system, and $(J/S)_{required}$ can be written as

$$\left(\frac{J}{S}\right)_{required} = \frac{W/R}{(E_b/J_0)_{required}} \quad (5.3)$$

The ratio $(J/S)_{required}$ is a figure of merit that provides a measure of how vulnerable a system is to interference. The larger the $(J/S)_{required}$, the greater is the system's jamming rejection capability [Ref. 2].

C. THEORY OF JAMMING FOR BFSK AND BPSK

Jamming is the deliberate radiation, reradiation, or reflection of electromagnetic energy for the purpose of impairing an adversary's use of electronic devices, equipment, or systems [Ref. 2].

The transmission of signals introduces an element of unpredictability or randomness (pseudo-randomness) in each of the transmitted coded signal waveforms that are not known to the jammer. As a result, the jammer must synthesize and transmit an interfering signal without knowledge of the pseudo-random pattern.

In order to disrupt a communication system, in a given location and at a given time, two fundamental questions arise for the jammer:

1. What is the best jamming waveform (shape of a signal) and strategy?
2. How effective will jamming be against the system?

The answers to these questions depend upon many factors: transmitted power levels, ranges, frequencies, system losses, system efficiencies, antenna patterns, noise levels, modulation methods, demodulation methods, error-control coding, data formats, environmental conditions (such as fading and nuclear effects), and self-interference levels. A system's vulnerability to EA can be described in terms of its interceptability, accessibility, and susceptibility. Interceptability is a measure of the ease with which an enemy can intercept and identify signals and determine enemy locations. Accessibility is a measure of the ease with which an enemy can reach a system with an appropriate jamming waveform and power level. Susceptibility is measure of the system's design that determines the effect of EA on system performance [Ref.1]. There are many different waveforms that can be used for jamming communications systems. The most appropriate choice depends on the target system. The primary jamming waveforms for BFSK and BPSK are barrage noise jamming, pulsed noise jamming, and tone jamming.

1. Barrage Noise Jamming

Barrage jammers are wideband noise transmitters designed to deny use of frequencies over wide portions of the electromagnetic spectrum. The advantages of barrage jammers are their simplicity and their ability to cover a wide portion of the electromagnetic spectrum.

In Chapter II it was shown that the bit error probability P_b for a coherently demodulated BFSK system in the presence of AWGN is

$$P_b = Q\left(\sqrt{\frac{E_b}{N_0}}\right). \quad (5.4)$$

The presence of the barrage noise jammer increases this noise power spectral density from N_0 to $(N_0 + J_0)$ where J_0 is the noise power spectral density due to the barrage noise jamming [Ref.11]. The bit error probability for a coherent BFSK system in the presence of barrage noise jamming can be defined as

$$P_b = Q\left(\sqrt{\frac{E_b}{N_0 + J_0}}\right). \quad (5.5)$$

In Chapter II it was illustrated that the bit error probability P_b for a noncoherently demodulated BFSK system is

$$P_b = \frac{1}{2} e^{\frac{-E_b}{2N_0}}. \quad (5.6)$$

The bit error probability for a noncoherent BFSK system in the presence of barrage noise jamming is

$$P_b = \frac{1}{2} e^{\frac{-E_b}{2(N_0 + J_0)}}. \quad (5.7)$$

In Chapter II it was shown that the bit error probability P_b for a coherently demodulated BPSK system is

$$P_b = Q\left(\sqrt{\frac{2E_b}{N_0}}\right). \quad (5.8)$$

The bit error probability for a coherent BPSK system in the presence of barrage noise jamming is therefore

$$P_b = Q\left(\sqrt{\frac{2E_b}{N_0 + J_0}}\right). \quad (5.9)$$

2. Pulsed Noise Jamming

In attempting to disrupt digital communications, it is often advantageous to concentrate the jamming energy in short pulses. Pulsed jamming can cause a substantial increase in the bit error rate relative to the rate caused by continuous jamming with the same power.

Pulsed noise jamming occurs when a jammer transmits with power $J = J_0/\rho$ where J_0 is jammer power at input to the intended receiver and ρ is a fraction of time the jammer is turned on [Ref. 11].

The bit error probability for a noncoherent BFSK system in the presence of pulsed noise jamming can be defined as

$$P_b = \frac{1-\rho}{2} e^{\frac{-E_b}{2N_0}} + \frac{\rho}{2} e^{\frac{-E_b}{2(N_0+J_0/\rho)}}. \quad (5.10)$$

The bit error probability for a coherent BPSK system in the presence of pulsed noise jamming is therefore

$$P_b = Q\left(\sqrt{\frac{2E_b}{N_0 + \frac{J_0}{\rho}}}\right) + (1-\rho)Q\left(\sqrt{\frac{2E_b}{N_0}}\right). \quad (5.11)$$

3. Tone Jamming

In the case of tone jamming for noncoherent BFSK, the communication system is attacked by a jamming tone $S_j(t) = \sqrt{2}A_j \cos[2\pi(f_c + \Delta f/2)t + \theta_j]$ where θ_j is a uniform random variable over the interval $[0, 2\pi]$. The bit error probability for a noncoherent BFSK system in the presence of tone noise jamming is

$$P_b = \frac{1}{2} Q \left[\left(\sqrt{\frac{P_j}{N_0/T_b}} \right), \left(\sqrt{\frac{P_c}{N_0/T_b}} \right) \right] \quad (5.12)$$

where $Q(\alpha, \beta)$ is Marcum's Q-function, P_j is jamming power, P_c is the carrier power [Ref. 11]. The generalization of Marcum's Q-function is

$$Q(\alpha, \beta) = \int_{\beta}^{\infty} x e^{\left(\frac{-x^2 + \alpha^2}{2} \right)} I_0(\alpha x) dx \quad (5.13)$$

where $I_0(x)$ is the Bessel Function of the first kind.

In the case of tone jamming for coherent BPSK, the communication system is attacked by a jamming tone $S_j(t) = \sqrt{2}A_j \cos[2\pi f_c t + \theta_j]$ where θ_j is a uniform random variable over the interval $[0, 2\pi]$.

The bit error probability for a coherent BPSK system in the presence of tone noise jamming is

$$P_b = \frac{1}{\pi} \int_0^\pi Q \left[\sqrt{\frac{2E_b}{N_0}} \left(1 + \sqrt{\frac{P_J}{P_C}} \cos \theta_J \right) \right] d\theta_J \quad (5.14)$$

where P_J is jamming power, P_C is the carrier power [Ref. 11].

D. THEORY OF JAMMING FOR SPREAD SPECTRUM

As indicated before, there are many different waveforms that can be used for jamming communications systems. The primary jamming waveforms for spread spectrum communications are broadband noise jamming, partial-band noise jamming, multiple-tone jamming, pulse jamming, and repeat-back jamming.

1. Broadband Noise Jamming

If the jammer strategy is to jam the entire spread spectrum bandwidth, W_{ss} , with its fixed power, the jammer is referred to as a wideband or broadband jammer, and the jammer power spectral density is

$$J_0 = \frac{J}{W_{ss}} \quad (5.15)$$

where J is a fixed jammer received power.

In Chapter II it was shown that the bit error probability P_b for a coherently demodulated BPSK system is

$$P_b = Q\left(\sqrt{\frac{2E_b}{N_0}}\right). \quad (5.16)$$

The noise power spectral density N_0 represents thermal noise at the front end of the receiver. The presence of the jammer increases this noise power spectral density from N_0 to $(N_0 + J_0)$. Thus the average bit error probability for a coherent BPSK system in the presence of broadband jamming is

$$P_b = Q\left(\sqrt{\frac{2E_b}{N_0 + J_0}}\right) = Q\left(\sqrt{\frac{2E_b/N_0}{1 + J_0/N_0}}\right). \quad (5.17)$$

By using Equation 5.3 we can write Equation 5.17 as

$$P_b = Q\left(\sqrt{\frac{2E_b/N_0}{1 + (E_b/N_0)(J/S)/(W_{ss}/R)}}\right) = Q\left(\sqrt{\frac{2E_b/N_0}{1 + (E_b/N_0)(J/S)/G_p}}\right) \quad (5.18)$$

where G_p is the processing gain (W_{ss}/R). For a given ratio of jammer power to signal power, the jammer will cause some irreducible error probability. The only way to reduce this error probability is to increase the processing gain [Ref. 2].

2. Partial-Band Noise Jamming

If the jammer strategy is to jam some frequency range of bandwidth which is subset of the entire spread spectrum bandwidth, W_{ss} , with its fixed power, the jammer is referred to as a partial-band jammer. A jammer can often increase the degradation to a frequency hopping (FH) system by employing partial-band jamming. Assuming that the frequency hopped modulation format is noncoherently detected binary FSK, and then the probability of a bit error is

$$P_b = \frac{1}{2} e^{\frac{-E_b}{2N_0}}. \quad (5.19)$$

Let us define a parameter, ρ , where $0 < \rho \leq 1$, representing the fraction of the band being jammed. The jammer can trade bandwidth jammed for in-band jammer power, such that by jamming a band $W = \rho W_{ss}$, the jammer noise power spectral density can be concentrated to level J_0/ρ , thus maintaining a constant average jamming received power J where $J = J_0 W_{ss}$.

In the case of partial-band jamming, the probability that a specific transmitted symbol will be received unjammed is $(1-\rho)$, and that it will be perturbed by

jammer power with spectral density J_0/ρ is ρ . Therefore, the average bit error probability can be written as

$$P_b = \frac{1-\rho}{2} e^{\frac{-E_b}{2N_0}} + \frac{\rho}{2} e^{\frac{-E_b}{2(N_0+J_0/\rho)}}. \quad (5.20)$$

Since, in a jamming environment, it is often the case that $J_0 \gg N_0$, we can simplify Equation (5.20) to the form

$$P_b = \frac{\rho}{2} e^{\frac{-\rho E_b}{2J_0}}. \quad (5.21)$$

An intelligent jammer, with fixed finite power, can produce significantly greater degradation with partial-band jamming than is possible with broadband jamming [Ref. 2].

3. Multiple-Tone Jamming

In the case of multiple-tone jamming, the jammer divides its total received power, J , into distinct, equal-power, random-phase CW tones. These are distributed over the spread-spectrum bandwidth, W_{ss} . The analysis of the effects of tone jamming is more complicated than that of noise jamming for DS systems. Therefore, the effect of a despread tone is often approximated as Gaussian noise. For a noncoherent FH/FSK system operating in the presence of partial-band tone jamming, the performance is often assumed the same as partial-band noise jamming. However, multiple-CW-tone

jamming can be more effective than partial-band noise against FH/MFSK signals because CW tones are the most efficient way for a jammer to inject energy into noncoherent detectors [Ref. 2].

4. Pulse Jamming

Consider a spread spectrum DS/BPSK communication system in the presence of a pulse-noise jammer. A pulse-noise jammer transmits pulses of bandlimited white Gaussian noise having a time-averaged received power, J , although the actual power during jamming pulse duration is larger. Assume that the jammer can choose the center frequency and bandwidth of the noise to be the same as the receiver's center frequency and bandwidth. Assume also that the jammer can trade duty cycle for increased jammer power, such that if the jamming is present for a fraction $0 < \rho < 1$ of the time, then during this time, the jammer power spectral density is increased to level J_0/ρ , thus maintaining a constant time-averaged power J . The bit error probability P_b for a coherently demodulated BPSK system was given in Equation 5.8. The noise power spectral density N_0 represents thermal noise at the front end of the receiver. The presence of the jammer increases this noise power spectral density from N_0 to $(N_0 + J_0/\rho)$. Since the jammer transmits with duty cycle (ρ), the average bit error probability is

$$P_b = (1 - \rho)Q\left(\sqrt{\frac{2E_b}{N_0}}\right) + \rho Q\left(\sqrt{\frac{2E_b}{N_0 + J_0/\rho}}\right). \quad (5.22)$$

We can generally assume that in a jamming environment N_0 can be neglected, therefore, we can write

$$P_b \approx \rho Q \left(\sqrt{\frac{2E_b \rho}{J_0}} \right). \quad (5.23)$$

The jammer will, of course, attempt to choose the duty cycle ρ that maximizes P_b . There is almost a 40-dB difference in E_b/J_0 between the broadband jammer and the worst-case pulse jammer. For the same jammer power, the jammer can do considerably more harm to a DS/BPSK system with pulse jamming than with constant power jamming. The effect of a pulse-noise jammer on DS/BPSK is similar to the effect of a partial-band noise jammer on FH/BFSK [Ref. 2].

5. Repeat-Back Jamming

It is clear that the faster the frequency hops, the easier it is to hide the signal from the jammer. The measure of jammer-rejection capability, namely processing gain, G_p , is based on the assumption that the jammer is a dumb jammer; that is, the jammer knows the extent of the spread-spectrum bandwidth, W_{ss} , but does not know the exact spectral location of the signal at any moment in time. We assume that the hopping rate is fast enough to preclude the jammer from monitoring the transmitted signal so as to usefully change this jamming strategy.

There are smart jammers that are known as repeat-back jammers or frequency-follower (FF) jammers. These jammers monitor a communicator's signal (usually

via a sidelobe beam from the transmitting antenna). They possess wideband receivers and high-speed signal processing capabilities that enable them to rapidly concentrate their jamming signal power in the spectral vicinity of a communicator's FH/FSK signal. By so doing, the smart jammer can increase the jamming power in the communicator's instantaneous bandwidth, thereby gaining an advantage over a wideband jammer. Notice that this strategy is useful only against frequency hopping signals. In direct-sequence systems, there is no instantaneous narrowband signal for the jammer to detect. What can be done to defeat the repeat-back jammer? One method is to simply hop so fast that by the time the jammer receives, detects, and transmits the jamming signal, the communicator is already transmitting at a new hop location (which of course will be unaffected by jamming at the frequency of the prior hop) [Ref. 2].

THIS PAGE INTENTIONALLY LEFT BLANK

VII. THEORY OF ANTI-JAMMING

A. INTRODUCTION

Anti-jamming consists of the design and operational steps taken in electronic devices or systems to limit the degradation performance that results from intentional electromagnetic interference or jamming.

Communications systems generally use a number of anti-jamming techniques that are listed in Figure 6.1.

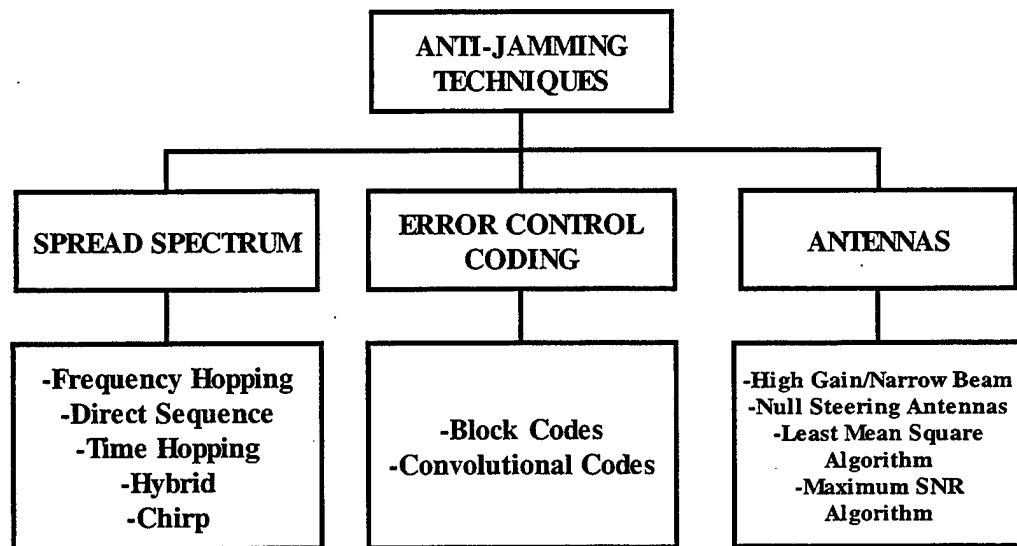


Figure 6.1 Communications Anti-jamming Techniques [From Ref. 5]

The usual design goal for an anti-jam (AJ) communication system is to force a jammer to expand its resources over a wide-frequency band, for a maximum time, and from a diversity of sites. The most prevalent design options are frequency

diversity, by the use of direct sequence and frequency hopping spread spectrum techniques; time diversity by the use of time hopping; spatial discrimination, by the use of narrow-beam antennas, and combinations of the above [Ref. 2]. Spread spectrum communications are discussed in Chapter V.

Error detection and correction coding is a structure, called code, by which information bits are transformed and augmented by additional binary digits such that errors occurring at the receiver and demodulator can be detected and corrected using the relationships between the transformed bits. The most common types of error detection and correction are block coding and convolutional coding. With block codes, information is accumulated in blocks of fixed length and represented by transmitted blocks of fixed larger length. Examples of block codes are Hamming codes, BCH codes, and Reed-Solomon codes. Convolutional codes offer an approach to error control substantially different from that of block codes. A convolutional encoder converts the entire data stream, regardless of its length, into a single code word. An optimum decoding algorithm for convolutional codes is the Viterbi algorithm.

Antenna patterns have an important role in anti-jamming techniques. Nulls in antenna radiation patterns can often be formed in nearly arbitrary directions outside the main beam. Thus, if the arrival angles of a desired signal and a jamming signal are known and adequately separated, it is possible to enhance the desired signal while nulling the jamming. However, a change in the geometry due to the movement of the intended transmitter, the receiver, or the jammer may cause the jamming signal initially in a null to leave the null. An adaptive antenna system can change the direction of a null to

accommodate geometrical changes. An adaptive antenna system automatically monitors its output and adjusts its parameters accordingly. It reduces the impact of the jamming signal that enters through the side lobes, or possibly the mainlobe, of its antenna radiation pattern, while still allowing reception of an intended transmission. The most common type for adaptive antenna systems is a phased-array antenna.

A phased-array antenna consists of a number K of antenna elements, the outputs of which are processed and combined to produce the designed antenna radiation pattern. With K antenna elements, it is possible to produce nulls for $K-1$ interfering jammers.

Another approach for interference rejection is the maximum SNR algorithm. Using an appropriately defined SNR, we can find the optimum set of weights for individual antennas to maximize this ratio.

The least mean square algorithm is the method that the reference signal is equal to the desired response of the antenna system. The algorithm updates the new equalizer weights based on the existing weights and a factor depending on the current input samples and the current estimation error.

B. ANTI-JAMMING TECHNIQUES

1. Error Control Coding

Error control codes are used to format the transmitted information so as to increase its immunity to noise. This is accomplished by inserting controlled redundancy into the transmitted information stream, allowing the receiver to detect and possibly correct errors.

There are primarily two types of errors that are introduced by a transmission channel, random errors and burst errors. Random errors are introduced by additive white Gaussian noise. Burst errors, which are a cluster of errors occurring in a relative short period of time, are caused when the received signal-to-noise ratio is subject to large fluctuations. Signal fading or a hostile noise jamming may cause these fluctuations.

The amount of inserted redundancy is usually expressed in terms of the code rate R . The code rate is the ratio of k , the number of data symbols transmitted per code word, to n , the total number of symbols transmitted per code word ($0 < R = k/n < 1$). Assuming that the data symbol transmission rate R_s is to remain constant, the added redundancy forces us to increase the overall symbol transmission rate to R_s/R . If the transmitted power level is constant, then the received energy per symbol is reduced from E_s to RE_s . The demodulated bit error rate (BER) is thus increased with respect to its previous value. However, when the degraded, demodulated data symbols and redundant symbols are sent to the error control decoder, the redundancy is used to correct some of errors, improving the reliability of the demodulated data. If the code is well selected, the BER at the output of the demodulator is better than that at the output of the demodulator in the original uncoded system.

The amount of improvement in BER is usually discussed in terms of the additional transmitted power that is required to obtain the same performance without coding. The difference in power is called the coding gain [Ref. 10].

The most common types of error detection and correction are block codes and convolutional codes.

a. Block Codes

With block codes, a block of k data bits are encoded into a block code of n coded bits which are then transmitted in blocks of fixed longer length. The code rate is $R = k/n$. There are 2^k possible output symbols. Since there are 2^n possible output code words and $k < n$, not all possible output code words are used.

Code words are represented by binary n -tuples, $X_m = (X_{m1}, X_{m2}, \dots, X_{mn})$, where $m = 0, 1, 2, \dots, (2^k - 1)$ is the message associated with the code word. Any two code words X_m and $X_{m'}$ which differ from one another in d_H places and agree in $n - d_H$ places are said to be separated by Hamming distance d_H . The minimum Hamming distance between any two of the 2^k code words in a code is the minimum distance d_{\min} of the code.

A (n, k) binary block code uses a fraction $2^k/2^n = 2^{k-n}$ of all possible output code words. A low-rate code uses a smaller fraction of the possible output words than a high-rate code and code words can therefore be separated further from one another. Thus low-rate codes typically have more error correction capability than high-rate codes.

An important property of block codes is that the symbol-by-symbol modulo-2 sum (\oplus) of any two words is another code word. This implies that the all zeros code word is a code word in block codes. The symbol \oplus represents modulo-2 sum which is equivalent to the logical exclusive-or operation. The rules of modulo-2 addition are: $0 \oplus 0 = 0$, $0 \oplus 1 = 1$, $1 \oplus 0 = 1$, and $1 \oplus 1 = 0$. Consider any two code words X_a

and X_b separated by Hamming distance d_H , and a third arbitrary code word X_c . Let $X_a' = X_a \oplus X_c$ and $X_b' = X_b \oplus X_c$, and notice that the Hamming distance between X_a' and X_b' is also d_H . Using these two properties, it can be demonstrated that the set of Hamming distances between a code word X_m and all other code words $X_{m'}$, $m' \neq m$, in the code is the same for all m . Denote the number of code words which are Hamming distance $d_H = d$ from the all zeros code word by A_d . The weight distribution of the code is the set of all A_d for $d = d_{\min}, \dots, n$ [Ref. 10].

Examples of block codes are Hamming codes, Bose-Chaudhuri-Hocquenghem (BCH) codes, and Reed-Solomon codes.

(1) Hamming Codes. Hamming codes are the first major class of linear block codes invented for error correction. The performance parameters for the Hamming codes are expressed as a function of single integer $m \geq 3$ where code length is $n = 2^m - 1$, number of information symbols is $k = 2^m - m - 1$, number of parity symbols is $n - k = m$, and error correcting capability $t = 1$. Regardless of n and k , all Hamming codes have a minimum distance $d_{\min} = 3$.

(2) BCH Codes. The most commonly used block codes for random error correction are the BCH codes. For block lengths of several hundred, binary BCH codes outperform all other binary block codes having the same block length and code rate. The performance parameters are code length $n = 2^m - 1$, number of parity symbols $n - k \leq mt$, minimum distance $d_{\min} \geq 2t + 1$, and error correcting capability $t \leq (d_{\min} - 1)/2$.

(3) **Reed-Solomon Codes.** Reed-Solomon codes are nonbinary BCH codes. For nonbinary codes, m bits at a time are combined to form a symbol. $M = 2^m$ symbols are required to represent all possible combinations of m bits. The performance parameters are code length $n = m(2^m - 1)$, number of parity symbols $n - k = 2t$, minimum distance $d_{\min} = 2t + 1$, and error correcting capability $t = (d_{\min} - 1)/2$.

b. Convolutional Codes

Convolutional codes offer an approach to error control substantially different from that of block codes. A convolutional encoder converts the entire data stream, regardless of its length, into a single code word.

In convolutional codes, the redundancy can be introduced into a data stream through the use of a linear shift register. A convolutional code is classified as a (n, k, m) code, where n coded bits are generated for every k bits, and m is the memory of the coder. A convolutional code produces n coded bits from k data bits where each set of n coded bits is determined by the k data bits and $v - 1$ and $k(v - 1)$ of the preceding data bits. The parameter v is the constraint length (the maximum number of shifts over a single information bit that can affect the encoder output). The code rate is $R = k/n$, and $1/R$ coded bits are generated for every data bit.

A general convolutional encoder can be implemented with k shift registers and n modulo-2 adders. At each clock, k data bits are multiplexed into the first stage of each of the k shift registers, and the previous data bits are all shifted one stage to the right. The outputs of the n modulo-2 adders are then sampled sequentially to

obtain the coded bits. Typical code rate is $7/8 \geq R \geq 1/4$, and typical constraint length is $9 \geq v \geq 2$ for convolutional codes.

An optimum-decoding algorithm for convolutional codes is the Viterbi algorithm. The Viterbi decoding algorithm is a path maximum-likelihood algorithm that takes advantage of convolutional codes. By path maximum-likelihood decoding we mean that the Viterbi decoder chooses the path, or one of the paths through the trellis (graphical representation of the convolutional codes).

Viterbi decoding algorithms may be implemented using hard or soft decision decoding. In hard-decision decoding, each received signal is examined and a hard decision is made as to whether the signal represents a transmitted zero or a one. For hard-decision decoding, the Viterbi algorithm is a minimum Hamming distance decoder and decodes a convolutional code by choosing a path through the code trellis which yields a code word that differs from the received code word in the fewest possible places. In soft-decision decoding, the receiver takes advantage of side information generated by the receiver bit decision circuitry. Rather than simply assign a zero or a one to each received noisy binary signal, a more flexible approach is taken through the use of multibit quantization. Four or more decision regions are established, ranging from a strong zero decision to a strong one decision. Intermediate values are given to the signals for which the decision is less clear [Ref. 10].

2. Antennas

a. High Gain/ Narrow Beam

Antennas can supply EP using their spatial filtering ability. In the microwave region (1 GHz - 100 GHz), highly directive antennas can be designed that are useful for point-to-point communication systems. These antennas have apparent gains because they concentrate the radiated power in a narrow beam rather than sending it uniformly in all directions. A narrow beamwidth minimizes the effects of interference from outside sources and adjacent antennas.

b. Null Steering Antennas

The side lobe canceller is a classic example of an adaptive antenna system. These systems utilize auxiliary or guard antennas to adaptively generate antenna patterns that provide nulls in the direction of jammers. In theory, a number of side lobe jammers equal to the number of auxiliary antennas can be nulled.

The potential for side lobe cancellation is increased when a phased array is used. An antenna array is formed when two or more antenna elements are combined to form a single antenna. An antenna element is an individual radiator such as a half-wave dipole. The elements are physically placed in such way that their radiation fields interact with each other, producing a total radiation pattern. The purpose of an array is to increase the directivity of an antenna system and concentrate the radiated power within a smaller spatial area.

c. Least Mean Square Algorithm

The least mean square algorithm is the method whereby the reference signal is equal to the desired response of the antenna system. The algorithm updates the new equalizer weights based on the existing weights and a factor depending on the current input samples and the current estimation error. The weights are selected to minimize the mean-square value of the error signal, which is the difference between the antenna output and the reference signal. The main idea is to minimize the total disturbance in the received signal.

d. Maximum SNR Algorithm

Another approach for interference rejection is the maximum SNR algorithm. Using an appropriately defined SNR, we can find the optimum set of weights for individual antennas to maximize this ratio. An antenna system based on these weights produces $K-1$ nulls (with K antenna elements) directed toward $K-1$ interfering transmitters spaced reasonably apart. In this approach, use is made of known direction from the signal transmitter. By maximizing the signal-to-noise ratio in the received signal we can minimize the effects of interference.

VIII. SIMULATION

A. INTRODUCTION

In the simulation of communication systems, there are two options for implementing the simulation, namely passband and baseband. In passband simulations, the carrier signal is included in the simulation model. By the Nyquist sampling theorem, the simulation sampling frequency must be greater than twice the highest frequency. Since the frequency of the carrier is usually much greater than the highest frequency of the input message signal, a passband simulation requires a very large number of samples and excessive simulation time. The simulation time can be dramatically reduced by using baseband-equivalent simulation. A baseband-equivalent model uses complex envelopes to reduce the simulation sampling rate and thus speeds up the simulation. The complex envelope is a complex function of time that carries information about both time-varying amplitude and the time-varying phase of a passband signal.

A passband signal can be expressed as

$$s(t) = A(t) \cos[2\pi f_c t + \phi(t)] \quad (8.1)$$

or,

$$s(t) = \text{Re}\{A(t)e^{j\phi(t)}e^{j2\pi f_c t}\} \quad (8.2)$$

where $A(t)$ is the envelope, f_c is the carrier frequency, and $\phi(t)$ is the phase of $s(t)$.

The corresponding baseband signal can be defined as

$$\tilde{s}(t) = A(t)e^{j\phi(t)} . \quad (8.3)$$

B. SIMULINK MODEL AND BLOCK ANALYSIS

Figure 8.1 shows the Simulink model that used for the simulation.

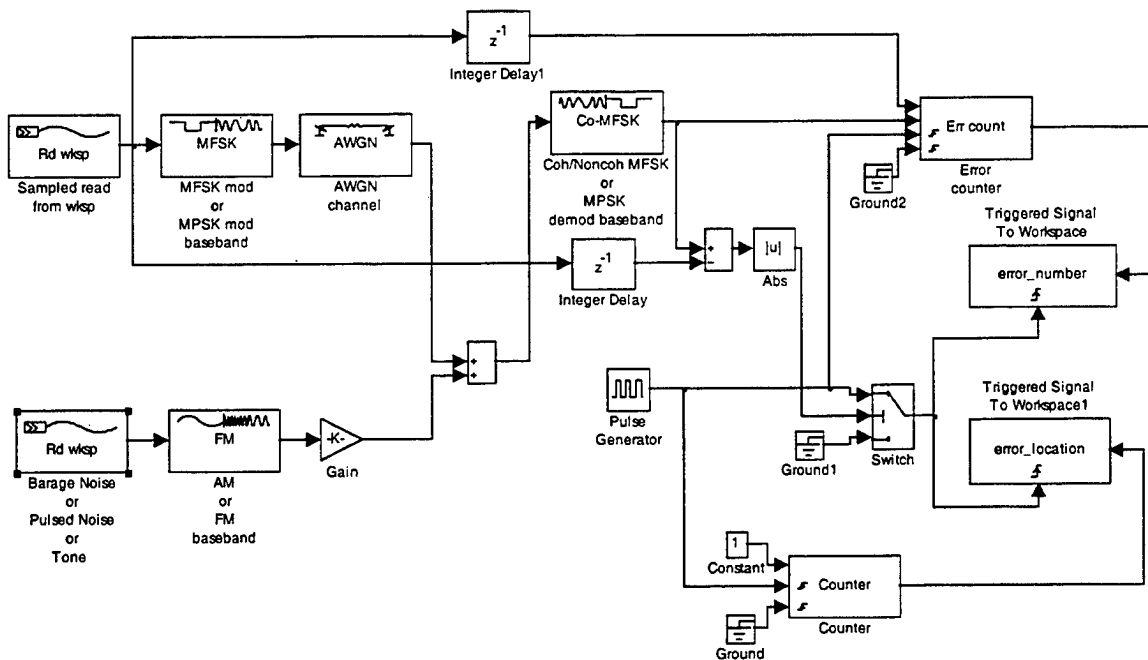


Figure 8.1 Simulink Model Used for the Simulation

The simulation model used in this study has the following main functional blocks: MFSK modulation and coherent and noncoherent MFSK demodulation blocks; MPSK modulation and MPSK demodulation blocks; AM modulation block; FM modulation block; Sampled Read from Workspace; Barrage Noise Jamming Block; Pulsed Noise

Jamming Block; Tone Jamming Block; AWGN channel; K-step Delay; Error Counter; Triggered Signal to Write Workspace; Pulse Generator; and Symbol Counter. In addition to these main blocks, auxiliary blocks such as sum, absolute value, gain, constant, ground, and switch are used.

The *MFSK Baseband Modulation Block* outputs the complex envelope of a MFSK modulated signal. The output is a unit-amplitude FSK modulated analog signal. The inputs are integers in the range $[0, M-1]$, where M is the M-ary number. The following four parameters must be defined for this block: Tone space (Δf = the frequency distance between two successive frequencies), symbol interval (T_s), initial phase, and sample frequency (f_{sampling}).

The *Coherent MFSK Baseband Demodulation Block* demodulates the input, which is a modulated complex analog signal. The output signals are digits in the range $[0, M-1]$. Five parameters define this block: M-ary number, tone space (Δf), symbol interval (T_s), initial phase and sample time ($\Delta t = 1/f_{\text{sampling}}$). The parameters mentioned above must match the ones used in the corresponding MFSK Baseband Modulation Block.

The *Noncoherent MFSK Baseband Demodulation Block* demodulates the complex envelope of a MFSK modulated signal using a noncoherent method. The output signals are digits in the range $[0, M-1]$. The following four parameters must be defined for this block: M-ary number, tone space (Δf), symbol interval (T_s), initial phase, and sample time (Δt). The parameters mentioned above must match the ones used in the corresponding MFSK Baseband Modulation Block.

The *MPSK Baseband Modulation Block* outputs the complex envelope of MPSK modulated signal. The inputs are integers in the range $[0, M-1]$, where M is the M-ary number. Three parameters define this block: M-ary number (2 for BPSK, 4 for QPSK), symbol interval (T_s), and initial phase.

The *MPSK Baseband Demodulation Block* outputs the complex envelope of a MPSK modulated signal using correlation method. The output signals are digits in the range $[0, M-1]$. Four parameters define this block: M-ary number (2 for BPSK), symbol interval (T_s), initial phase, and sample time (Δt).

The *AM Modulation Block* causes the amplitude of the sinusoid carrier to depend on the message signal. An offset is added to the input signal before modulation. The output of this block is a complex signal.

The *FM Modulation Block* outputs the complex envelope of the frequency-modulated signal, a complex signal. This block resets the phase at the very beginning of the symbol interval.

The *Sampled Read from Workspace Block* reads a row of data for a workspace variable at every data sampling point. If the workspace variable is a matrix, the size of the block output vector corresponds to the number of columns in the matrix. If the "cyclic repeat" box is checked, after reading the last row of the variable the block will return to the first row of the variable. Otherwise, the block will output zeros after reading the last row of the variable. The following two parameters must be defined for this block: Signal source and data output sample time (T_s).

The *Barrage Noise Jamming Block*, the *Pulsed Noise Jamming Block*, and the *Tone Jamming Block* are created by using the *Sampled Read from Workspace Block*. With this method signals other than the “canned” or standard signals within SIMULINK can be generated.

The *Barrage Noise Jamming Block* is created by using Weibull function of the statistics toolbox. Weibull is a distribution that delivers noise with a distribution different than Gaussian as shown in the top part of Figure 8.2. Preliminary simulation results indicated that Weibull Noise might be more detrimental to communication signals than Gaussian. Further simulations revealed that values of $A=2$ and $B=2$ were the most damaging. A vector of $R = \text{weibrnd}(A, B)$ generates Weibull random numbers from the Weibull distribution with parameters A and B which control the mean, variance, and shape of the distribution. The bottom part of Figure 8.2 shows the power spectral density (PSD) of the noise modulated carrier as compared to the carrier alone. This shows the two sidebands are white with infinite bandwidth.

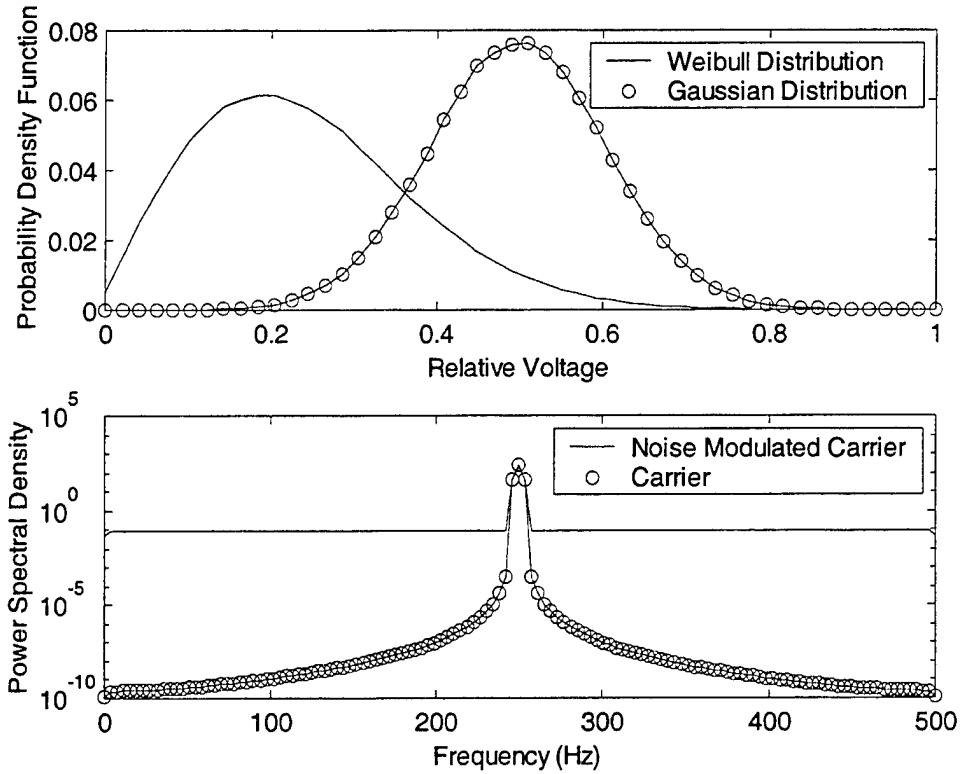


Figure 8.2 The Top Part is the Pdfs of Weibull and Gaussian Distributions. The Bottom Part is the PSDs of the Noise Modulated Carrier and the Carrier Alone

The *Pulsed Noise Jamming Block* is created by a sine wave whose amplitude is Rayleigh distributed (a matrix of $R = \text{raylrm}(B)$ returns a matrix of random numbers chosen from the Rayleigh distribution with parameter B), and phase is uniformly distributed between 0 and 2π .

The *Tone Jamming Block* is created by a sine wave whose phase is Rayleigh distributed.

The variances of the input signal and the jamming signal, and the output signal-to-jamming ratios are tabulated in Table 8.1 and Table 8.2 for input SJR of 4.5 dB. The output signal-to-jamming ratios, which are very close to the input signal-to-jamming ratios, validate the Simulink model that designed for the simulation.

Digital Mod. Tech. \ Jamming Type	AM by Weibull Noise Jamming			AM-Modulated Pulsed Noise Jamming			AM-Modulated Tone Jamming		
	Input Signal Var.	Jam. Signal Var.	Output SJR	Input Signal Var.	Jam. Signal Var.	Output SJR	Input Signal Var.	Jam. Signal Var.	Output SJR
Coherent BFSK	1.10	0.41	4.30	1.20	0.43	4.50	1.23	0.45	4.40
Noncoherent BFSK	0.99	0.38	4.20	1.05	0.39	4.30	1.10	0.40	4.44
BPSK	1.12	0.40	4.47	1.24	0.45	4.44	1.13	0.42	4.30
QPSK	0.98	0.35	0.46	0.999	0.37	4.30	0.99	0.36	4.39

Table 8.1 The Variances of the Input Signal and the Jamming Signal, and the Signal-to-Jamming ratio (SJR) for Input SJR of 4.5 dB.

Digital Mod. Tech. \ Jamming Type	FM by Weibull Noise Jamming			FM-Modulated Pulsed Noise Jamming			FM-Modulated Tone Jamming		
	Input Signal Var.	Jam. Signal Var.	Output SJR	Input Signal Var.	Jam. Signal Var.	Output SJR	Input Signal Var.	Jam. Signal Var.	Output SJR
Coherent BFSK	0.99	0.38	4.20	0.98	0.36	4.30	0.95	0.34	4.46
Noncoherent BFSK	1.08	0.40	4.30	1.18	0.43	4.40	0.999	0.38	4.20
BPSK	1.10	0.39	4.50	0.99	0.36	4.40	1.05	0.40	4.20
QPSK	0.98	0.34	4.47	0.97	0.37	4.20	0.99	0.36	4.40

Table 8.2 The Variances of the Input Signal and the Jamming Signal, and the Signal-to-Jamming ratio (SJR) for Input SJR of 4.5 dB.

The *AWGN Channel Block* adds white Gaussian noise to a real or complex input signal. When the input signal is real, this block adds real Gaussian noise and produces a real output signal. When the input signal is complex, this block adds complex Gaussian noise and produces a complex output signal. This block inherits its sample time from the input signal, and uses the DSP Blockset's Random Source block to generate the noise. The vector length N for the initial seed entry determines the output vector size. The initial seed parameter in this block seeds the noise generator. The initial seed can be either a scalar or a vector whose length matches the number of channels parameter. The mean and the variance of the noise are specified such that the mean can be either a vector of length equal to the seed length N or a scalar, in which case all the elements of the noise vector share the same mean value.

The *K-step Delay Block* delays its input by the number of sample intervals specified in the delay in samples parameter.

The *Error Counter Block* detects the difference between the first and the second ports signals at the times of the rising edge of the third port. If the signals at the first and second port do not match at the rising edge of the third port pulse, the counter increases by one. The rising edge of the fourth port resets the counter to zero.

The *Triggered Signal to Write Workspace Block* creates a matrix variable in the workspace, where it stores the acquired inputs at the end of a simulation. Each row of the workspace matrix represents an input sample, with the most recent sample occupying the last row. The maximum size of this variable is limited to the size specified by the maximum number of rows P parameter. If the simulation progresses long enough for the block to trigger more than P times, it stores only the last P samples. The decimation

factor parameter D allows storage of only every D th sample. The block acquires and buffers a single sample from input 1 whenever it is triggered by the control signal at input two. At all other times, the block ignores input one. The triggering event at input two is specified by the trigger type pop-up menu, and can be one of the following: Rising edge triggers execution of the block when the trigger input rises from a negative value to zero or a positive value, or from zero to a positive value. A falling edge triggers execution of the block when the trigger input falls from a positive value to zero or a negative value, or from zero to a negative value. Either edge triggers execution of the block when either a rising or falling edge (as described above) occurs.

The *Pulse Generator Block* generates a series of pulses at regular intervals. Four parameters define this block: Period (the pulse period in seconds), duty cycle (the percentage of the pulse period that the signal is on), amplitude, start time (the delay before the pulse is generated, in seconds).

The *Symbol Counter Block* counts the number of symbols. There are three input ports to the counter block. If the signal at the first port is larger than or equal to the given threshold at the rising edge of the second port, the counter increases by one. The rising edge of the third port resets the counter to zero.

The *Sum Block* adds scalar and/or vector inputs, or elements of a single vector input, depending on the number of block inputs. It accepts real or complex-valued signals of any data type. All the inputs must be of the same data type. The output data type is the same as the input data type.

The *Absolute Value Block* generates as output the absolute value of the input. It accepts a real or complex-valued input and generates a real output.

The *Gain Block* generates its output by multiplying its input by a specified constant, variable, or expression. You can enter the gain as a numeric value, or as a variable or expression.

The *Constant Block* generates one output, which can be scalar or vector, depending on the length of the constant value parameter.

The *Ground Block* can be used to connect blocks whose input ports are not connected to other blocks. It outputs a signal with zero value. The data type of the signal is the same as that of the port to which it is connected.

The *Switch Block* propagates one of two inputs to its output depending on the value of a third input, called the control input. If the signal on the control (second) input is greater than or equal to the threshold parameter, the block propagates the first input; otherwise, it propagates the third input.

C. PERFORMANCE OF DIGITAL COMMUNICATION SYSTEMS WITH BARRAGE NOISE JAMMING

1. Performance of Coherent BFSK with Barrage Noise Jamming

a. AM by Weibull Noise

Figure 8.3 shows the Simulink model for coherent BFSK with AM by Weibull Noise jamming. The simulation model and the blocks used in this study are explained above.

The AM by Weibull Noise jamming is created by first generating a baseband Weibull noise signal. The bandwidth of this noise signal is much greater than that of the message signal. This baseband signal is used to AM modulate the carrier at

100% modulation index. This barrage noise is then shifted using complex amplitude to baseband for analysis.

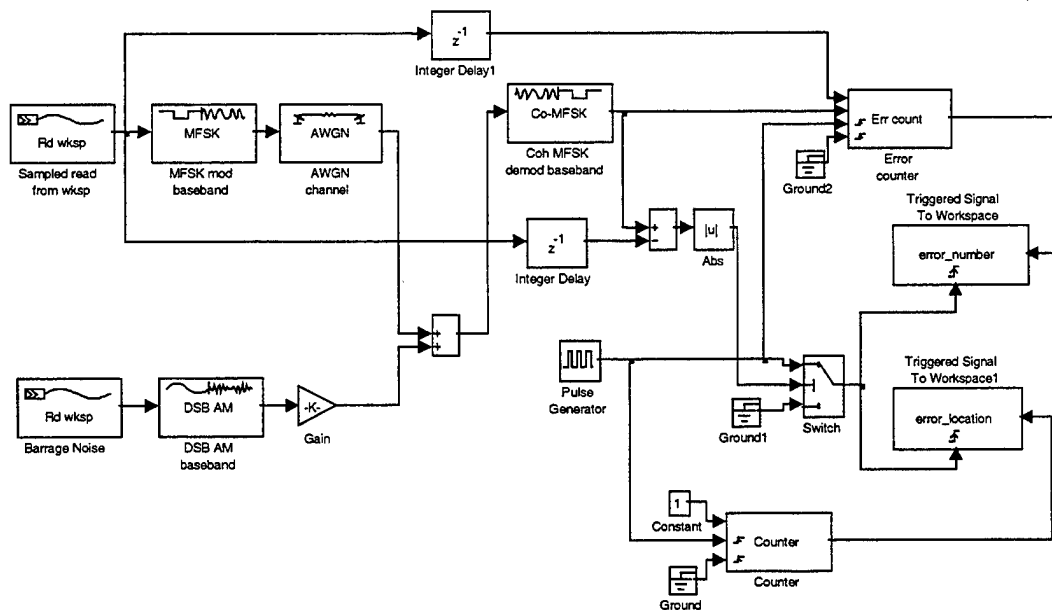


Figure 8.3 Simulink Model for Coherent BFSK with AM by Weibull Noise

The bit error rate (BER) for coherent BFSK with AM by Weibull Noise jamming as a function of the signal-to-noise ratio (SNR), with the signal-to-jamming ratio (SJR) as parameter, is shown in Figure 8.4 (a). The BER increases as SNR decreases. The selected range for SNR was from -5 dB to $+15$ dB, and the selected range for SJR was from -5 dB to $+12$ dB. The solid line is the probability of bit error for coherent BFSK without jamming.

The BER for coherent BFSK with AM-modulated AWGN jamming as a function of the SNR, with the SJR as parameter, is shown in Figure 8.4 (b). The solid line is the probability of bit error for coherent BFSK without jamming.

In Chapter VI it was shown that the presence of the barrage noise jammer increases the noise power spectral density of AWGN from N_0 to $(N_0 + J_0)$ where J_0 is the noise power spectral density due to the barrage noise jamming. We note the dramatic increase in the BER due to AM by Weibull Noise jamming, relative to AM-modulated AWGN jamming.

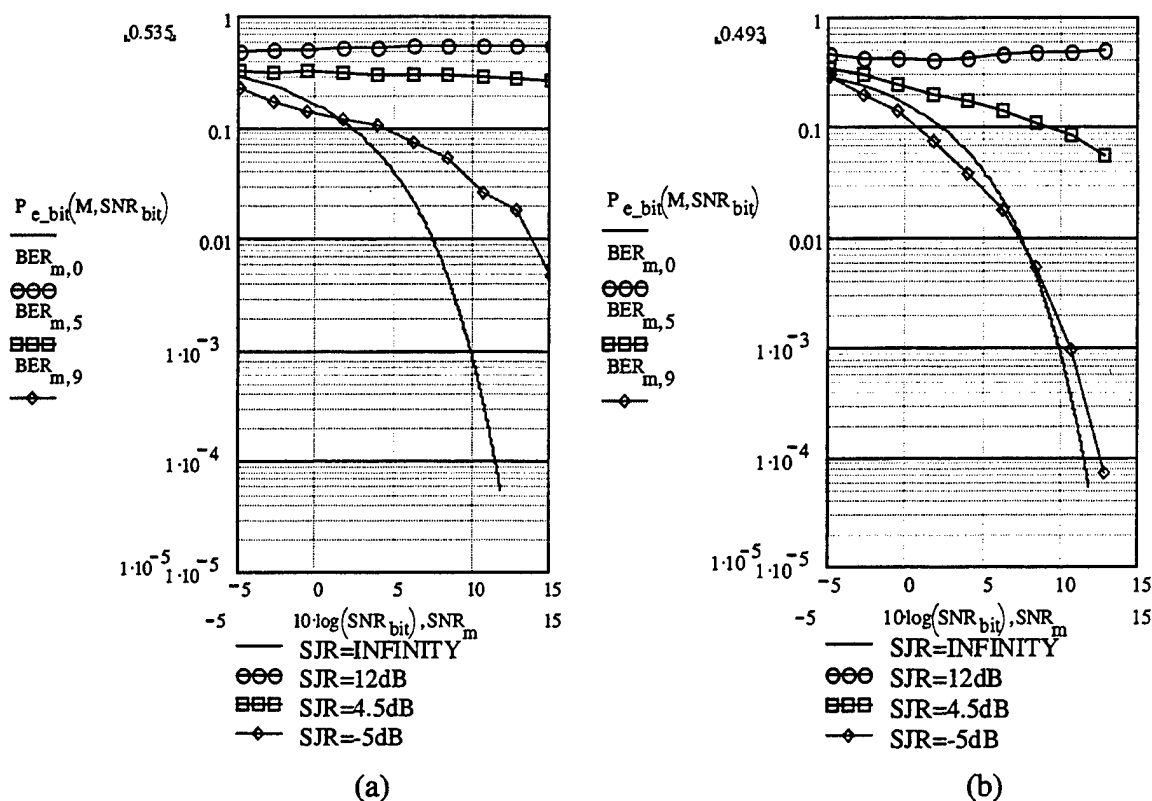


Figure 8.4 (a) The BER for coherent BFSK with AM by Weibull Noise jamming as a function of the SNR (b) The BER for coherent BFSK with AM-modulated AWGN jamming as a function of the SNR

b. FM by Weibull Noise

Figure 8.5 shows the Simulink model for coherent BFSK with FM by Weibull Noise jamming.

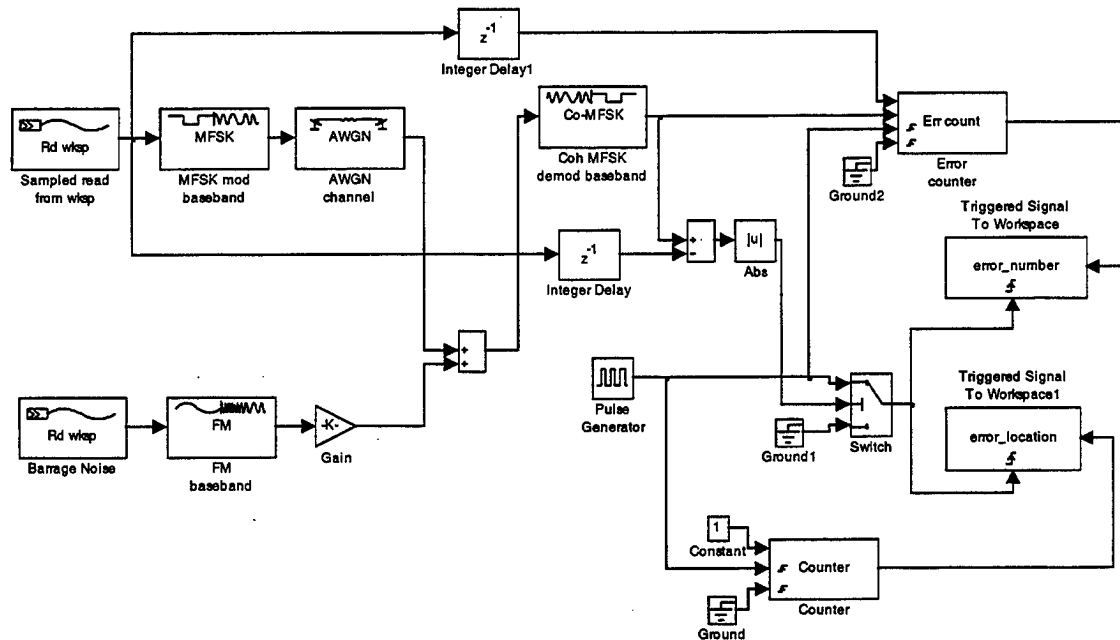


Figure 8.5 Simulink Model for Coherent BFSK with AM by Weibull Noise

The barrage noise signal begins with a baseband Weibull noise signal whose bandwidth is much greater than that of the message signal. This baseband signal is used to FM modulate the carrier using a modulation index of 1 Hertz per volt. Using Carson's Rule the modulated resulting bandwidth is more than twice that of the original broadband noise signal. This FM-modulated signal is then shifted to baseband using complex envelope.

The bit error rate (BER) for coherent BFSK with FM by Weibull Noise jamming as a function of the signal-to-noise ratio (SNR), with the signal-to-jamming

ratio (SJR) as parameter, is shown in Figure 8.6 (a). The BER increases as SNR decreases. The selected range for SNR was from -5 dB to $+15$ dB, and the selected range for SJR was from -5 dB to $+12$ dB. The solid line is the probability of bit error for coherent BFSK without jamming.

The BER for coherent BFSK with FM-modulated AWGN jamming as a function of the SNR, with the SJR as parameter, is shown in Figure 8.6 (b). The solid line is the probability of bit error for coherent BFSK without jamming.

We observe the dramatic increase in the BER due to FM by Weibull Noise jamming, relative to FM-modulated AWGN jamming.

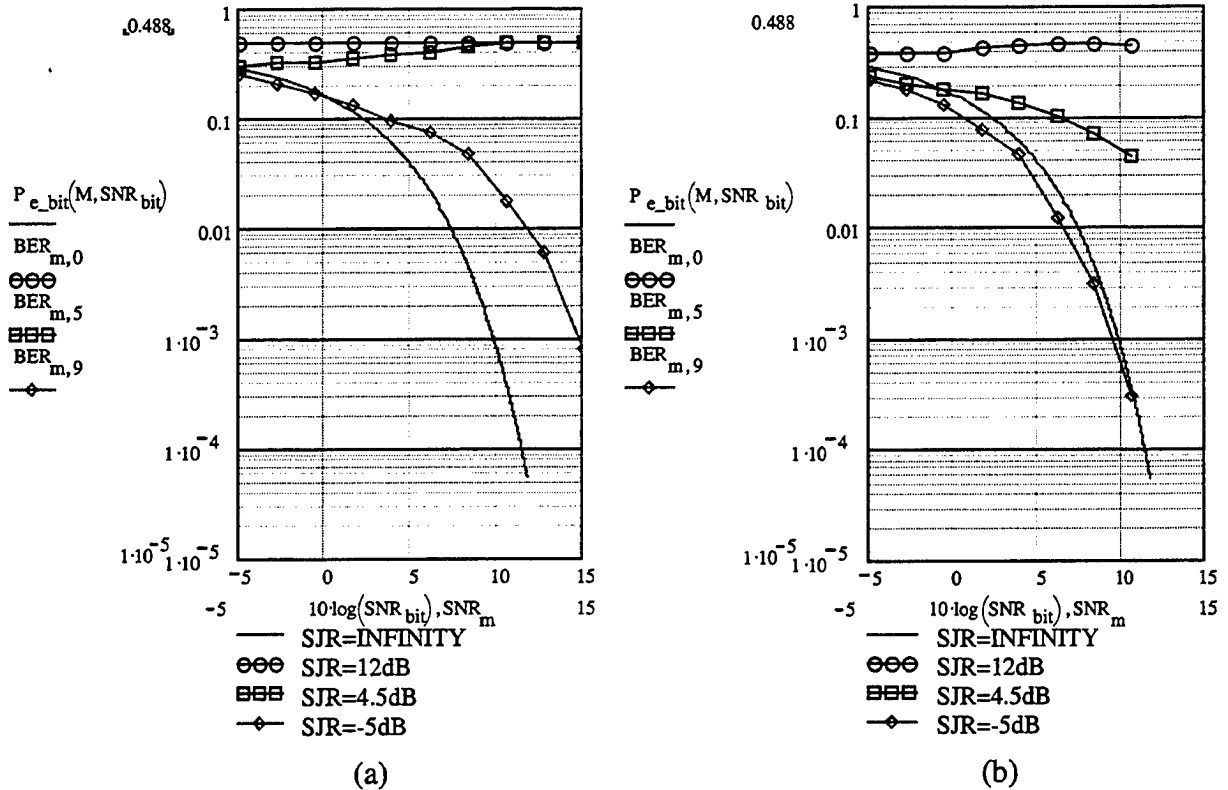


Figure 8.6 (a) The BER for coherent BFSK with FM by Weibull Noise jamming as a function of the SNR (b) The BER for coherent BFSK with FM-modulated AWGN jamming as a function of the SNR

2. Performance of Noncoherent BFSK with Barrage Noise Jamming

a. AM by Weibull Noise

Figure 8.7 shows the Simulink model for noncoherent BFSK with AM by Weibull Noise jamming.

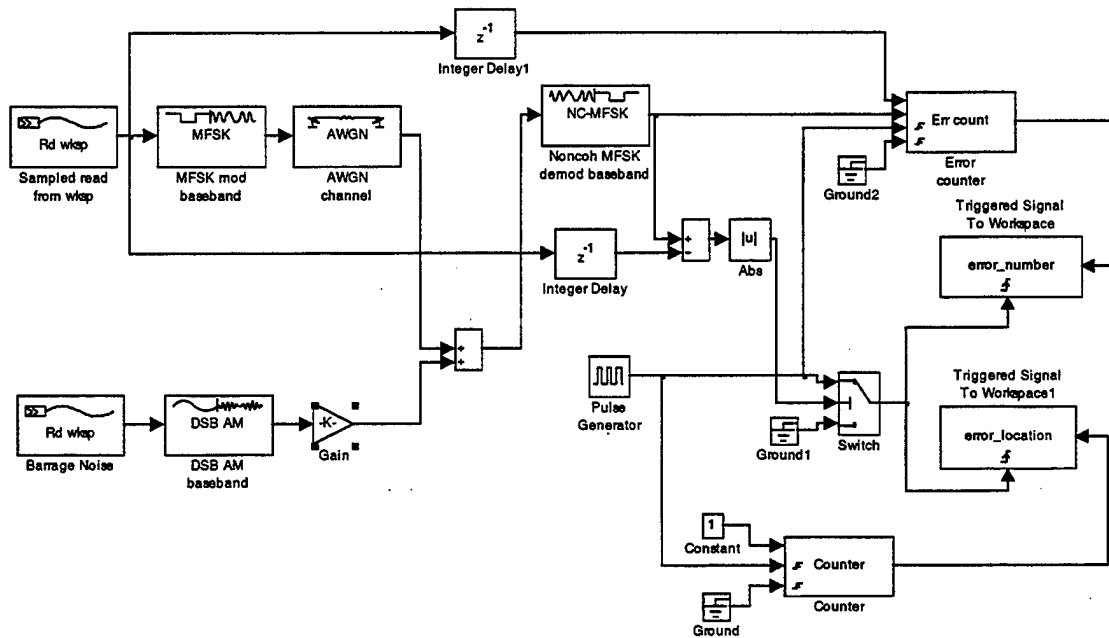
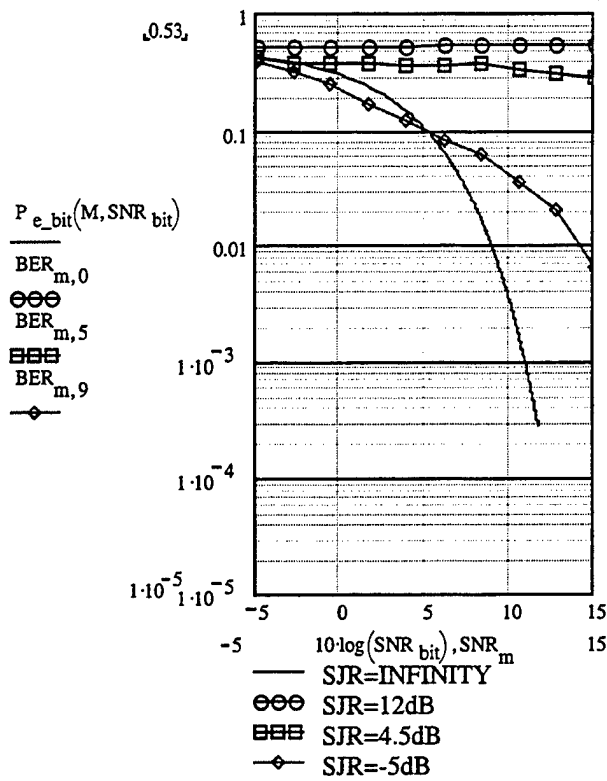


Figure 8.7 Simulink Model for Noncoherent BFSK with AM by Weibull Noise

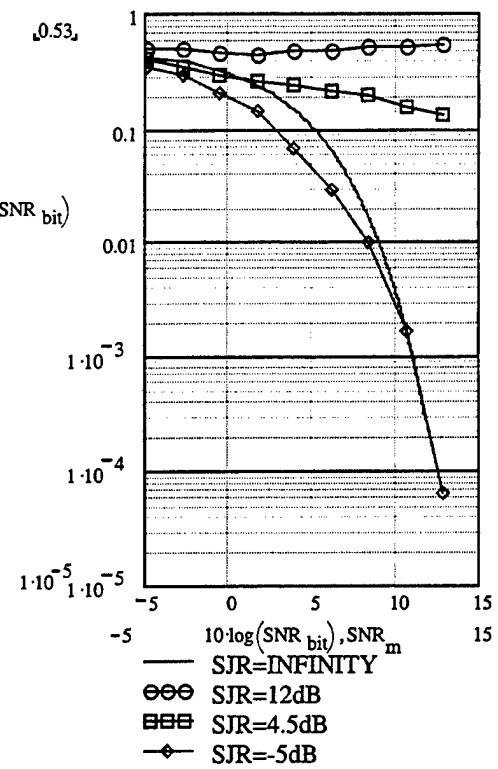
The bit error rate (BER) for noncoherent BFSK with AM by Weibull Noise jamming as a function of the signal-to-noise ratio (SNR), with the signal-to-jamming ratio (SJR) as parameter, is shown in Figure 8.8 (a). The BER increases as SNR decreases. The selected range for SNR was from -5 dB to $+15$ dB, and the selected range for SJR was from -5 dB to $+12$ dB. The solid line is the probability of bit error for noncoherent BFSK without jamming.

The BER for noncoherent BFSK with AM- modulated AWGN jamming as a function of the SNR, with the SJR as parameter, is shown in Figure 8.8 (b). The solid line is the probability of bit error for noncoherent BFSK without jamming.

We note the change in the BER due to AM by Weibull Noise jamming, relative to AM-modulated AWGN jamming.



(a)



(b)

Figure 8.8 (a) The BER for noncoherent BFSK with AM by Weibull Noise jamming as a function of the SNR (b) The BER for noncoherent BFSK with AM- modulated AWGN jamming as a function of the SNR

b. FM by Weibull Noise

Figure 8.9 shows the Simulink model for noncoherent BFSK with FM by Weibull Noise jamming.

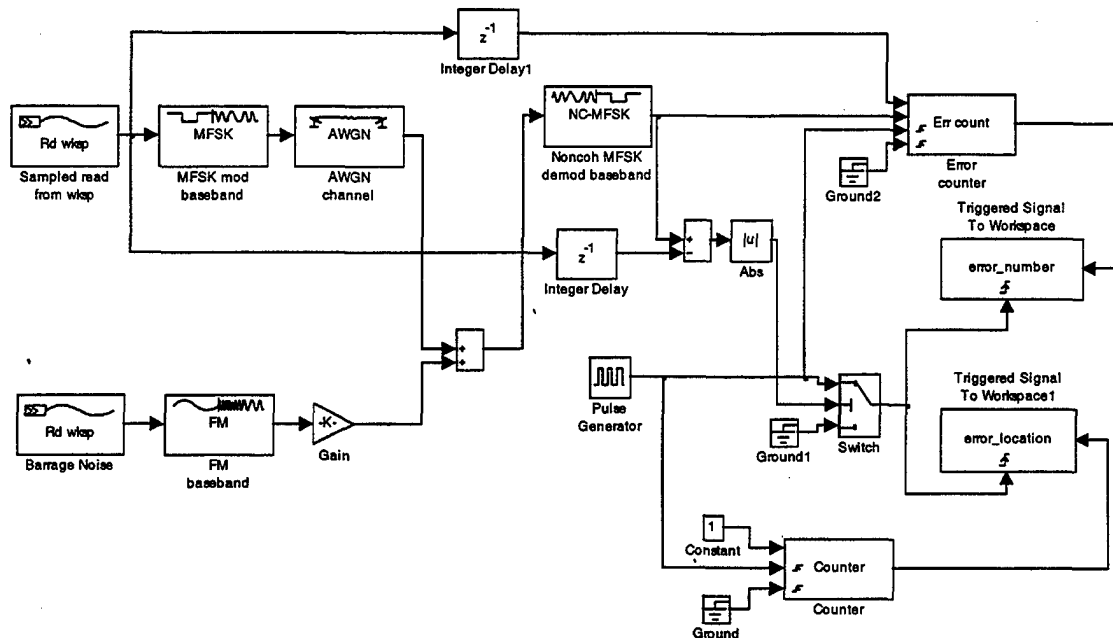
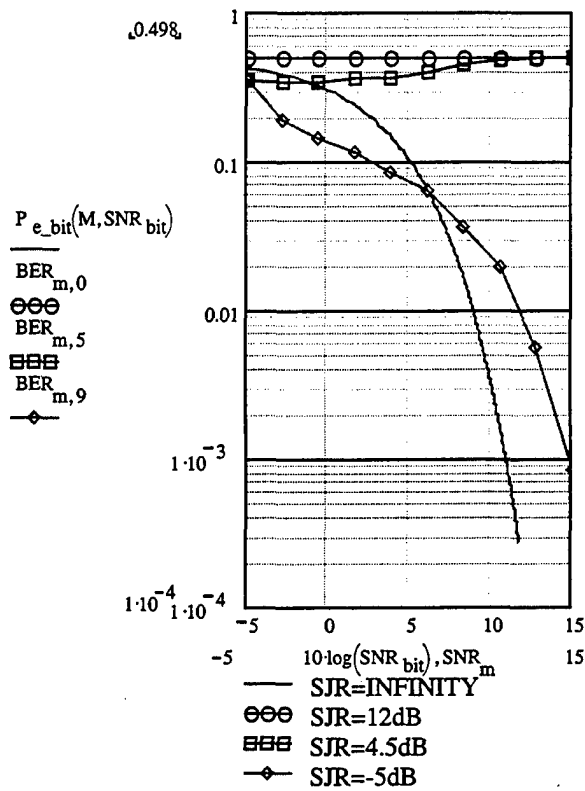


Figure 8.9 Simulink Model for Noncoherent BFSK with FM by Weibull Noise

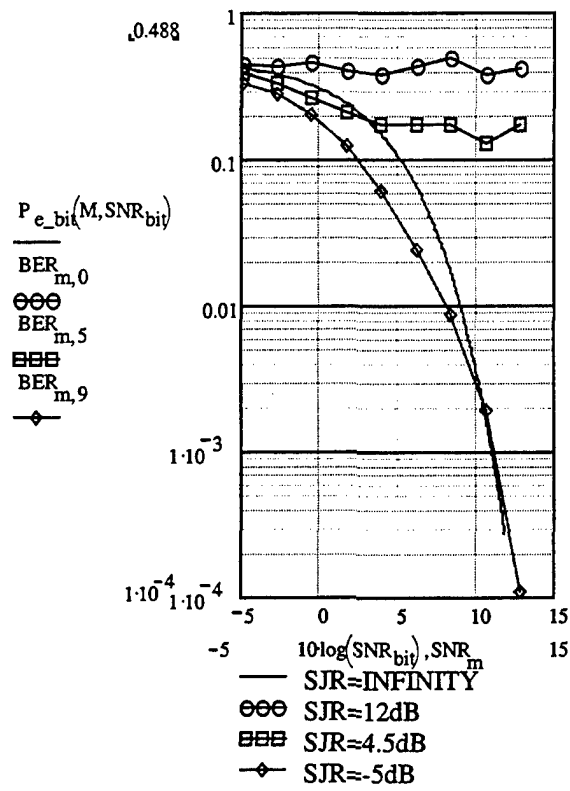
The bit error rate (BER) for noncoherent BFSK with FM by Weibull Noise jamming as a function of the signal-to-noise ratio (SNR), with the signal-to-jamming ratio (SJR) as parameter, is shown in Figure 8.10 (a). The BER increases as SNR decreases. The selected range for SNR was from -5 dB to +15 dB, and the selected range for SJR was from -5 dB to +12 dB. The solid line is the probability of bit error for noncoherent BFSK without jamming.

The BER for noncoherent BFSK with FM- modulated AWGN jamming as a function of the SNR, with the SJR as parameter, is shown in Figure 8.10 (b). The solid line is the probability of bit error for noncoherent BFSK without jamming.

We observe the change in the BER due to FM by Weibull Noise jamming, relative to FM-modulated AWGN jamming.



(a)



(b)

Figure 8.10 (a) The BER for noncoherent BFSK with FM by Weibull Noise jamming as a function of the SNR (b) The BER for noncoherent BFSK with FM- modulated AWGN jamming as a function of the SNR

3. Performance of BPSK with Barrage Noise Jamming

a. AM by Weibull Noise

Figure 8.11 shows the Simulink model for BPSK with AM by Weibull Noise jamming.

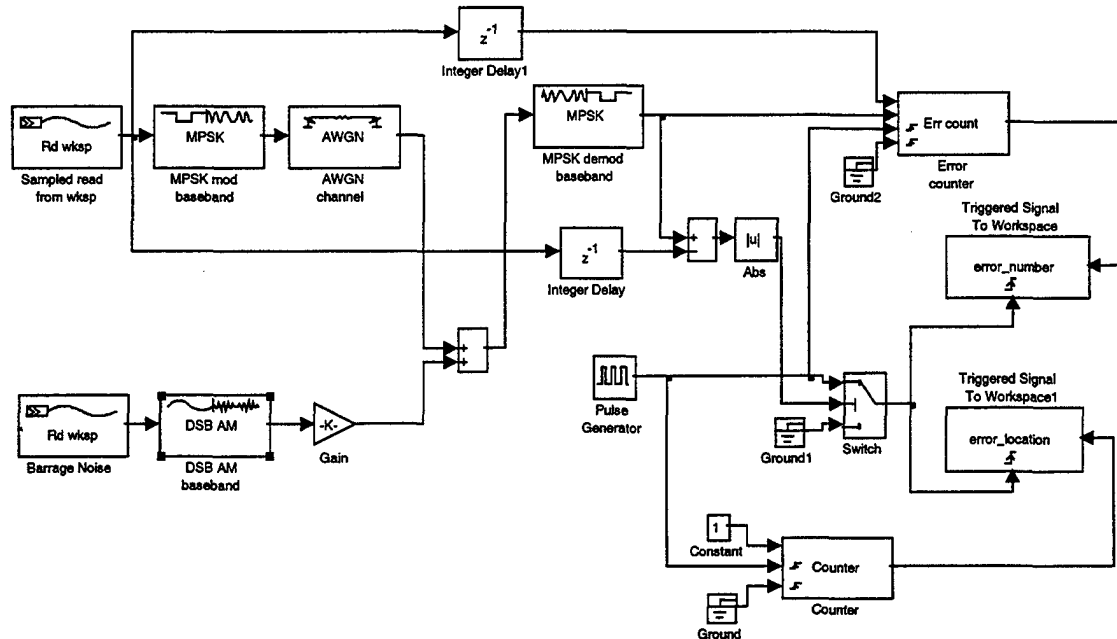


Figure 8.11 Simulink Model for BPSK with AM by Weibull Noise Jamming

The bit error rate (BER) for BPSK with AM by Weibull Noise jamming as a function of the signal-to-noise ratio (SNR), with the signal-to-jamming ratio (SJR) as parameter, is shown in Figure 8.12 (a). The BER increases as SNR decreases. The selected ranges for SNR and SJR were from -5 dB to $+12$ dB. The solid line is the probability of bit error for BPSK without jamming.

The BER for BPSK with AM-modulated AWGN jamming as a function of the SNR, with the SJR as parameter, is shown in Figure 8.12 (b). The solid line is the probability of bit error for BPSK without jamming.

We note the increase in the BER due to AM by Weibull Noise jamming, relative to AM-modulated AWGN jamming.

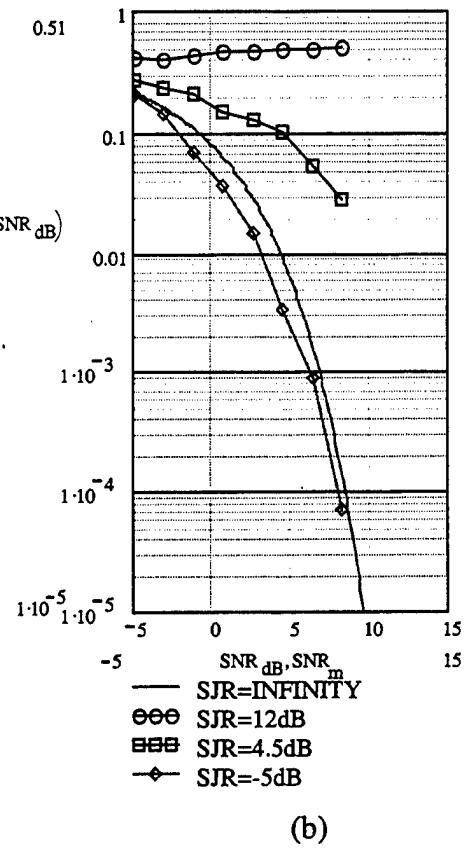
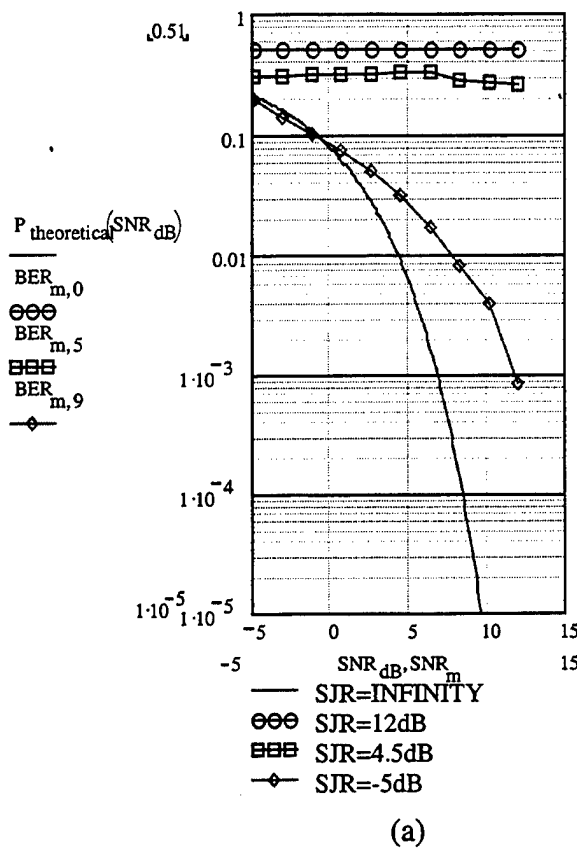


Figure 8.12 (a) The BER for BPSK with AM by Weibull Noise jamming as a function of the SNR (b) The BER for BPSK with AM-modulated AWGN jamming as a function of the SNR

b. FM by Weibull Noise

Figure 8.13 shows the Simulink model for BPSK with FM by Weibull Noise jamming.

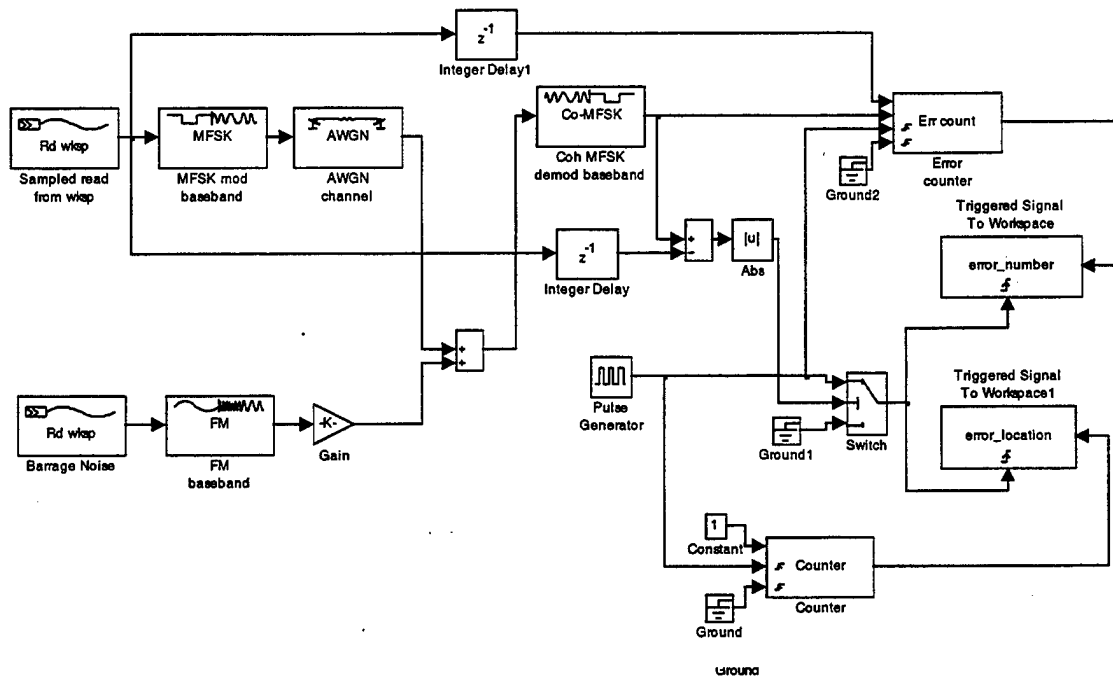
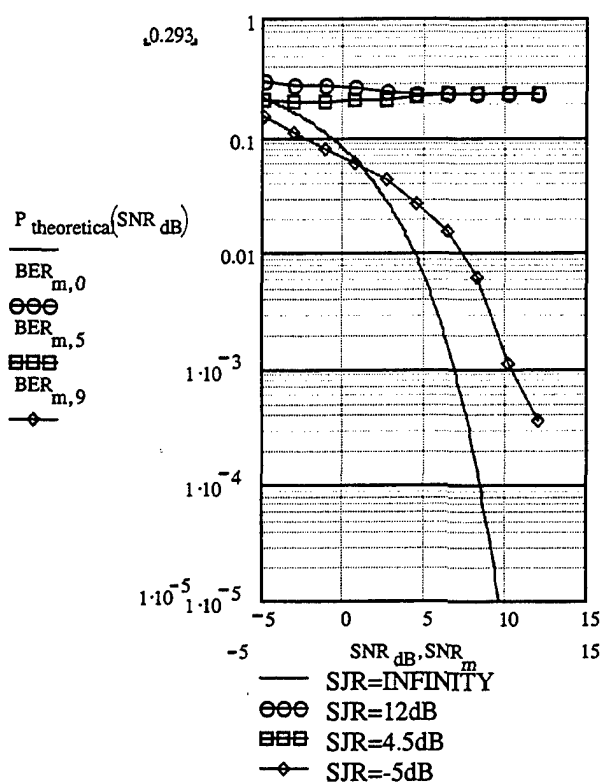


Figure 8.13 Simulink Model for BPSK with FM by Weibull Noise Jamming

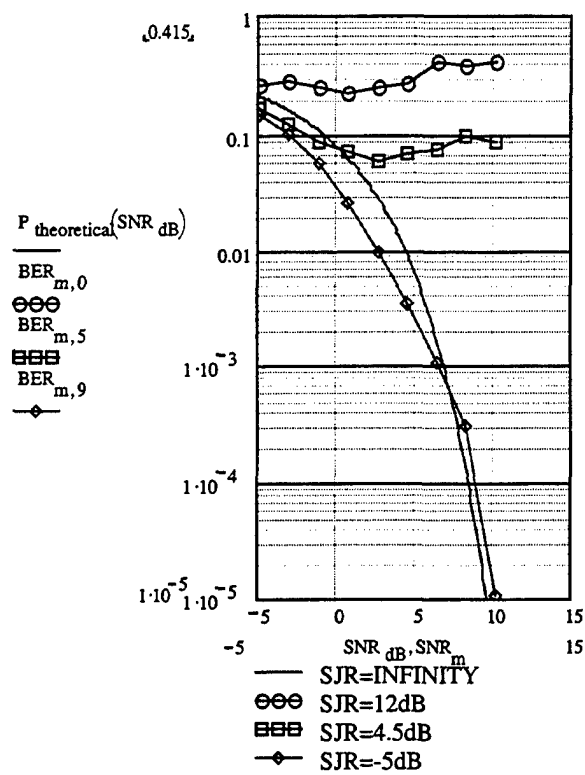
The bit error rate (BER) for BPSK with FM by Weibull Noise jamming as a function of the signal-to-noise ratio (SNR), with the signal-to-jamming ratio (SJR) as parameter, is shown in Figure 8.14 (a). The BER increases as SNR decreases. The selected ranges for SNR and SJR were from -5 dB to $+12$ dB. The solid line is the probability of bit error for BPSK without jamming.

The BER for BPSK with FM-modulated AWGN jamming as a function of the SNR, with the SJR as parameter, is shown in Figure 8.14 (b). The solid line is the probability of bit error for BPSK without jamming.

We observe the change in the BER due to FM by Weibull Noise jamming, relative to FM-modulated AWGN jamming.



(a)



(b)

Figure 8.14 (a) The BER for BPSK with FM by Weibull Noise jamming as a function of the SNR (b) The BER for BPSK with FM-modulated AWGN jamming as a function of the SNR

4. Performance of QPSK with Barrage Noise Jamming

a. AM by Weibull Noise

Figure 8.15 shows the Simulink model for QPSK with AM by Weibull Noise jamming.

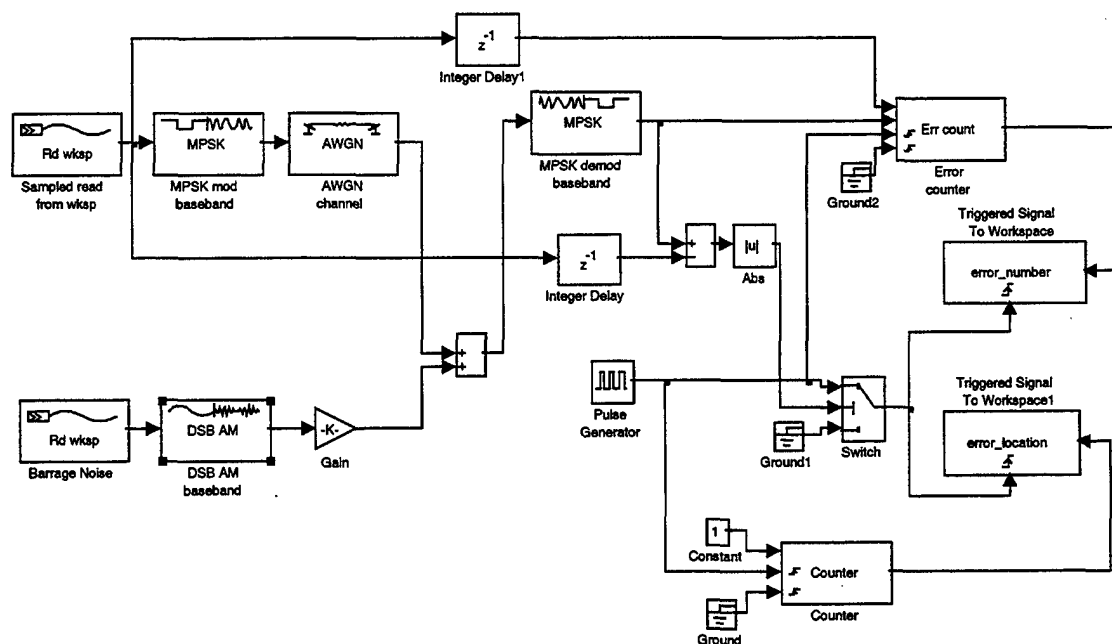


Figure 8.15 Simulink Model for QPSK with AM by Weibull Noise Jamming

The bit error rate (BER) for QPSK with AM by Weibull Noise jamming as a function of the signal-to-noise ratio (SNR), with the signal-to-jamming ratio (SJR) as parameter, is shown in Figure 8.16 (a). The BER increases as SNR decreases. The selected ranges for SNR and SJR were from -5 dB to $+12$ dB. The solid line is the probability of bit error for QPSK without jamming.

The BER for QPSK with AM-modulated AWGN jamming as a function of the SNR, with the SJR as parameter, is shown in Figure 8.16 (b). The solid line is the probability of bit error for QPSK without jamming.

We note the dramatic increase in the BER due AM by Weibull Noise jamming, relative to AM-modulated AWGN jamming.

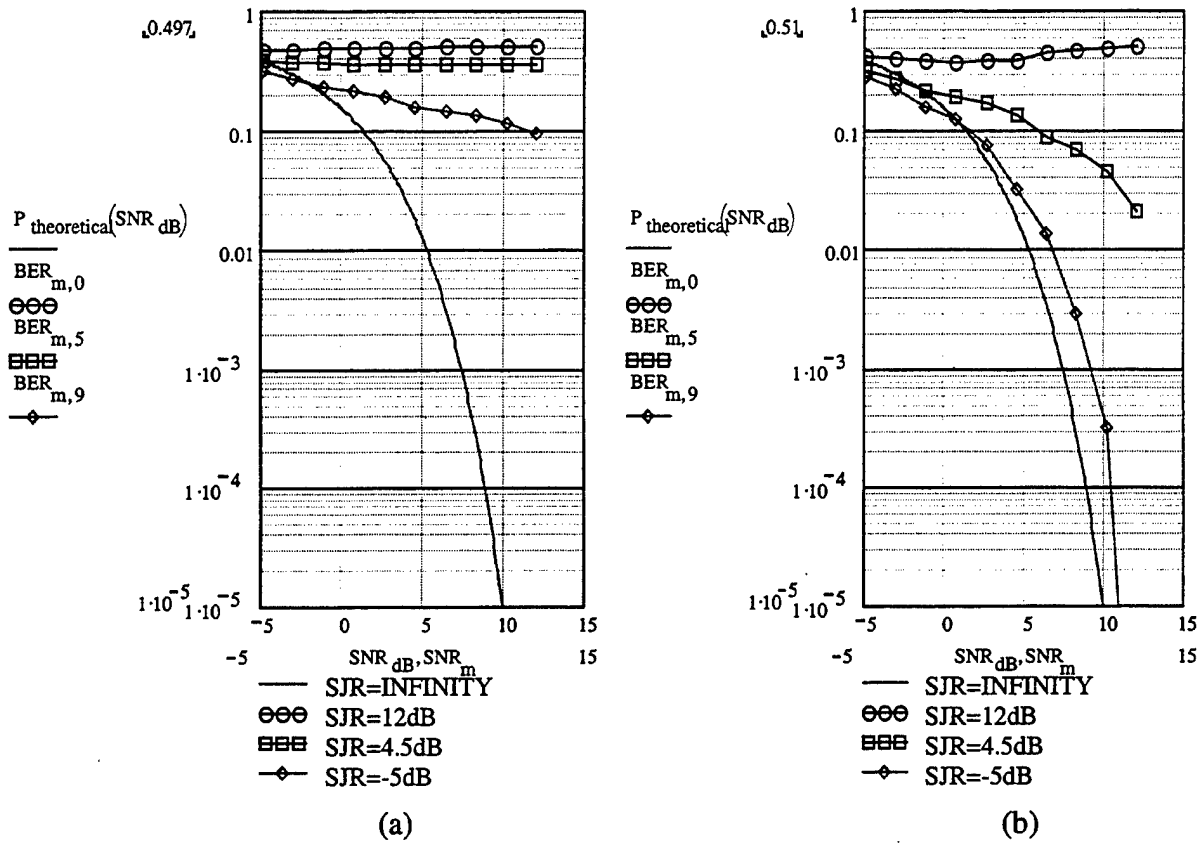


Figure 8.16 (a) The BER for QPSK with AM by Weibull Noise jamming as a function of the SNR (b) The BER for QPSK with AM-modulated AWGN jamming as a function of the SNR

b. FM by Weibull Noise

Figure 8.17 shows the Simulink model for QPSK with FM by Weibull Noise jamming.

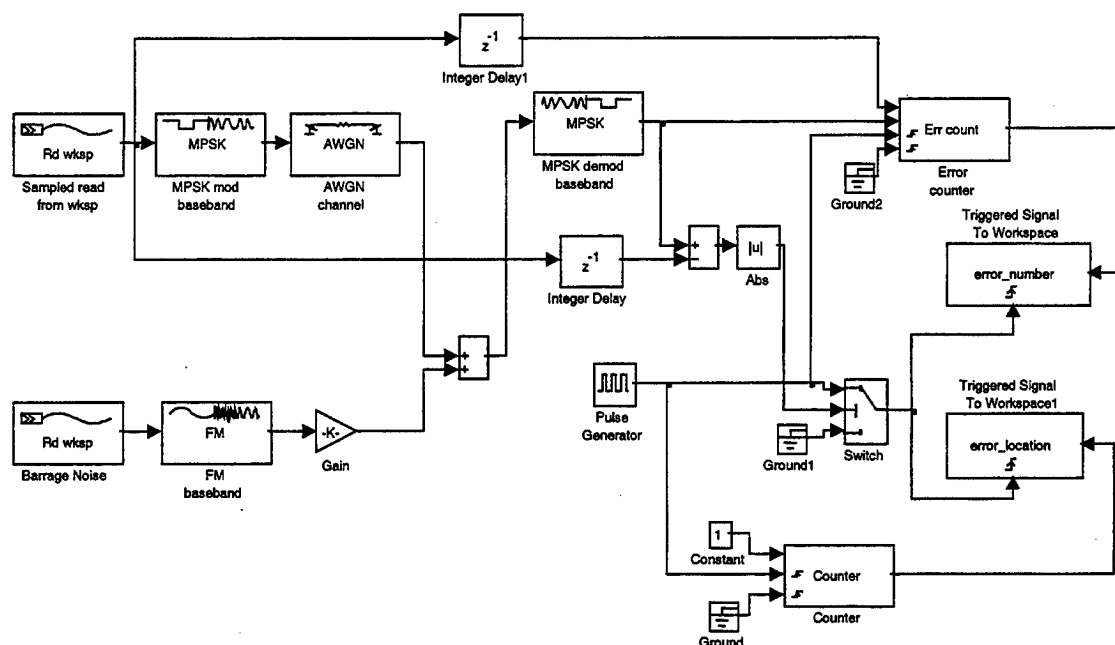
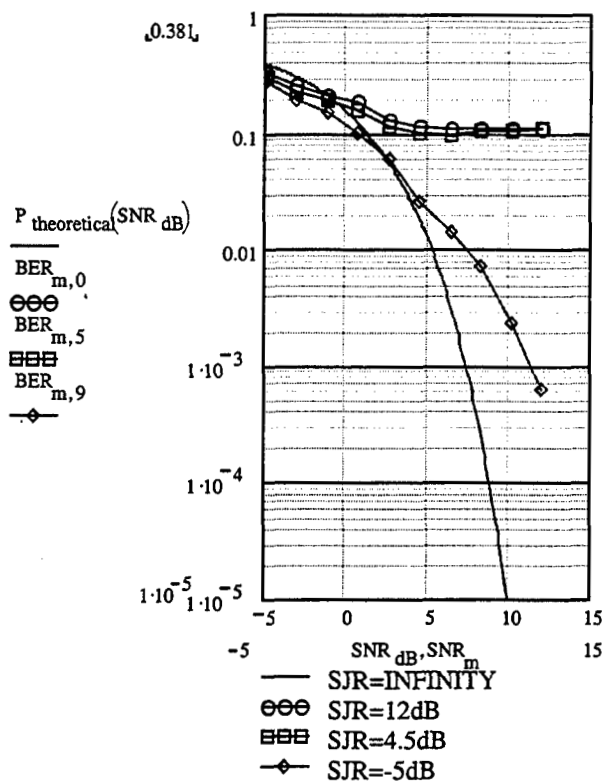


Figure 8.17 Simulink Model for QPSK with FM by Weibull Noise Jamming

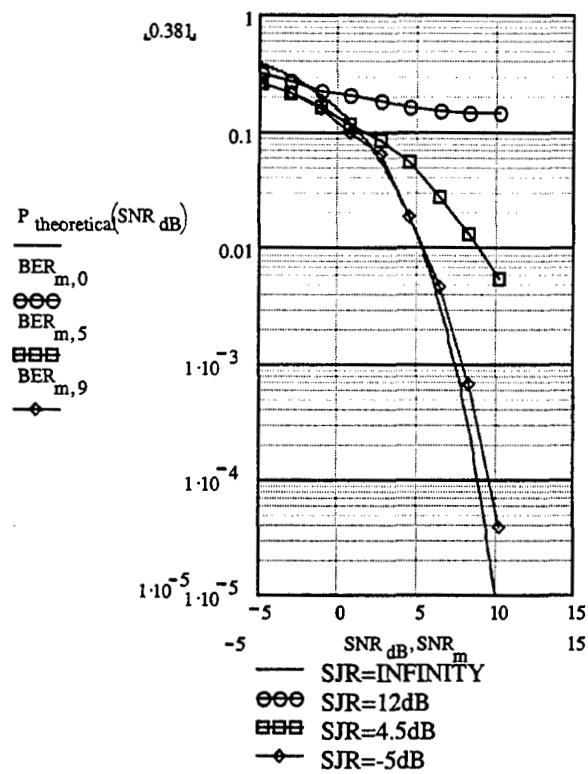
The bit error rate (BER) for QPSK with FM by Weibull Noise jamming as a function of the signal-to-noise ratio (SNR), with the signal-to-jamming ratio (SJR) as parameter, is shown in Figure 8.18 (a). The BER increases as SNR decreases. The selected ranges for SNR and SJR were from -5 dB to $+12$ dB. The solid line is the probability of bit error for QPSK without jamming.

The BER for QPSK with FM-modulated AWGN jamming as a function of the SNR, with the SJR as parameter, is shown in Figure 8.18 (b). The solid line is the probability of bit error for QPSK without jamming.

We note the change in the BER due to FM by Weibull Noise jamming, relative to FM-modulated AWGN jamming.



(a)



(b)

Figure 8.18 (a) The BER for QPSK with FM by Weibull Noise jamming as a function of the SNR (b) The BER for QPSK with FM-modulated AWGN jamming as a function of the SNR

D. PERFORMANCE OF DIGITAL COMMUNICATION SYSTEMS WITH PULSED NOISE JAMMING

1. Performance of Coherent BFSK with Pulsed Noise Jamming

a. AM-Modulated Pulsed Noise Jamming

Figure 8.19 shows the Simulink model for coherent BFSK with AM-modulated pulsed noise jamming.

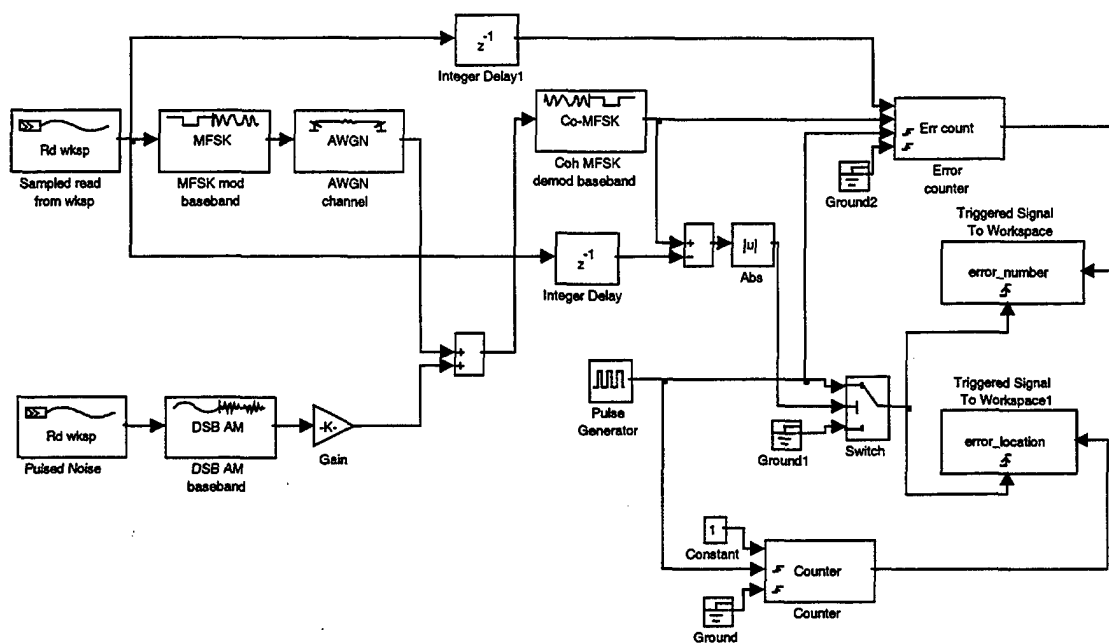


Figure 8.19 Simulink Model for Coherent BFSK with AM-Modulated Pulsed Noise Jamming

The bit error rate (BER) for coherent BFSK with AM-modulated pulsed noise jamming as a function of the signal-to-noise ratio (SNR), with the signal-to-jamming ratio (SJR) as parameter, is shown in Figure 8.20 (a). The BER increases as SNR decreases. The selected range for SNR was from -5 dB to $+15$ dB, and the selected

range for SJR was from -5 dB to $+12$ dB. The solid line is the probability of bit error for coherent BFSK without jamming.

The BER for coherent BFSK with AM-modulated AWGN jamming as a function of the SNR, with the SJR as parameter, is shown in Figure 8.20 (b). The solid line is the probability of bit error for coherent BFSK without jamming.

We note the dramatic increase in the BER due to AM-modulated pulsed noise jamming, relative to AM-modulated AWGN jamming.

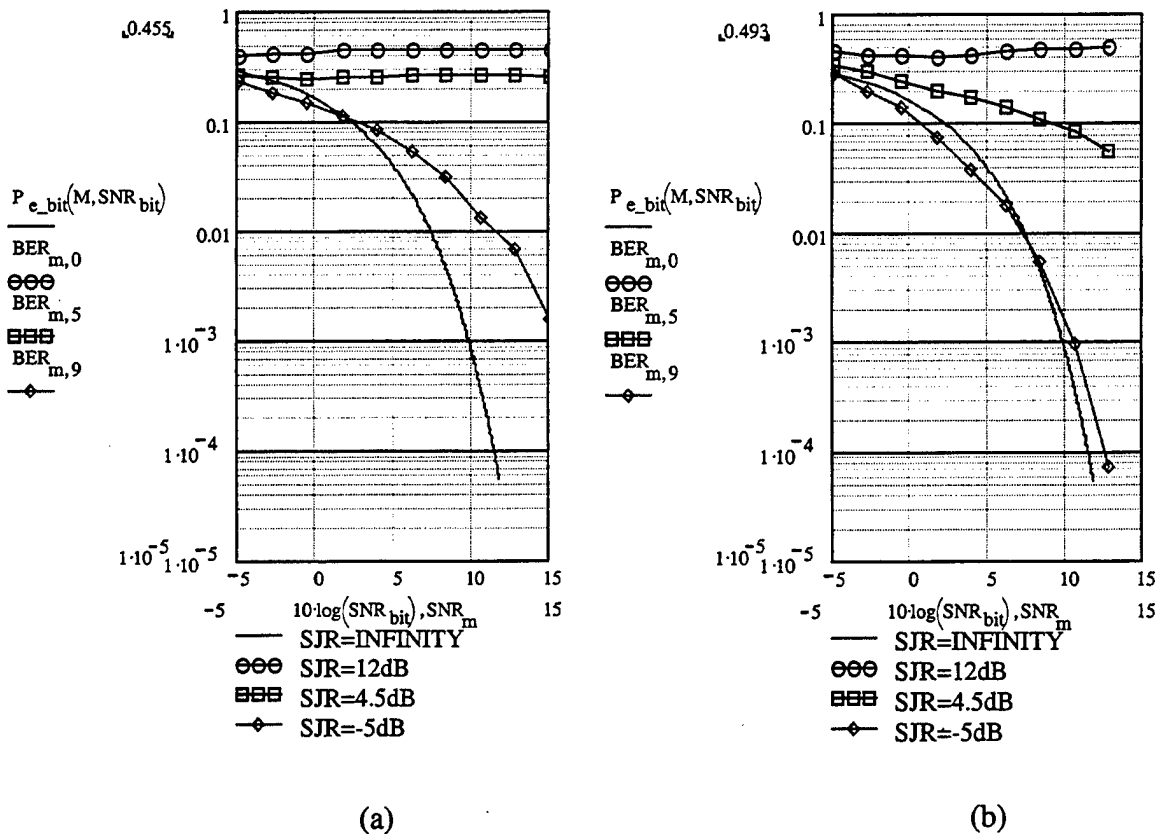


Figure 8.20 (a) The BER for coherent BFSK with AM-modulated pulsed noise jamming as a function of the SNR (b) The BER for coherent BFSK with AM-modulated AWGN jamming as a function of the SNR

b. *FM-Modulated Pulsed Noise Jamming*

Figure 8.21 shows the Simulink model for coherent BFSK with FM-modulated pulsed noise jamming.

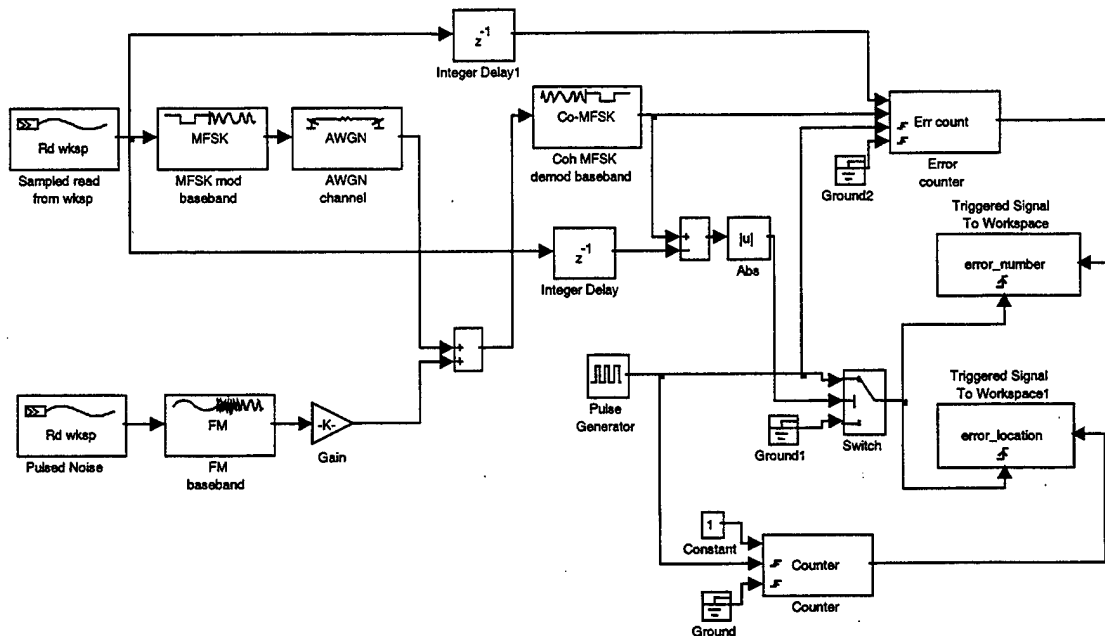


Figure 8.21 Simulink Model for Coherent BFSK with FM-Modulated Pulsed Noise Jamming

The bit error rate (BER) for coherent BFSK with FM-modulated pulsed noise jamming as a function of the signal-to-noise ratio (SNR), with the signal-to-jamming ratio (SJR) as parameter, is shown in Figure 8.22 (a). The BER increases as SNR decreases. The selected range for SNR was from -5 dB to $+15$ dB, and the selected range for SJR was from -5 dB to $+12$ dB. The solid line is the probability of bit error for coherent BFSK without jamming.

The BER for coherent BFSK with FM-modulated AWGN jamming as a function of the SNR, with the SJR as parameter, is shown in Figure 8.22 (b). The solid line is the probability of bit error for coherent BFSK without jamming.

We observe the change in the BER due to FM-modulated pulsed noise jamming, relative to FM-modulated AWGN jamming.

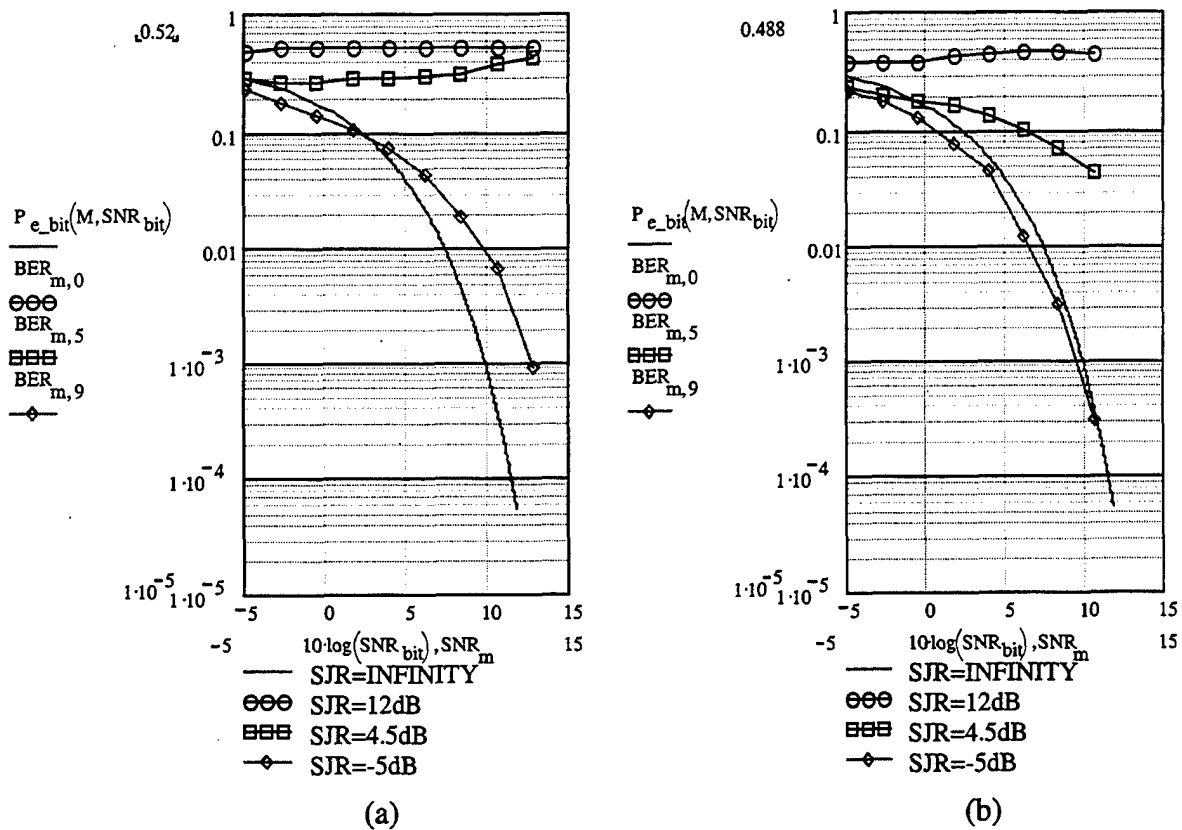


Figure 8.22 (a) The BER for coherent BFSK with FM-modulated pulsed noise jamming as a function of the SNR (b) The BER for coherent BFSK with FM-modulated AWGN jamming as a function of the SNR

2. Performance of Noncoherent BFSK with Pulsed Noise Jamming

a. AM-Modulated Pulsed Noise Jamming

Figure 8.23 shows the Simulink model for noncoherent BFSK with AM-modulated pulsed noise jamming.

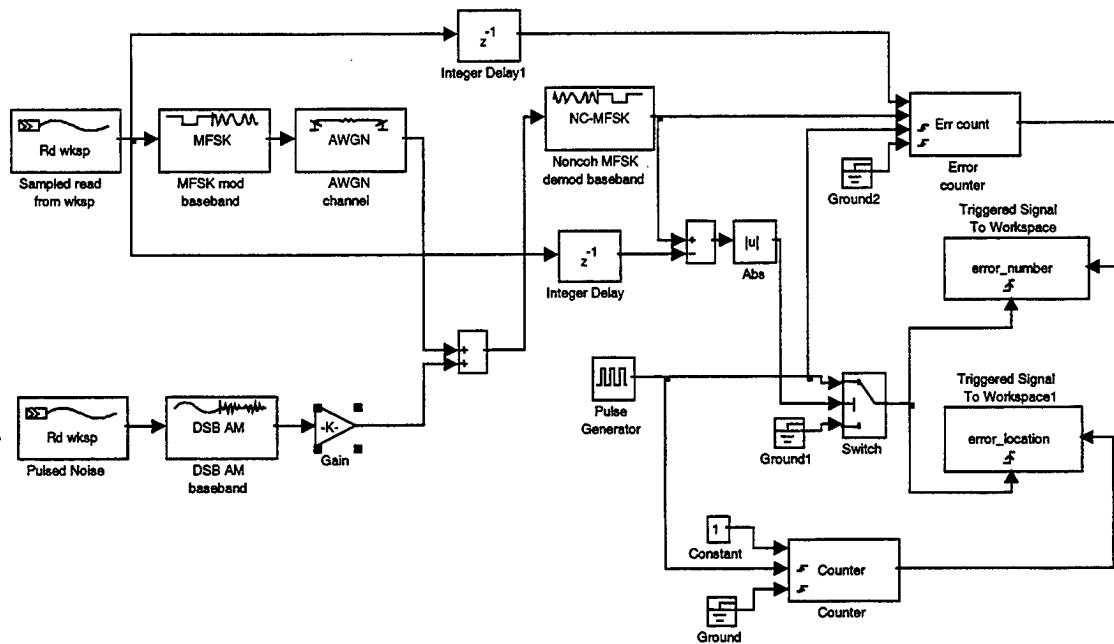


Figure 8.23 Simulink Model for Noncoherent BFSK with AM-Modulated Pulsed Noise Jamming

The probability of bit error (BER) for noncoherent BFSK with AM-modulated pulsed noise jamming as a function of the signal-to-noise ratio (SNR), with the signal-to-jamming ratio (SJR) as parameter, is shown in Figure 8.24 (a). The BER increases as SNR decreases. The selected range for SNR was from -5 dB to $+15$ dB, and the selected range for SJR was from -5 dB to $+12$ dB. The solid line is the probability of bit error for noncoherent BFSK without jamming.

The BER for noncoherent BFSK with AM- modulated AWGN jamming as a function of the SNR, with the SJR as parameter, is shown in Figure 8.24 (b). The solid line is the probability of bit error for noncoherent BFSK without jamming.

We note the change in the BER due to AM-modulated pulsed noise jamming, relative to AM-modulated AWGN jamming.

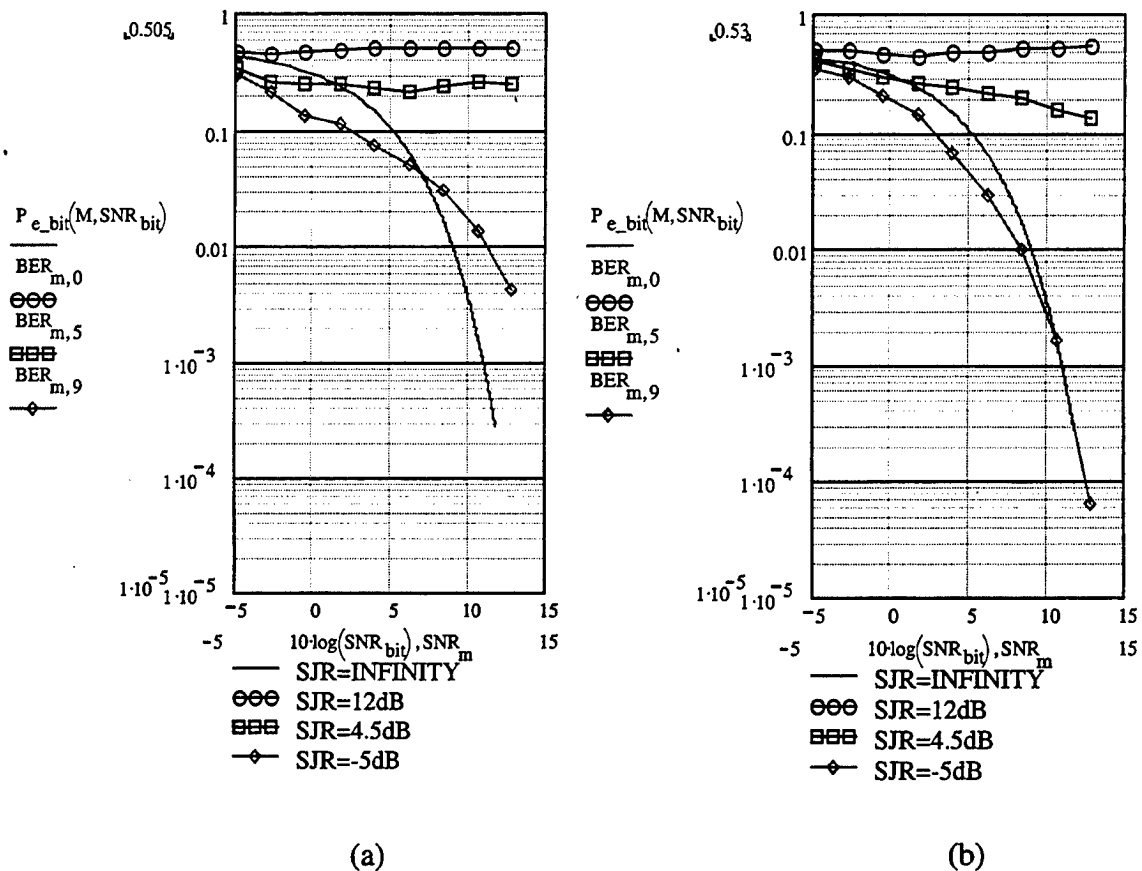


Figure 8.24 (a) The BER for noncoherent BFSK with AM-modulated pulsed noise jamming as a function of the SNR (b) The BER for noncoherent BFSK with AM-modulated AWGN jamming as a function of the SNR

b. FM-Modulated Pulsed Noise Jamming

Figure 8.25 shows the Simulink model for noncoherent BFSK with FM-modulated pulsed noise jamming.

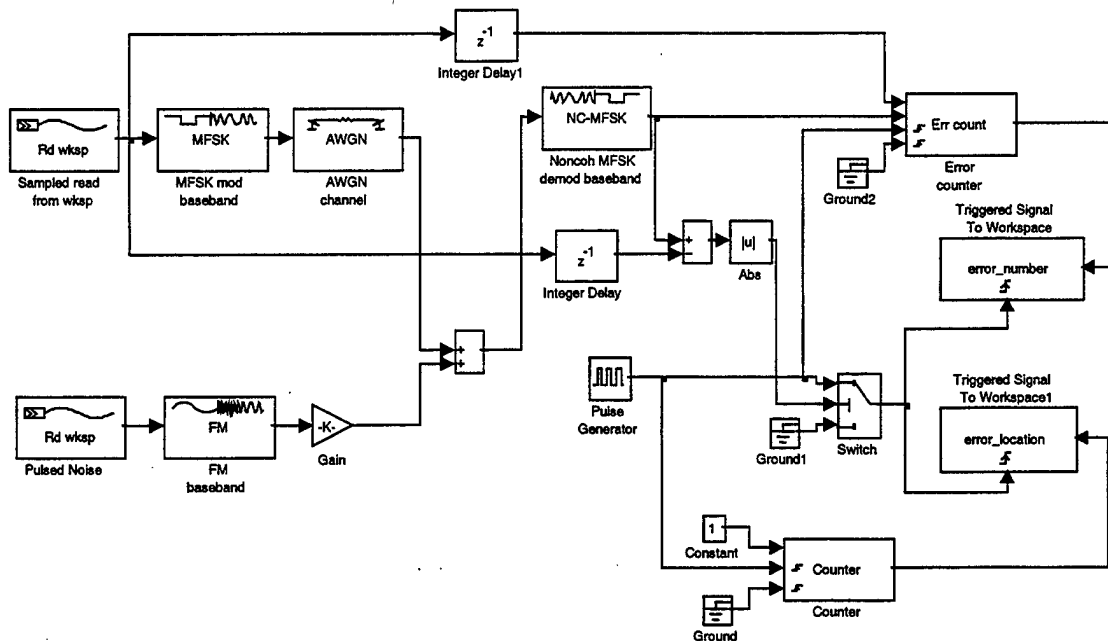


Figure 8.25 Simulink Model for Noncoherent BFSK with FM-Modulated Pulsed Noise Jamming

The bit error rate (BER) for noncoherent BFSK with FM- modulated pulsed noise jamming as a function of the signal-to-noise ratio (SNR), with the signal-to-jamming ratio (SJR) as parameter, is shown in Figure 8.26 (a). The BER increases as SNR decreases. The selected range for SNR was from -5 dB to $+15$ dB, and the selected range for SJR was from -5 dB to $+12$ dB. The solid line is the probability of bit error for noncoherent BFSK without jamming.

The BER for noncoherent BFSK with FM- modulated AWGN jamming as a function of the SNR, with the SJR as parameter, is shown in Figure 8.26 (b). The solid line is the probability of bit error for noncoherent BFSK without jamming.

We note the dramatic increase in the BER due to FM-modulated pulsed noise jamming, relative to FM-modulated AWGN jamming.

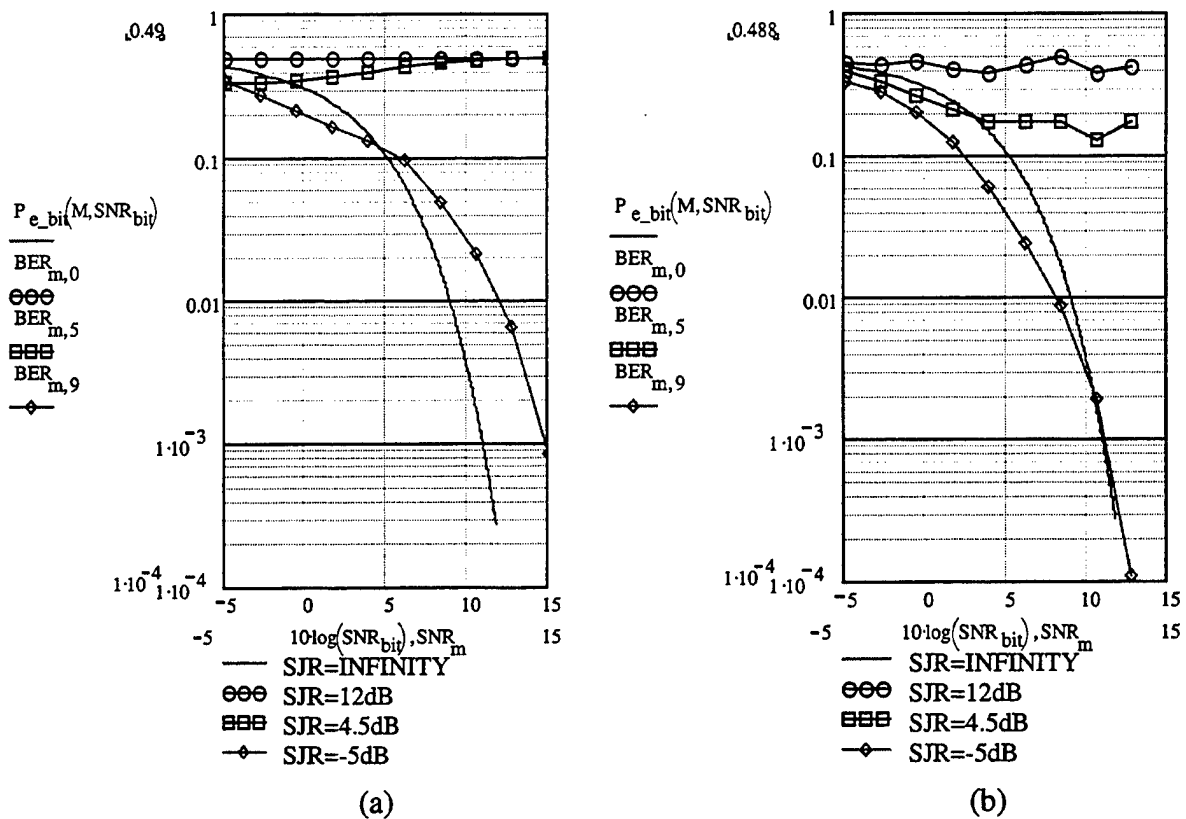


Figure 8.26 (a) The BER for noncoherent BFSK with FM-modulated pulsed noise jamming as a function of the SNR (b) The BER for noncoherent BFSK with FM-modulated AWGN jamming as a function of the SNR

3. Performance of BPSK with Pulsed Noise Jamming

a. AM-Modulated Pulsed Noise Jamming

Figure 8.27 shows the Simulink model for BPSK with AM-modulated pulsed noise jamming.

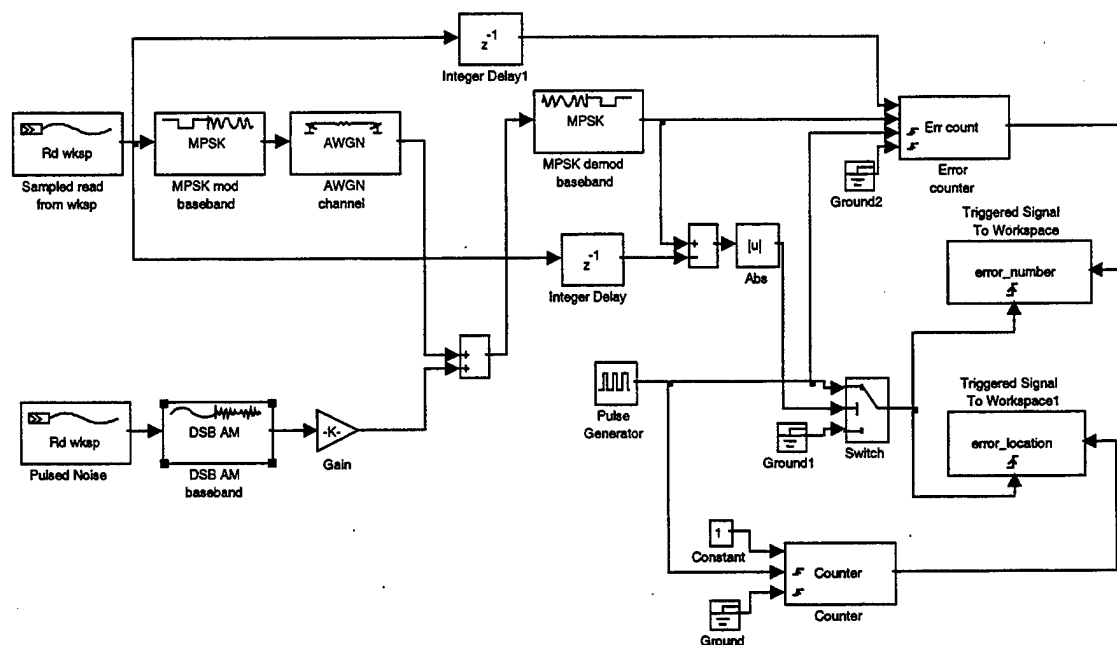


Figure 8.27 Simulink Model for BPSK with AM-Modulated Pulsed Noise Jamming

The bit error rate (BER) for BPSK with AM-modulated pulsed noise jamming as a function of the signal-to-noise ratio (SNR), with the signal-to-jamming ratio (SJR) as parameter, is shown in Figure 8.28 (a). The BER increases as SNR decreases. The selected ranges for SNR and SJR were from -5 dB to $+12$ dB. The solid line is the probability of bit error for BPSK without jamming.

The BER for BPSK with AM-modulated AWGN jamming as a function of the SNR, with the SJR as parameter, is shown in Figure 8.28 (b). The solid line is the probability of bit error for BPSK without jamming.

We observe the dramatic increase in the BER due to AM-modulated pulsed noise jamming, relative to AM-modulated AWGN jamming.

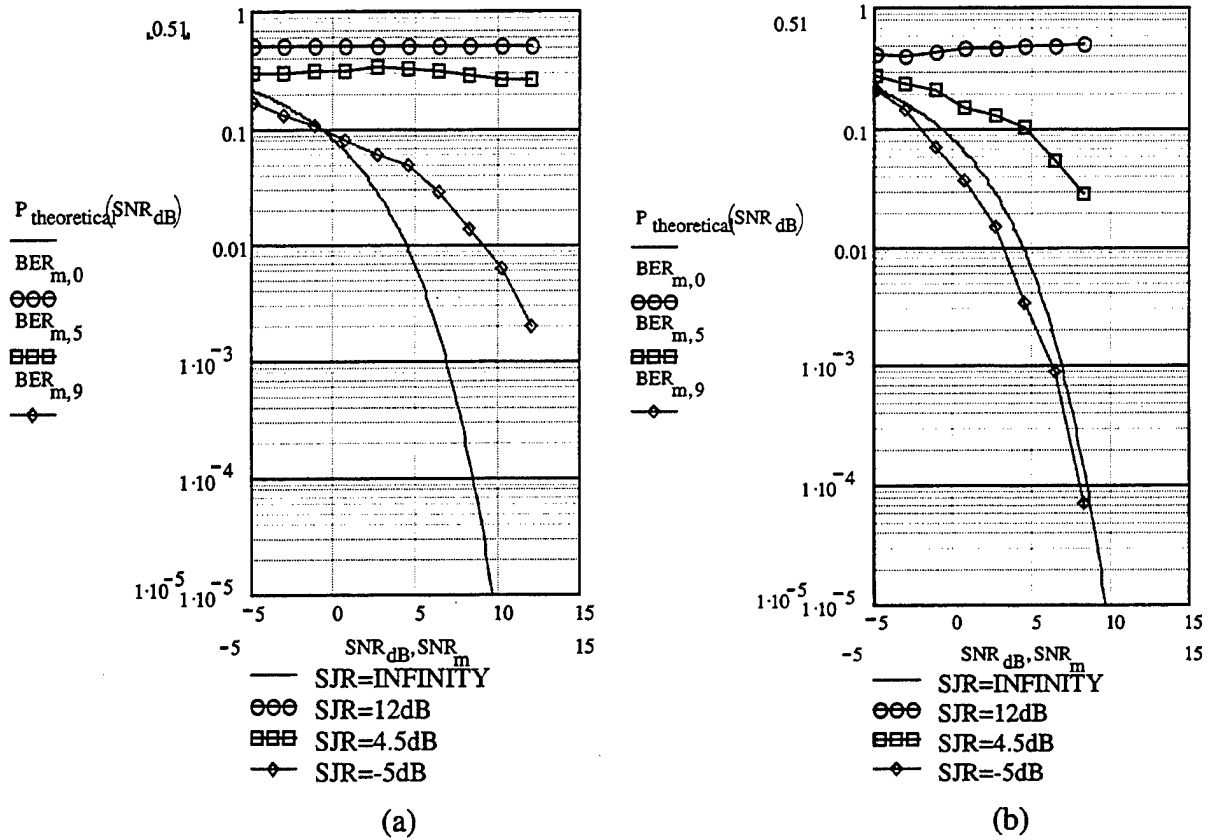


Figure 8.28 (a) The BER for BPSK with AM-modulated pulsed noise jamming as a function of the SNR (b) The BER for BPSK with AM-modulated AWGN jamming as a function of the SNR

The BER for BPSK with FM-modulated AWGN jamming as a function of the SNR, with the SJR as parameter, is shown in Figure 8.30 (b). The solid line is the probability of bit error for BPSK without jamming.

We note that the dramatic increase in the BER due to FM-modulated pulsed noise jamming, relative to FM-modulated AWGN jamming.

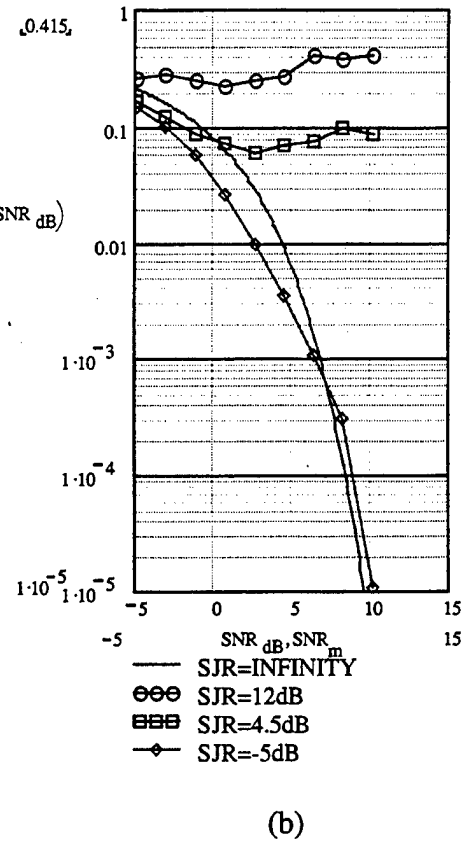
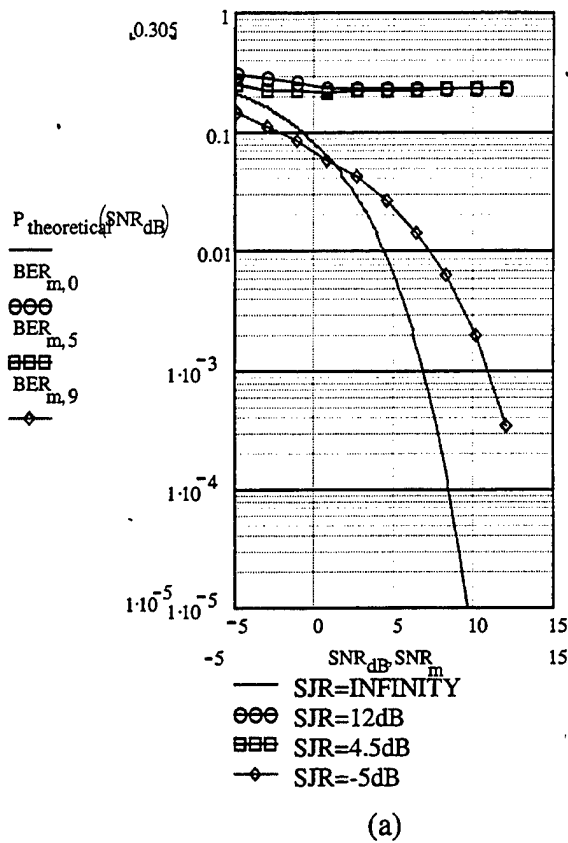


Figure 8.30 (a) The BER for BPSK with FM-modulated pulsed noise jamming as a function of the SNR (b) The BER for BPSK with FM-modulated AWGN jamming as a function of the SNR

4. Performance of QPSK with Pulsed Noise Jamming

a. AM-Modulated Pulsed Noise Jamming

Figure 8.31 shows the Simulink model for QPSK with AM-modulated pulsed noise jamming.

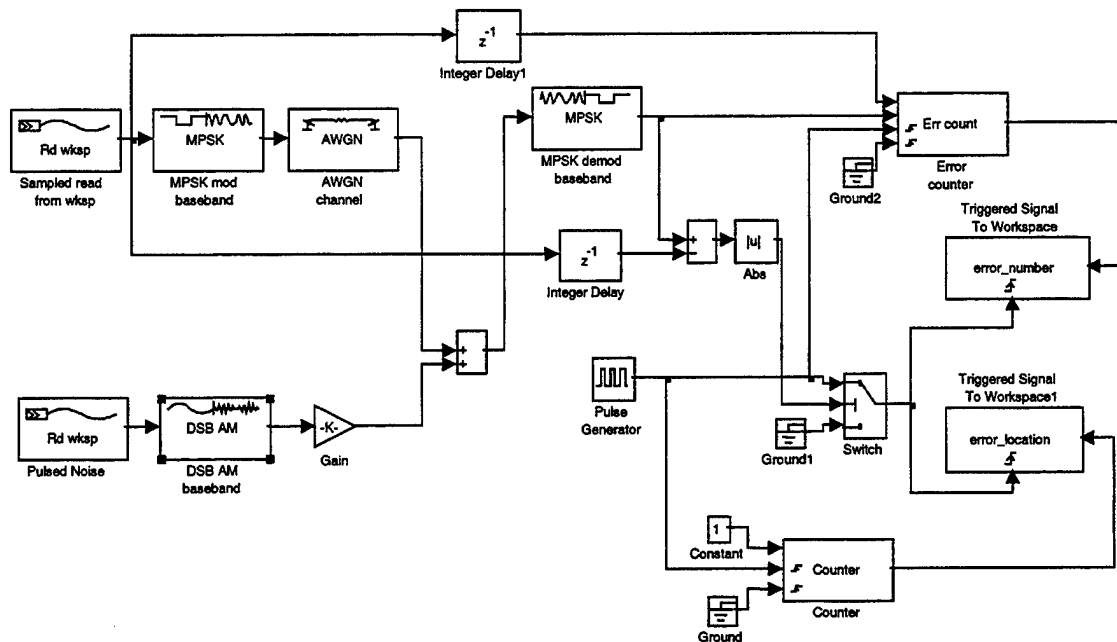


Figure 8.31 Simulink Model for QPSK with AM-Modulated Pulsed Noise Jamming

The bit error rate (BER) for QPSK with AM-modulated pulsed noise jamming as a function of the signal-to-noise ratio (SNR), with the signal-to-jamming ratio (SJR) as parameter, is shown in Figure 8.32 (a). The BER increases as SNR decreases. The selected ranges for SNR and SJR were from -5 dB to $+12$ dB. The solid line is the probability of bit error for QPSK without jamming.

The BER for QPSK with AM-modulated AWGN jamming as a function of the SNR, with the SJR as parameter, is shown in Figure 8.32 (b). The solid line is the probability of bit error for QPSK without jamming.

We note the dramatic increase in the BER due to AM-modulated pulsed noise jamming, relative to AM-modulated AWGN jamming.

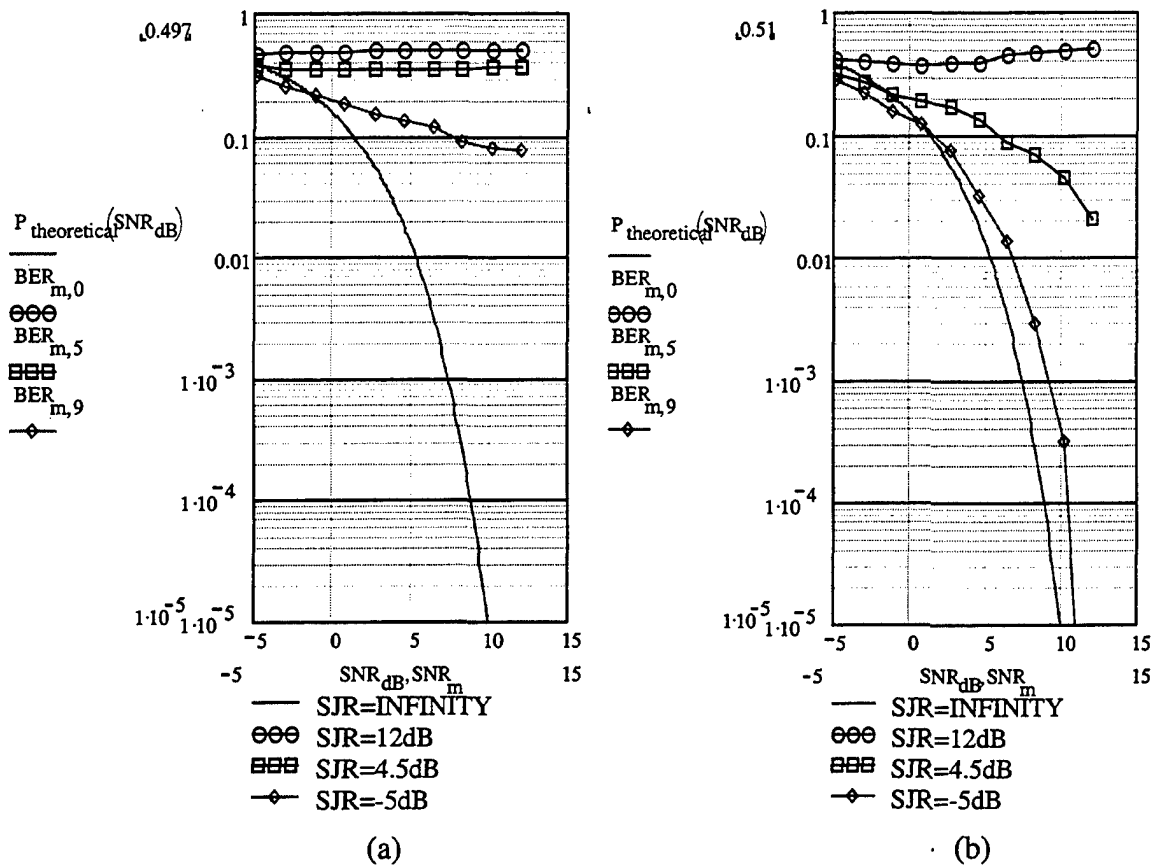


Figure 8.32 (a) The BER for QPSK with AM-modulated pulsed noise jamming as a function of the SNR (b) The BER for QPSK with AM-modulated AWGN jamming as a function of the SNR

a. FM-Modulated Pulsed Noise Jamming

Figure 8.33 shows the Simulink model for QPSK with FM-modulated pulsed noise jamming.

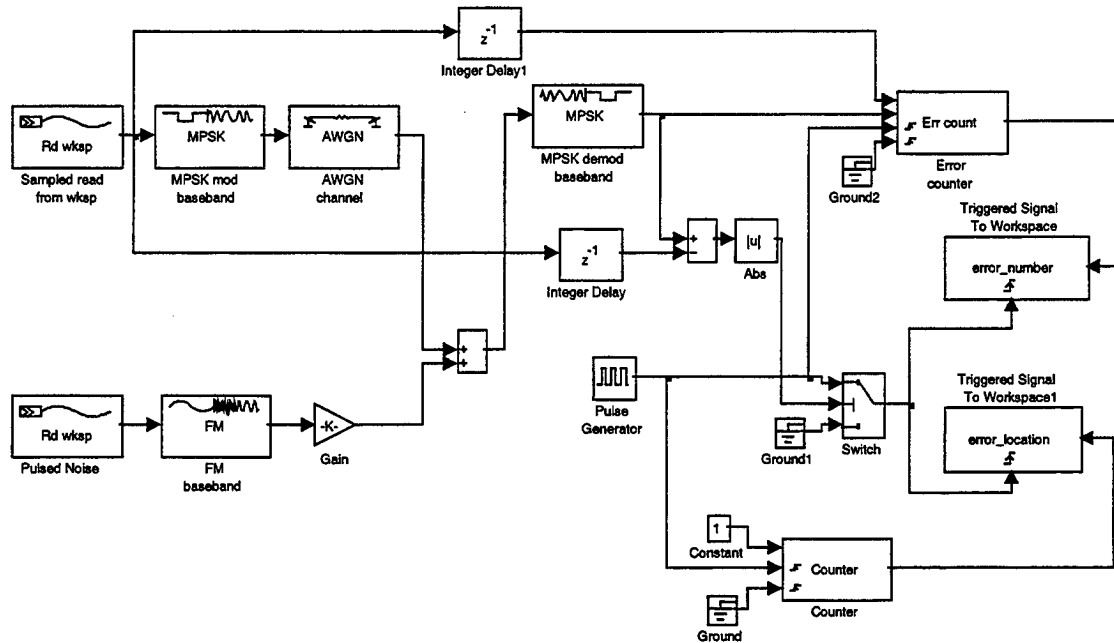


Figure 8.33 Simulink Model for QPSK with FM-Modulated Pulsed Noise Jamming

The bit error rate (BER) for QPSK with FM-modulated barrage noise jamming as a function of the signal-to-noise ratio (SNR), with the signal-to-jamming ratio (SJR) as parameter, is shown in Figure 8.34 (a). The BER increases as SNR decreases. The selected ranges for SNR and SJR were from -5 dB to $+12$ dB. The solid line is the probability of bit error for QPSK without jamming.

The BER for QPSK with FM-modulated AWGN jamming as a function of the SNR, with the SJR as parameter, is shown in Figure 8.34 (b). The solid line is the probability of bit error for QPSK without jamming.

We note the change in the BER due to FM-modulated pulsed noise jamming, relative to FM-modulated AWGN jamming.

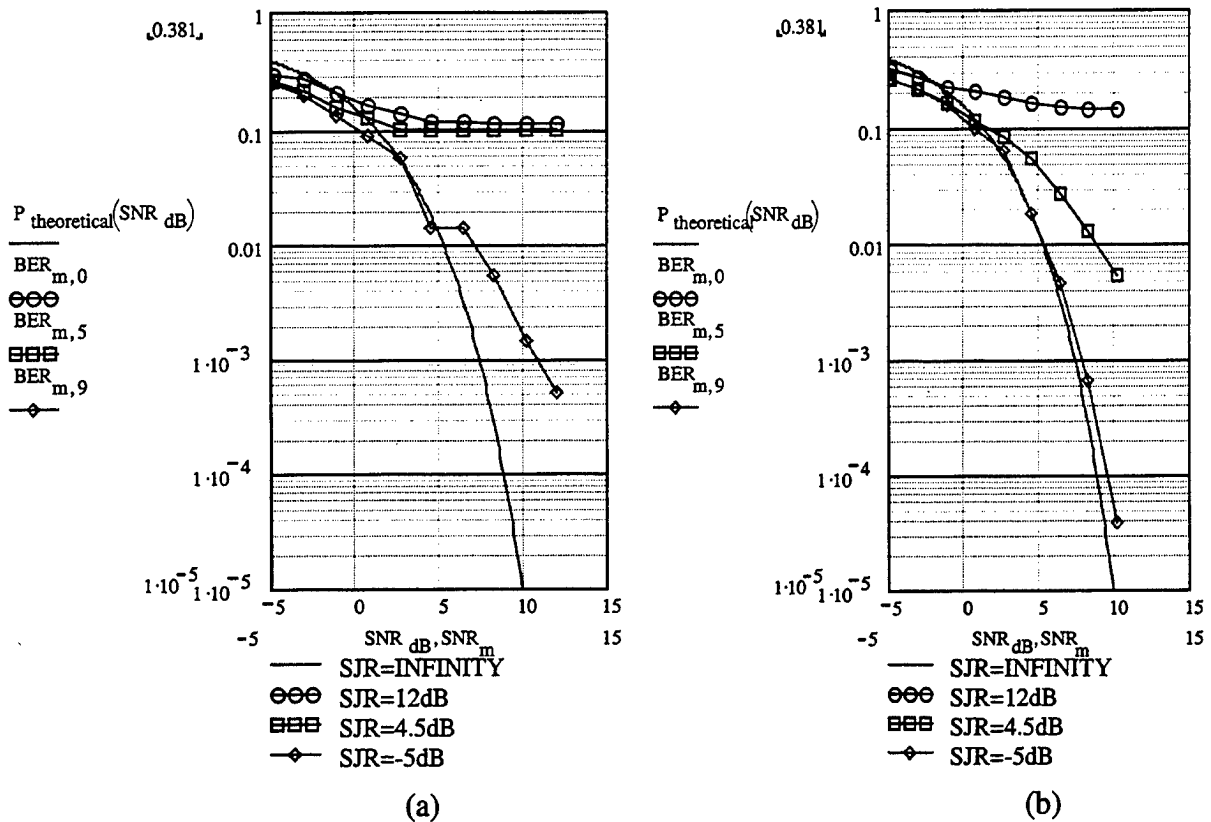


Figure 8.34 (a) The BER for QPSK with FM-modulated pulsed noise jamming as a function of the SNR (b) The BER for QPSK with FM-modulated AWGN jamming as a function of the SNR

E. PERFORMANCE OF DIGITAL COMMUNICATION SYSTEMS WITH TONE JAMMING

1. Performance of Coherent BFSK with Tone Jamming

a. AM-Modulated Tone Jamming

Figure 8.35 shows the Simulink model for coherent BFSK with AM-modulated tone jamming.

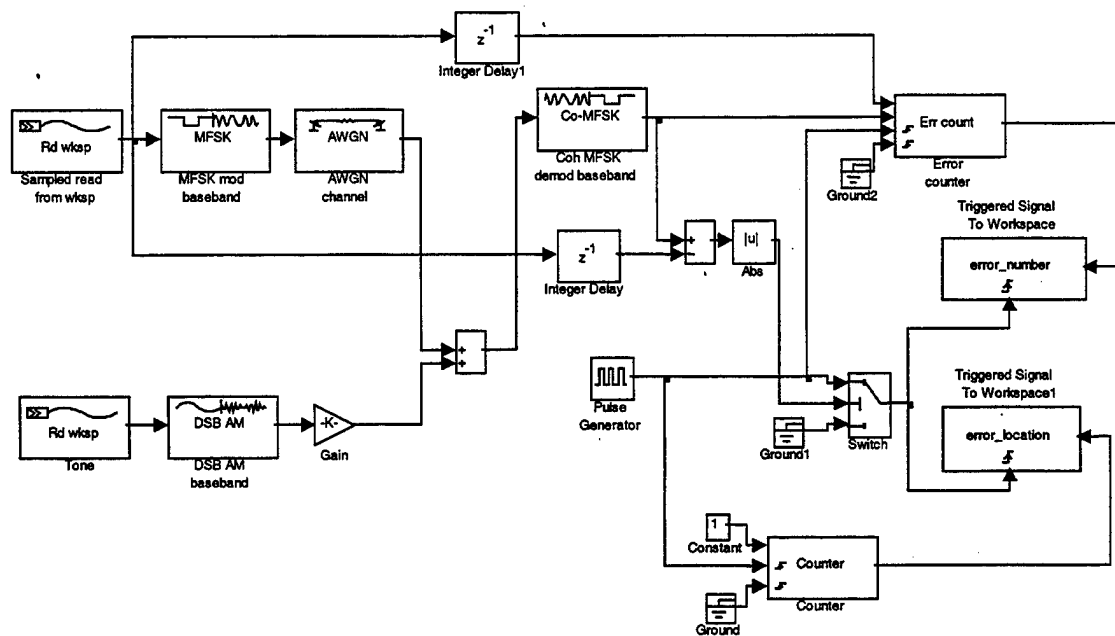


Figure 8.35 Simulink Model for Coherent BFSK with AM-Modulated Tone Jamming

The bit error rate (BER) for coherent BFSK with AM-modulated tone jamming as a function of the signal-to-noise ratio (SNR), with the signal-to-jamming ratio (SJR) as parameter, is shown in Figure 8.36 (a). The BER increases as SNR decreases. The selected range for SNR was from -5 dB to $+15$ dB, and the selected range

for SJR was from -5 dB to $+12$ dB. The solid line is the probability of bit error for coherent BFSK without jamming.

The BER for coherent BFSK with AM-modulated AWGN jamming as a function of the SNR, with the SJR as parameter, is shown in Figure 8.36 (b). The solid line is the probability of bit error for coherent BFSK without jamming.

We observe the dramatic increase in the BER due to AM-modulated tone jamming, relative to AM-modulated AWGN jamming.

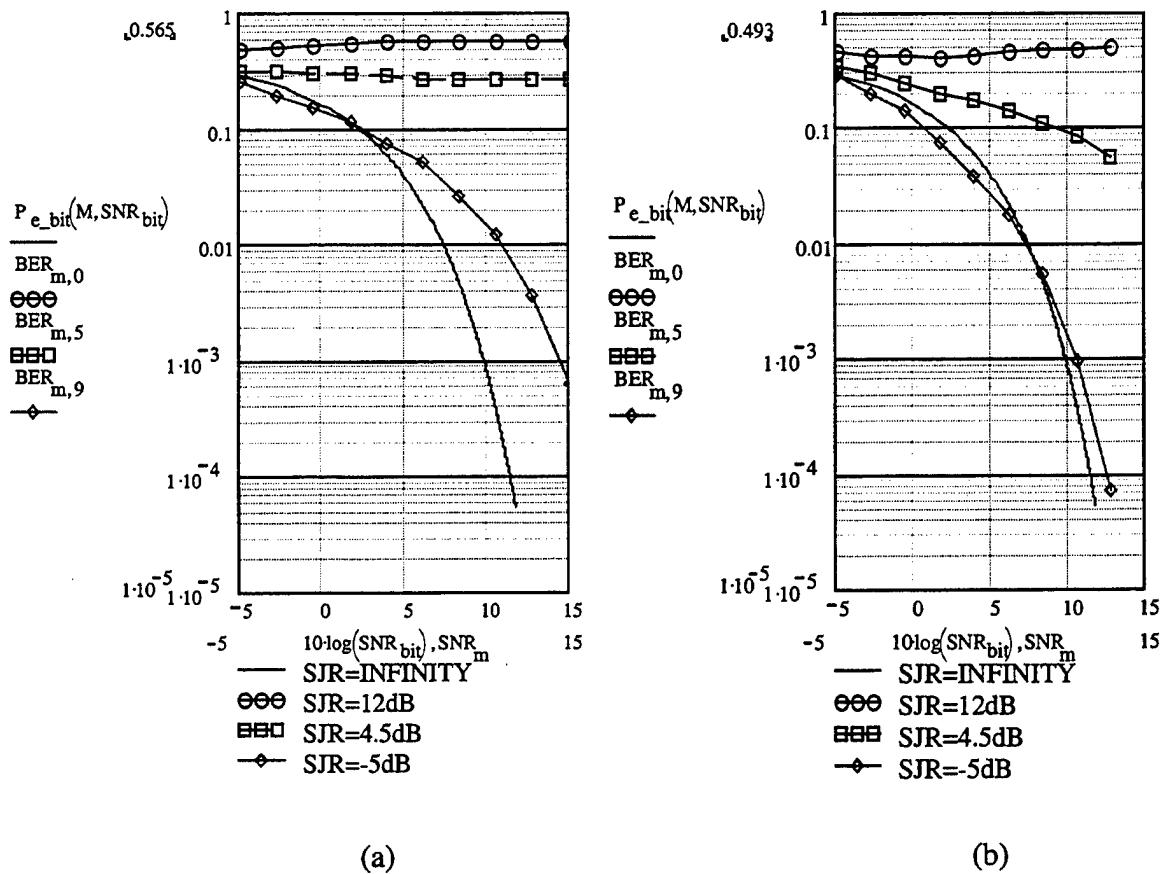


Figure 8.36 (a) The BER for coherent BFSK with AM-modulated tone jamming as a function of the SNR (b) The BER for coherent BFSK with AM-modulated AWGN jamming as a function of the SNR

b. FM-Modulated Tone Jamming

Figure 8.37 shows the Simulink model for coherent BFSK with FM-modulated tone jamming.

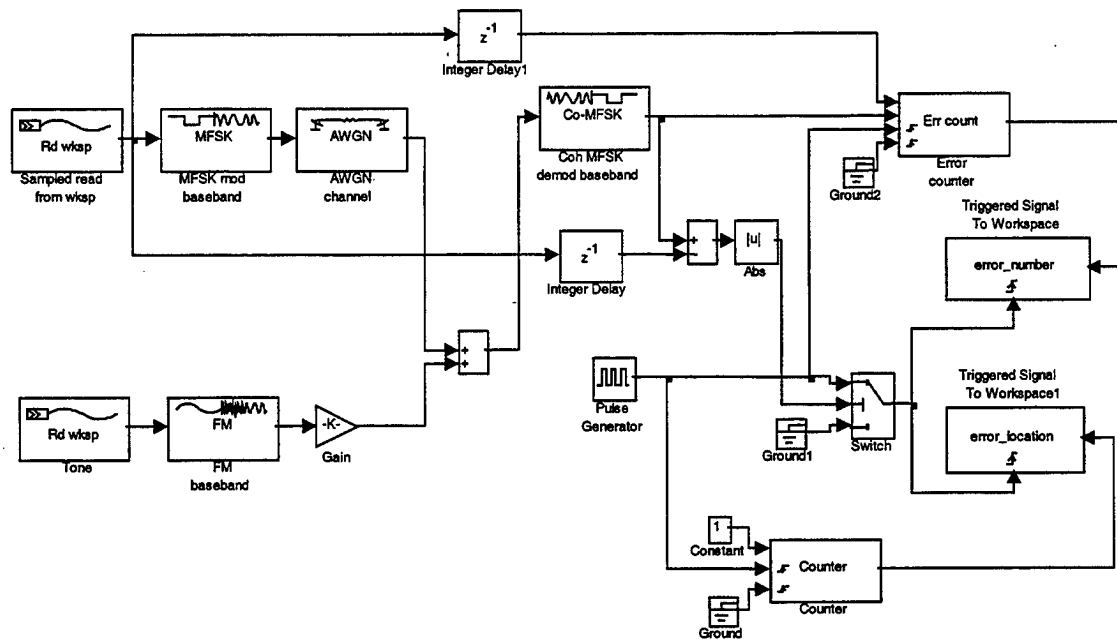


Figure 8.37 Simulink Model for Coherent BFSK with FM-Modulated Tone Jamming

The bit error rate (BER) for coherent BFSK with FM-modulated tone jamming as a function of the signal-to-noise ratio (SNR), with the signal-to-jamming ratio (SJR) as parameter, is shown in Figure 8.38 (a). The BER increases as SNR decreases. The selected range for SNR was from -5 dB to $+15$ dB, and the selected range for SJR was from -5 dB to $+12$ dB. The solid line is the probability of bit error for coherent BFSK without jamming.

The BER for coherent BFSK with FM-modulated AWGN jamming as a function of the SNR, with the SJR as parameter, is shown in Figure 8.38 (b). The solid line is the probability of bit error for coherent BFSK without jamming.

We note the dramatic increase in the BER due to FM-modulated tone jamming, relative to FM-modulated AWGN jamming.

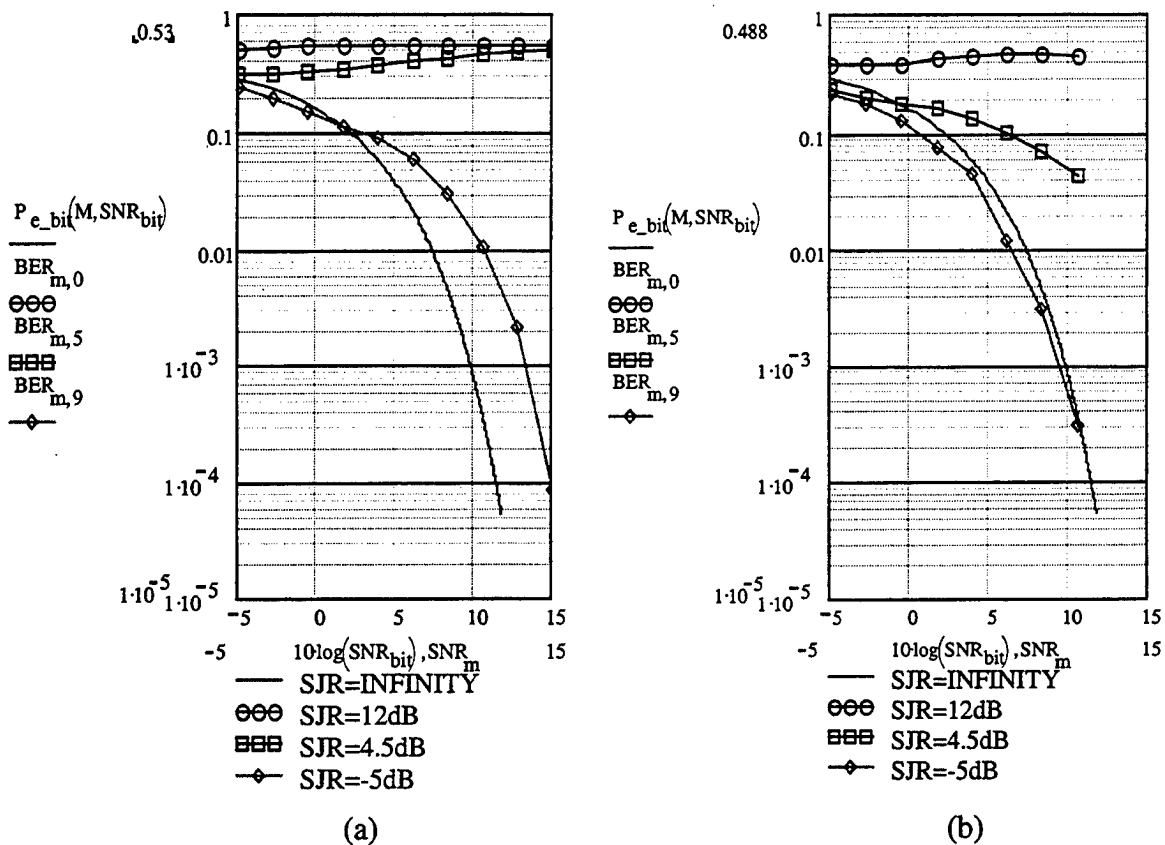


Figure 8.38 (a) The BER for coherent BFSK with FM-modulated tone jamming as a function of the SNR (b) The BER for coherent BFSK with FM-modulated AWGN jamming as a function of the SNR

2. Performance of Noncoherent BFSK with Tone Jamming

a. AM-Modulated Tone Jamming

Figure 8.39 shows the Simulink model for noncoherent BFSK with AM-modulated tone jamming.

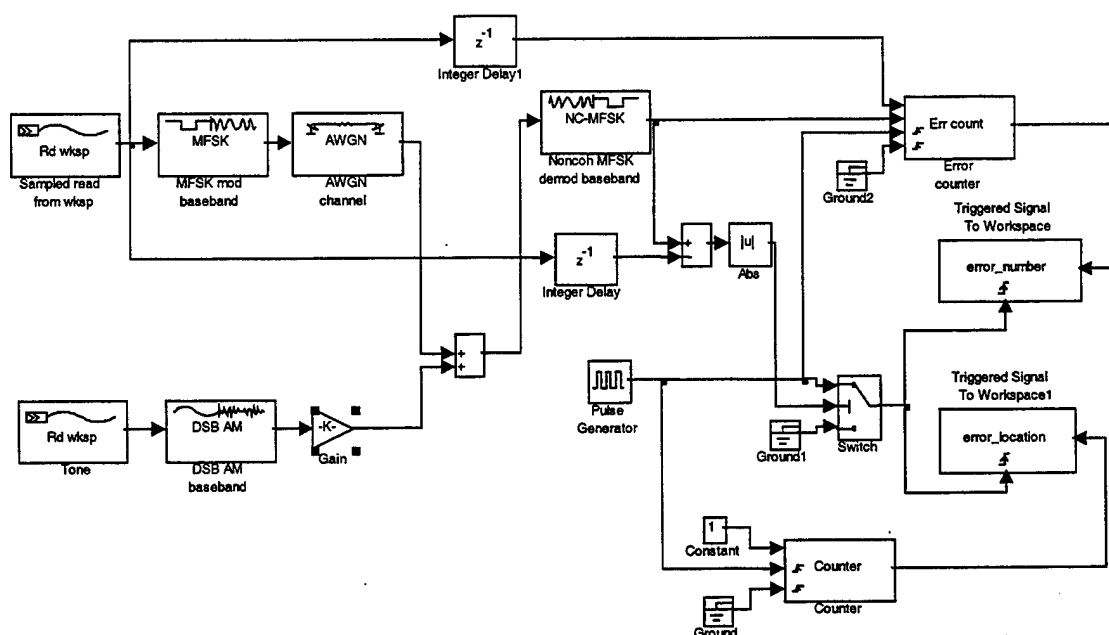


Figure 8.39 Simulink Model for Noncoherent BFSK with AM-Modulated Tone Jamming

The bit error rate (BER) for noncoherent BFSK with AM-modulated tone jamming as a function of the signal-to-noise ratio (SNR), with the signal-to-jamming ratio (SJR) as parameter, is shown in Figure 8.40 (a). The BER increases as SNR decreases. The selected range for SNR was from -5 dB to $+15$ dB, and the selected range for SJR was from -5 dB to $+12$ dB. The solid line is the probability of bit error for noncoherent BFSK without jamming.

The BER for noncoherent BFSK with AM- modulated AWGN jamming as a function of the SNR, with the SJR as parameter, is shown in Figure 8.40 (b). The solid line is the probability of bit error for noncoherent BFSK without jamming.

We observe the change in the BER due to AM-modulated tone jamming, relative to AM-modulated AWGN jamming.

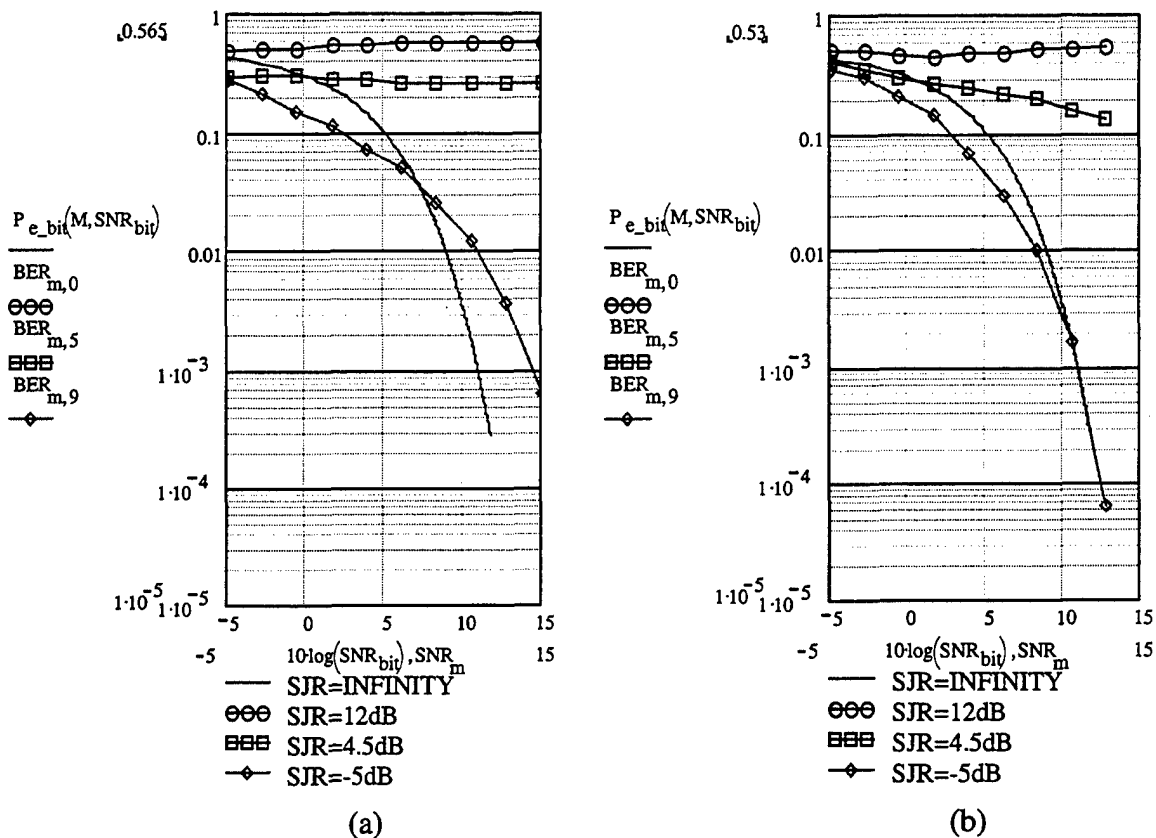


Figure 8.40 (a) The BER for noncoherent BFSK with AM-modulated tone jamming as a function of the SNR (b) The BER for noncoherent BFSK with AM-modulated AWGN jamming as a function of the SNR

b. FM-Modulated Tone Jamming

Figure 8.41 shows the Simulink model for noncoherent BFSK with FM-modulated tone jamming.

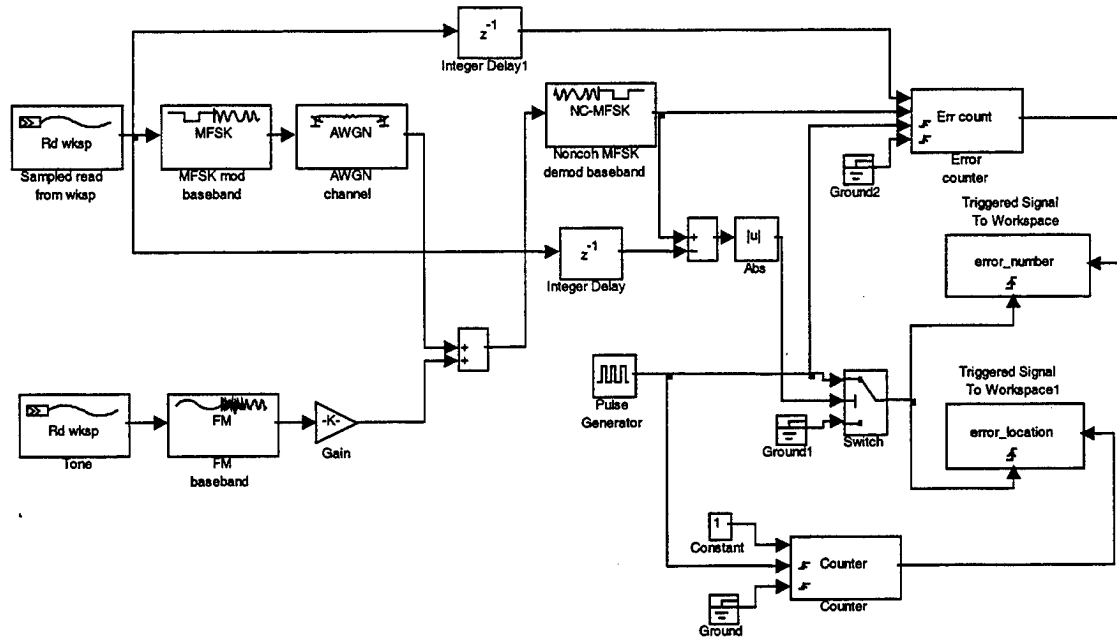


Figure 8.41 Simulink Model for Noncoherent BFSK with FM-Modulated Tone Jamming

The bit error rate (BER) for noncoherent BFSK with FM-modulated tone jamming as a function of the signal-to-noise ratio (SNR), with the signal-to-jamming ratio (SJR) as parameter, is shown in Figure 8.42 (a). The BER increases as SNR decreases. The selected range for SNR was from -5 dB to +15 dB, and the selected range for SJR was from -5 dB to +12 dB. The solid line is the probability of bit error for noncoherent BFSK without jamming.

The BER for noncoherent BFSK with FM- modulated AWGN jamming as a function of the SNR, with the SJR as parameter, is shown in Figure 8.42 (b). The solid line is the probability of bit error for noncoherent BFSK without jamming.

We note the change in the BER due to FM-modulated tone jamming, relative to FM-modulated AWGN jamming.

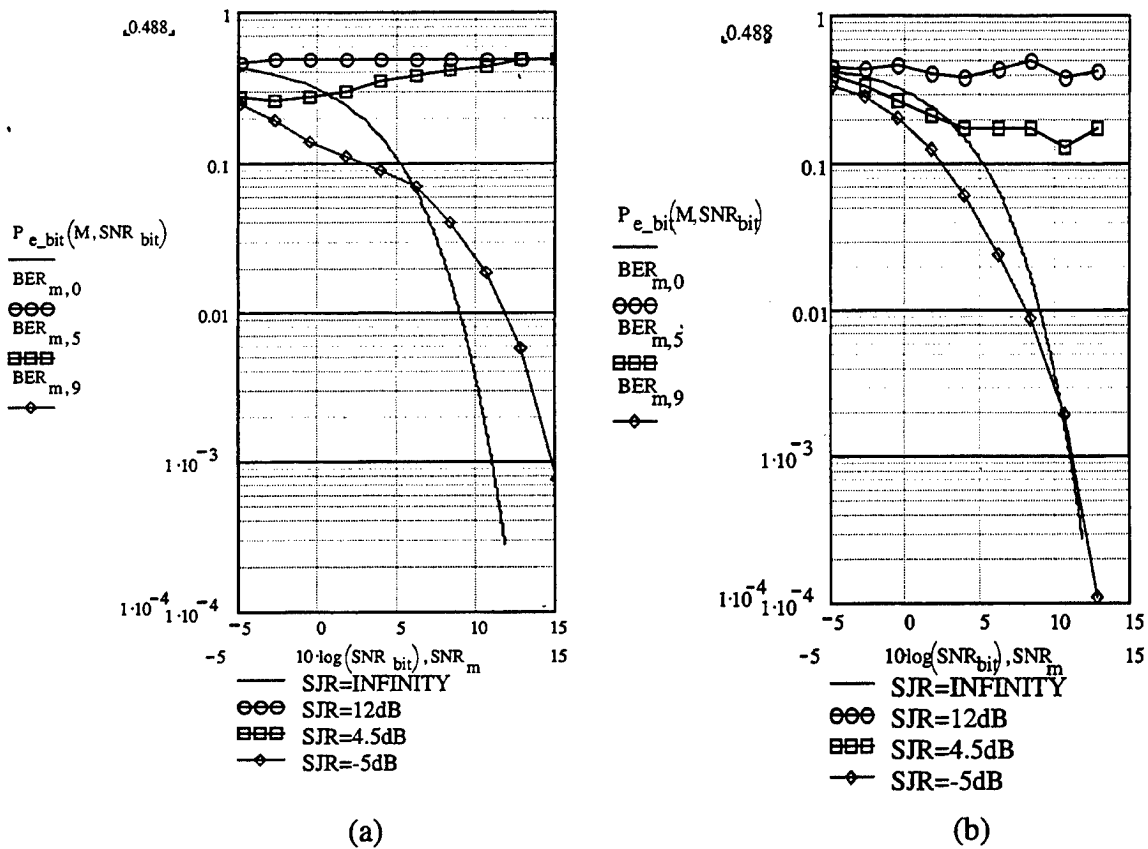


Figure 8.42 (a) The BER for noncoherent BFSK with FM-modulated tone jamming as a function of the SNR (b) The BER for noncoherent BFSK with FM-modulated AWGN jamming as a function of the SNR

3. Performance of BPSK with Tone Jamming

a. AM-Modulated Tone Jamming

Figure 8.43 shows the Simulink model for BPSK with AM-modulated tone jamming.

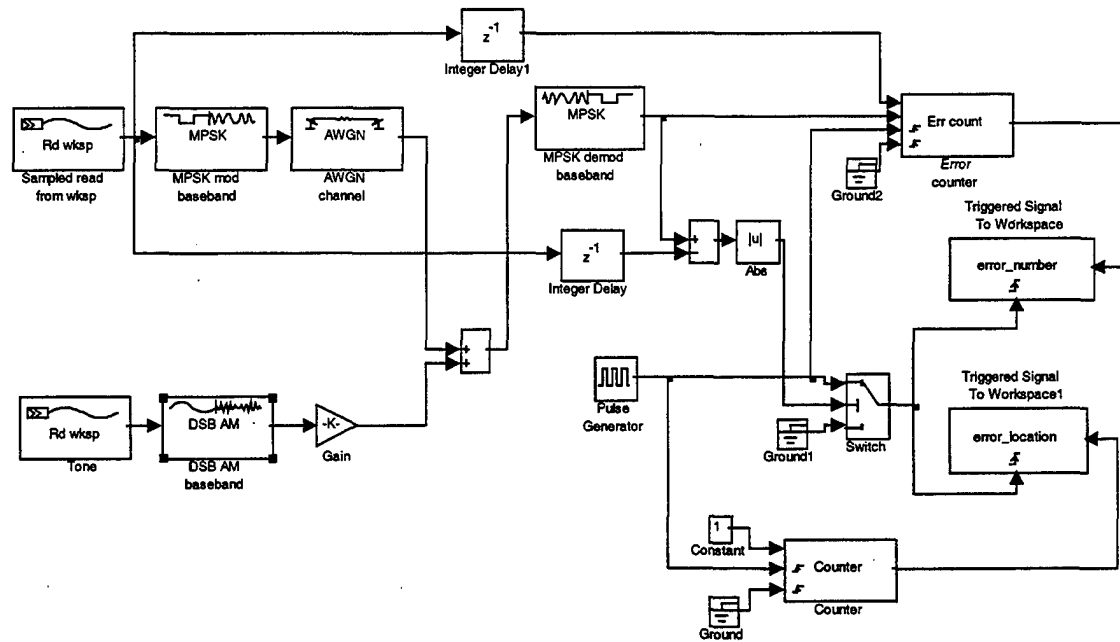


Figure 8.43 Simulink Model for BPSK with AM-Modulated Tone Jamming

The bit error rate (BER) for BPSK with AM-modulated tone jamming as a function of the signal-to-noise ratio (SNR), with the signal-to-jamming ratio (SJR) as parameter, is shown in Figure 8.44 (a). The BER increases as SNR decreases. The selected ranges for SNR and SJR were from -5 dB to $+12$ dB. The solid line is the probability of bit error for BPSK without jamming.

The BER for BPSK with AM-modulated AWGN jamming as a function of the SNR, with the SJR as parameter, is shown in Figure 8.44 (b). The solid line is the probability of bit error for BPSK without jamming.

We observe the dramatic increase in the BER due to AM-modulated tone jamming, relative to AM-modulated AWGN jamming.

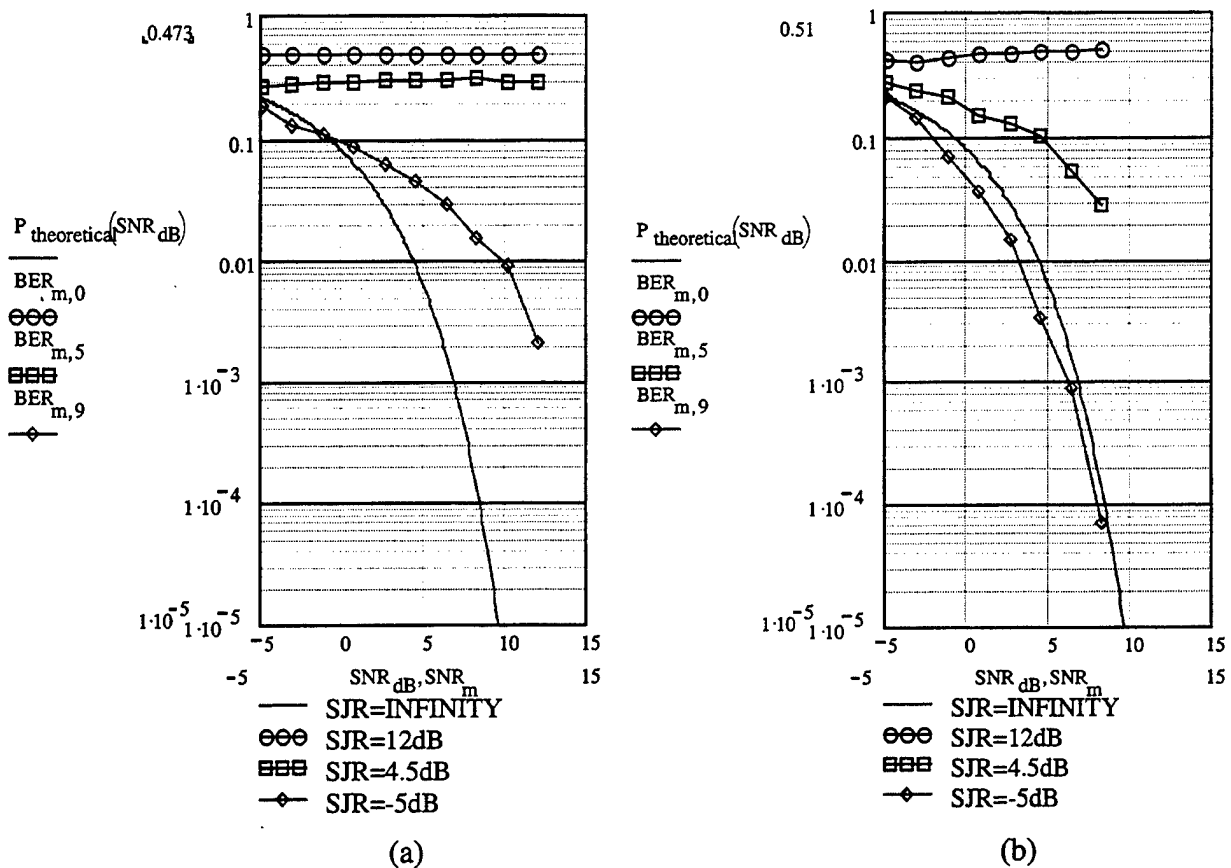


Figure 8.44 (a) The BER for BPSK with AM-modulated tone jamming as a function of the SNR (b) The BER for BPSK with AM-modulated AWGN jamming as a function of the SNR

b. FM-Modulated Tone Jamming

Figure 8.45 shows the Simulink model for BPSK with FM-modulated tone jamming.

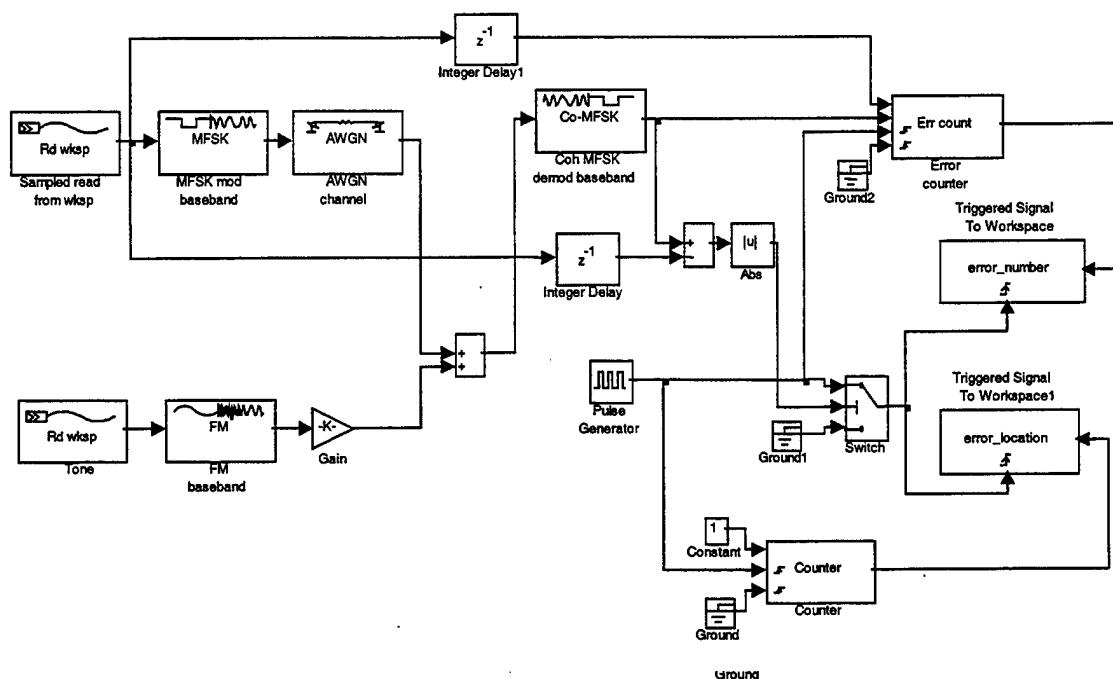


Figure 8.45 Simulink Model for BPSK with FM-Modulated Tone Jamming

The bit error rate (BER) for BPSK with FM-modulated tone jamming as a function of the signal-to-noise ratio (SNR), with the signal-to-jamming ratio (SJR) as parameter, is shown in Figure 8.46 (a). The BER increases as SNR decreases. The selected ranges for SNR and SJR were from -5 dB to $+12$ dB. The solid line is the probability of bit error for BPSK without jamming.

The BER for BPSK with FM-modulated AWGN jamming as a function of the SNR, with the SJR as parameter, is shown in Figure 8.46 (b). The solid line is the probability of bit error for BPSK without jamming.

We note the dramatic increase in the BER due to FM-modulated tone jamming, relative to FM-modulated AWGN jamming.

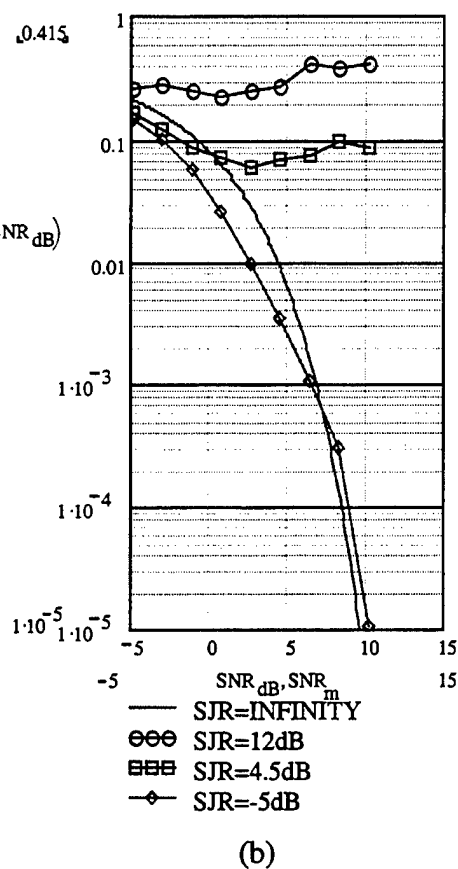
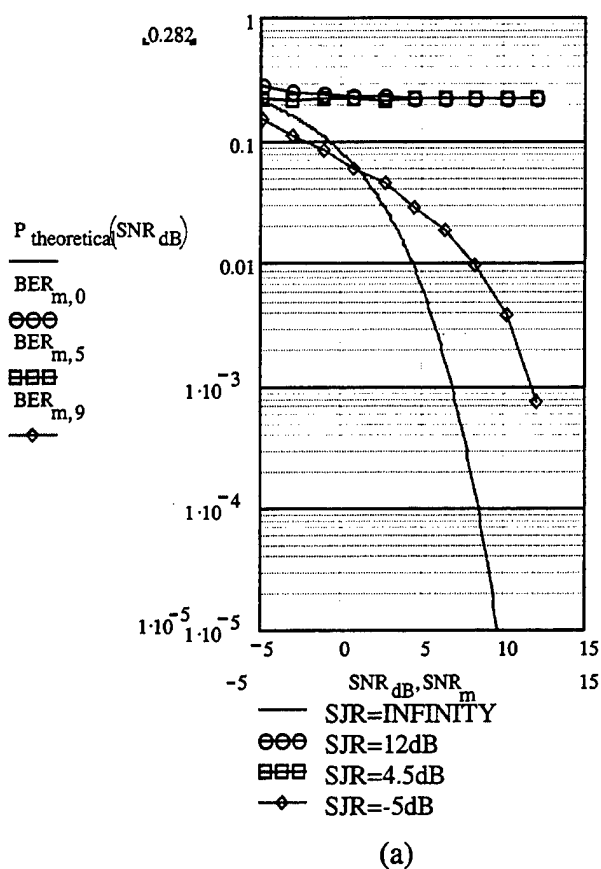


Figure 8.46 (a) The BER for BPSK with FM-modulated tone jamming as a function of the SNR (b) The BER for BPSK with FM-modulated AWGN jamming as a function of the SNR

4. Performance of QPSK with Tone Jamming

a. AM-Modulated Tone Jamming

Figure 8.47 shows the Simulink model for QPSK with AM-modulated tone jamming.

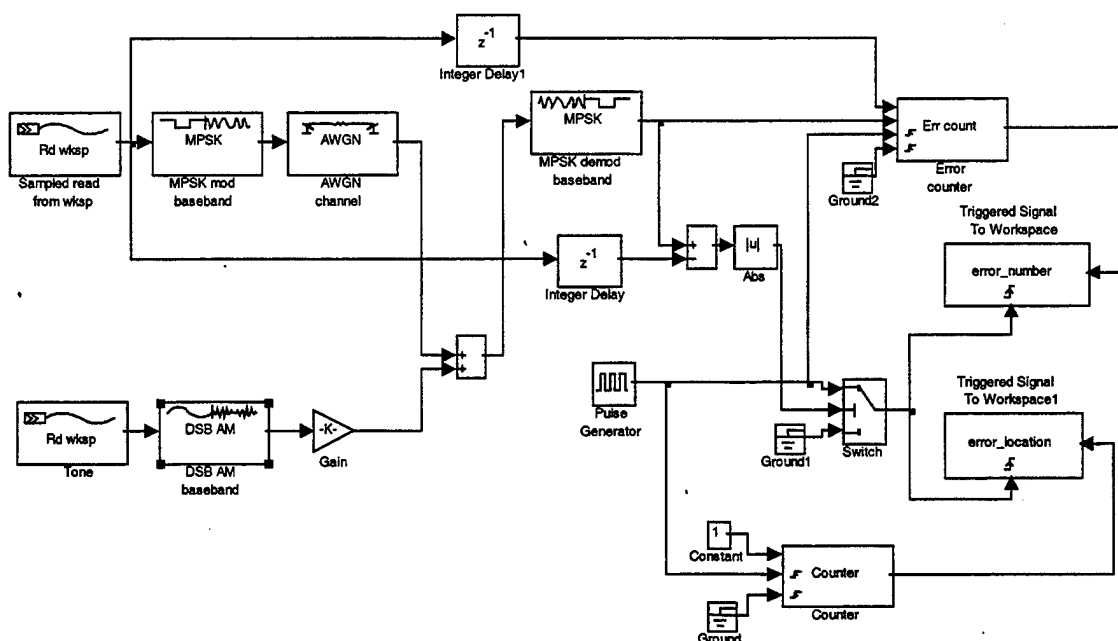


Figure 8.47 Simulink Model for QPSK with AM-Modulated Tone Jamming

The bit error rate (BER) for QPSK with AM-modulated tone jamming as a function of the signal-to-noise ratio (SNR), with the signal-to-jamming ratio (SJR) as parameter, is shown in Figure 8.48 (a). The BER increases as SNR decreases. The selected ranges for SNR and SJR were from -5 dB to $+12$ dB. The solid line is the probability of bit error for QPSK without jamming.

The BER for QPSK with AM-modulated AWGN jamming as a function of the SNR, with the SJR as parameter, is shown in Figure 8.48 (b). The solid line is the probability of bit error for QPSK without jamming.

We note the dramatic increase in the BER due to AM-modulated tone jamming, relative to AM-modulated AWGN jamming.

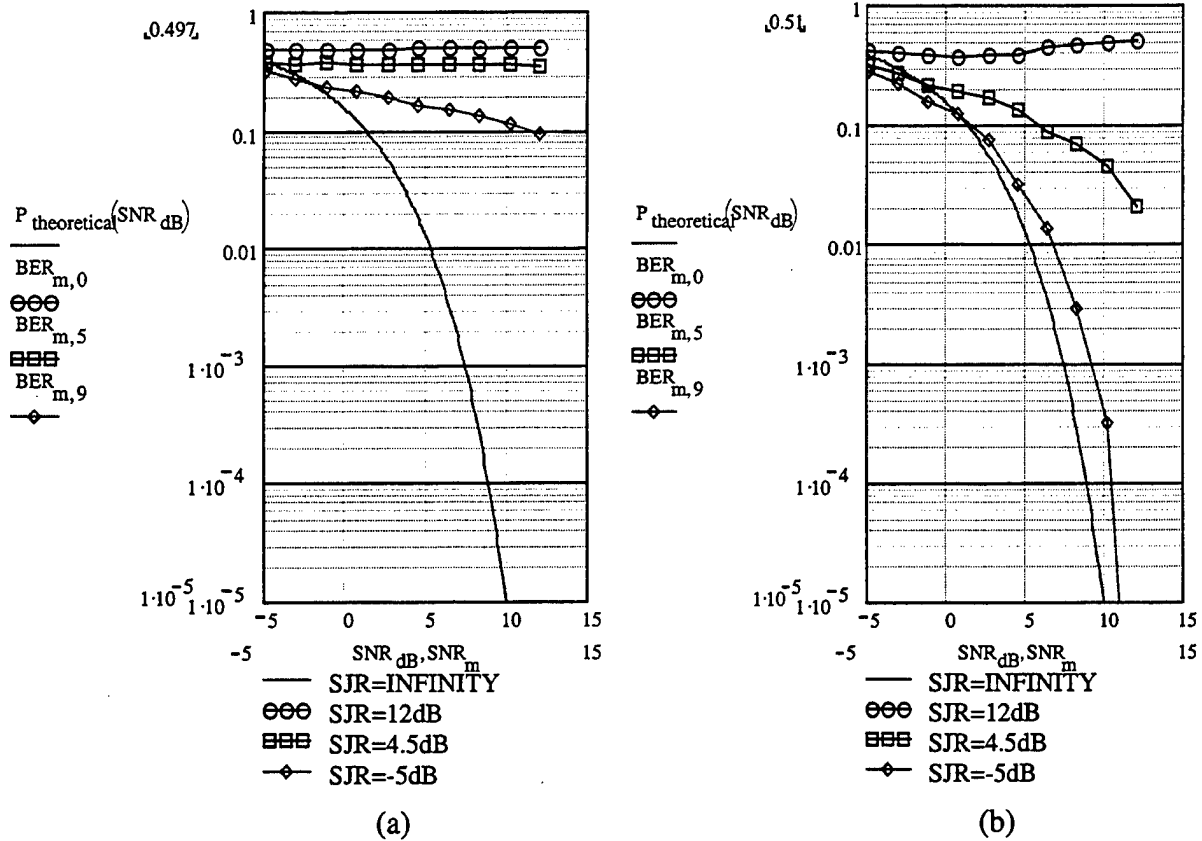


Figure 8.48 (a) The BER for QPSK with AM-modulated tone jamming as a function of the SNR (b) The BER for QPSK with AM-modulated AWGN jamming as a function of the SNR

b. FM-Modulated Tone Jamming

Figure 8.49 shows the Simulink model for QPSK with FM-modulated tone jamming.

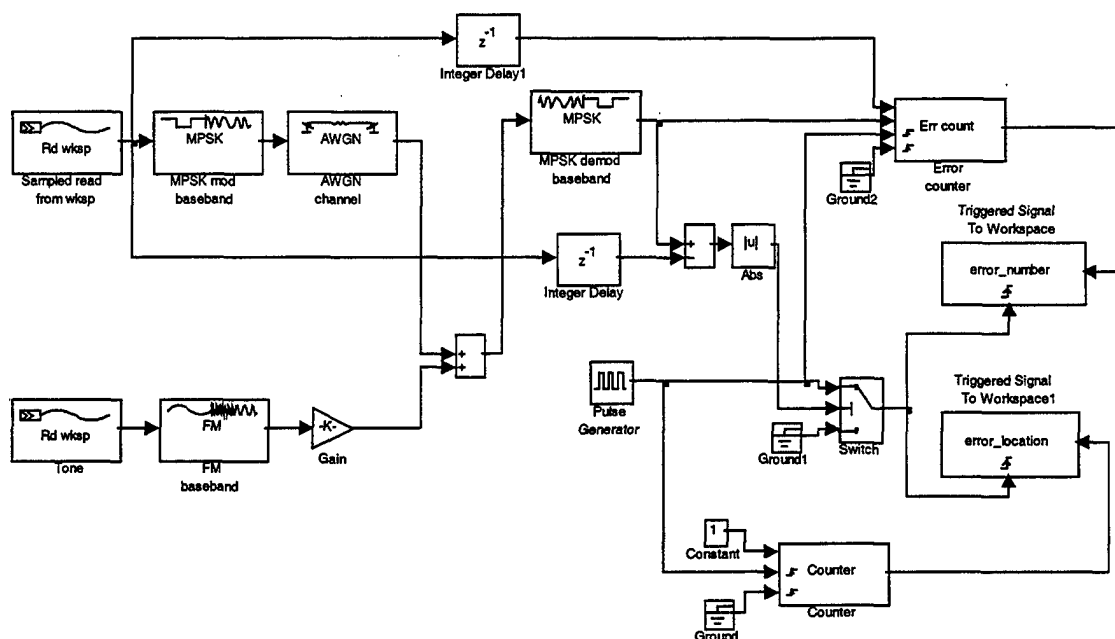


Figure 8.49 Simulink Model for QPSK with FM-Modulated Tone Jamming

The bit error rate (BER) for QPSK with FM-modulated tone jamming as a function of the signal-to-noise ratio (SNR), with the signal-to-jamming ratio (SJR) as parameter, is shown in Figure 8.50 (a). The BER increases as SNR decreases. The selected ranges for SNR and SJR were from -5 dB to $+12$ dB. The solid line is the probability of bit error for QPSK without jamming.

The BER for QPSK with FM-modulated AWGN jamming as a function of the SNR, with the SJR as parameter, is shown in Figure 8.50 (b). The solid line is the probability of bit error for QPSK without jamming.

We observe the dramatic increase in the BER due to FM-modulated tone jamming, relative to FM-modulated AWGN jamming.

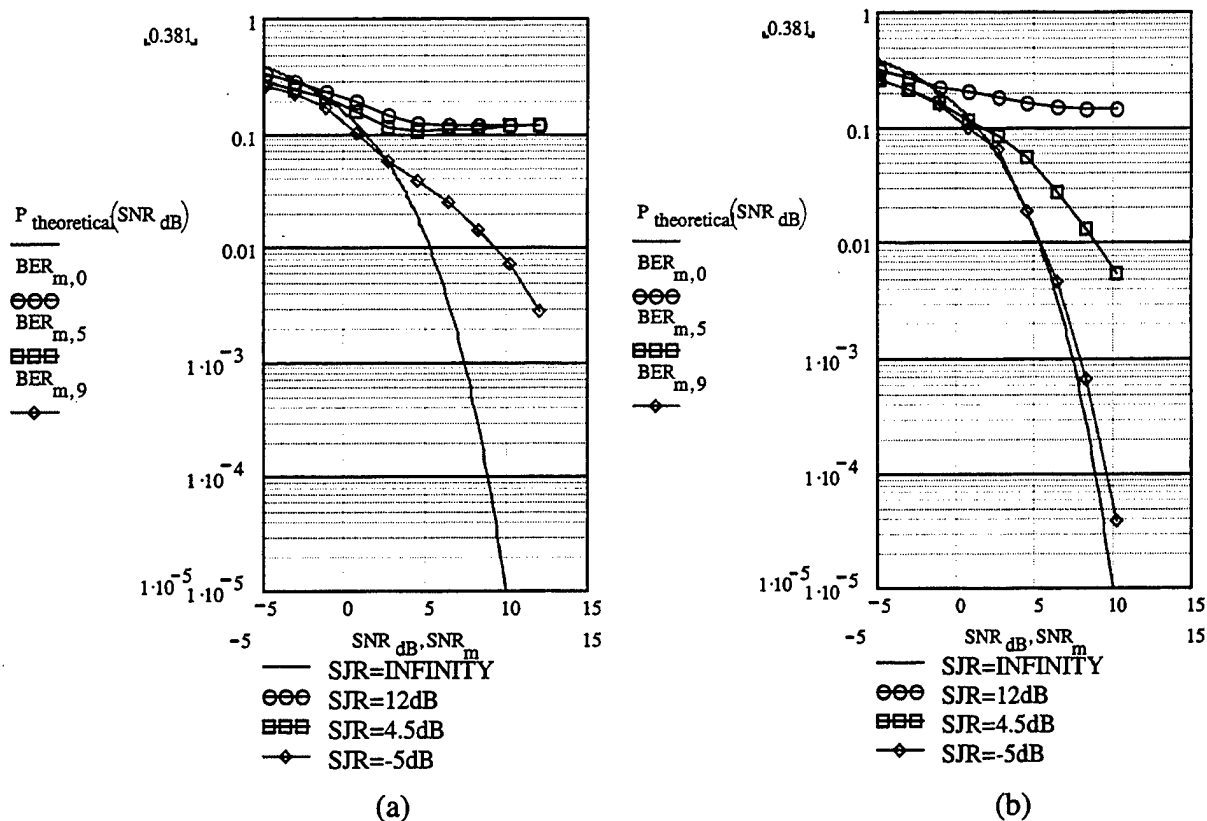


Figure 8.50 (a) The BER for QPSK with FM-modulated tone jamming as a function of the SNR (b) The BER for QPSK with FM-modulated AWGN jamming as a function of the SNR

IX. CONCLUSIONS AND RECOMMENDATIONS

In this study coherently detected BFSK, BPSK, QPSK, and noncoherently detected BFSK communication systems, in the presence of additive white Gaussian Noise (AWGN) and different types of jamming signals (barrage, pulsed and tone) were simulated by using MATLAB Communications Toolbox and Simulink. The bit error probabilities were determined by simulation and verified against the theoretical bit error probabilities for the case of AWGN.

As observed from the simulation results, different types of jamming affect each digital modulation technique differently. We determined that in attempting to disrupt digital communications, it is often advantageous to concentrate the jamming energy in short pulses. Pulsed jamming can cause a substantial increase in the bit error rate relative to the rate caused by continuous jamming with the same average power. By comparing the effects of different jammer types used in the simulation, we observed that AM-modulated jammers caused more damage to digital communication systems than FM-modulated jammers.

Table 9.1 shows the summary of the simulation results regarding the effects of each AM-modulated jamming technique on the digital modulation types.

Jamming Type Digital Mod. Tech.	AM by Weibull Noise Jamming	AM-Modulated Pulsed Noise Jamming	AM-Modulated Tone Jamming
Coherent BFSK	2	1	3
Noncoherent BFSK	1	3	2
BPSK	3	2	1
QPSK	2	3	1

Table 9.1 The Summary of the Simulation Results According to Effect of each AM-Modulated Jamming Technique on the Digital Modulation Types

Here, number one in the table refers to the most effective jamming technique, number two refers to the second most effective jamming technique, and number three refers to the least effective jamming technique. As can be seen from the table, AM by Weibull Noise jamming caused worst-case bit error probability for noncoherent BFSK, AM-modulated pulsed noise jamming caused worst-case bit error probability coherent BFSK, and AM-modulated tone jamming caused worst-case bit error probability for BPSK and QPSK.

Table 9.2 shows the summary of the simulation results regarding the effects of each FM-modulated jamming technique on the digital modulation types.

Jamming Type Digital Mod. Tech.	FM by Weibull Noise Jamming	FM- Modulated Pulsed Noise Jamming	FM- Modulated Tone Jamming
Coherent BFSK	1	3	2
Noncoherent BFSK	3	1	2
BPSK	3	2	1
QPSK	3	2	1

Table 9.2 The Summary of the Simulation Results According to Effect of each FM-Modulated Jamming Technique on the Digital Modulation Types

Here again, number one in the table refers to the most effective jamming technique, number two refers to the second most effective jamming technique, and number three refers to the least effective jamming technique. As can be seen from the table, FM by Weibull Noise jamming caused worst-case bit error probability for coherent BFSK, FM-modulated pulsed noise jamming caused worst-case bit error probability for noncoherent BFSK, and FM-modulated tone jamming caused worst-case bit error probability for BPSK and QPSK.

The theoretical bit error probability (explained on page 49) and the simulated bit error probability for AM and FM by Weibull Noise jamming for the digital modulation types are tabulated in Table 9.3 (for input SJR of 12 dB). The number of transmitted symbols is one million.

Jamming Types \ BER	Theoretical P_b	Simulated P_b	Difference in BER
AM by Weibull Noise Jamming for Coherent BFSK	0.01980	0.020	1.00 %
FM by Weibull Noise Jamming for Coherent BFSK	0.01488	0.015	0.80 %
AM by Weibull Noise Jamming for Noncoherent BFSK	0.034775	0.035	0.64 %
FM by Weibull Noise Jamming for Noncoherent BFSK	0.01490	0.015	0.67 %
AM by Weibull Noise Jamming for BPSK	0.00099	0.001	1.00 %
FM by Weibull Noise Jamming for BPSK	0.000395	0.0004	1.25 %
AM by Weibull Noise Jamming for QPSK	0.14876	0.150	0.83 %
FM by Weibull Noise Jamming for QPSK	0.000495	0.0005	0.94 %

Table 9.3 The Theoretical and the Simulated Bit Error Probabilities for AM and FM by Weibull Noise Jamming for the Digital Modulation Types (for Input SJR of 12 dB).

The theoretical bit error probability (explained on page 51) and the simulated bit error probability for AM and FM-modulated pulsed noise jamming for the digital modulation types are tabulated in Table 9.4 (for input SJR of 12 dB).

Jamming Types	BER	Theoretical P_b	Simulated P_b	Difference in BER
AM-Modulated Pulsed Noise Jamming for Coherent BFSK		0.00993	0.010	0.70%
FM-Modulated Pulsed Noise Jamming for Coherent BFSK		0.00290	0.003	0.67%
AM-Modulated Pulsed Noise Jamming for Noncoherent BFSK		0.00790	0.008	1.25%
FM-Modulated Pulsed Noise Jamming for Noncoherent BFSK		0.00988	0.010	1.20%
AM-Modulated Pulsed Noise Jamming for BPSK		0.0019823	0.002	0.89%
FM-Modulated Pulsed Noise Jamming for BPSK		0.0002475	0.0003	0.83%
AM-Modulated Pulsed Noise Jamming for QPSK		0.07950	0.080	0.63%
FM-Modulated Pulsed Noise Jamming for QPSK		0.000695	0.0007	0.64%

Table 9.4 The Theoretical and the Simulated Bit Error Probabilities for AM and FM-Modulated Pulsed Noise Jamming for the Digital Modulation Types (for Input SJR of 12 dB).

The theoretical bit error probability (explained on page 52) and the simulated bit error probability for AM and FM-modulated tone jamming for the digital modulation types are tabulated in Table 9.5 (for input SJR of 12 dB).

Jamming Types \ BER	Theoretical P_b	Simulated P_b	Difference in BER
AM-Modulated Tone Jamming for Coherent BFSK	0.00494	0.005	1.20 %
FM-Modulated Tone Jamming for Coherent BFSK	0.00396	0.004	0.95 %
AM-Modulated Tone Jamming for Noncoherent BFSK	0.00791	0.008	1.25 %
FM-Modulated Tone Jamming for Noncoherent BFSK	0.01980	0.020	1.00 %
AM-Modulated Tone Jamming for BPSK	0.002977	0.003	0.77 %
FM-Modulated Tone Jamming for BPSK	0.000992	0.001	0.80 %
AM-Modulated Tone Jamming for QPSK	0.009910	0.010	1.00 %
FM-Modulated Tone Jamming for QPSK	0.002964	0.003	1.20 %

Table 9.3 The Theoretical and the Simulated Bit Error Probabilities for AM and FM-Modulated Tone Jamming for the Digital Modulation Types (for Input SJR of 12 dB).

As can be seen from the tables, for the input SJR of 12 dB, the simulated results approach to the theoretical results.

For the continuation of this research, error-correction-coding and adaptive antennas can be added to the simulation model, and noise and jamming effects on the probability-of-error for spread spectrum communication systems can also be investigated.

APPENDIX. MATLAB COMMUNICATIONS TOOLBOX AND SIMULINK

The Communications Toolbox is a collection of computation functions and simulation blocks for research, development, system design, analysis, and simulation in the communications area. The toolbox contains ready-to-use functions and blocks, which we can easily modify to implement our own schemes, methods, and algorithms. The Communications Toolbox is designed for use with MATLAB and SIMULINK. The Communications Toolbox includes SIMULINK blocks and MATLAB functions. The blocks and functions are organized in the following sub-categories: Data source, source coding/decoding, error-control coding, modulation/demodulation, transmission/reception filters, transmitting channel, multiple access, synchronization, and utilities.

SIMULINK is a program for modeling linear and nonlinear dynamic systems in the time-domain. Models in SIMULINK are represented in block-diagram form and can be assembled from block libraries and sub-libraries. Furthermore, SIMULINK allows the display of results and changes of certain model parameters without interrupting the simulation. Since SIMULINK is built upon MATLAB numeric computation system, it offers direct access to the MATLAB workspace and MATLAB's mathematical and engineering functions. SIMULINK's main features are:

1. Modeling and analysis of dynamic systems, including linear, nonlinear, continuous, discrete, and hybrid.
2. Flexible "open system" environment that allows addition of new blocks to SIMULINK.

3. Seamless interface with MATLAB's built-in math functions, 2D and 3D graphics, and add-on toolboxes for specialized applications.
4. Choice of methods of running a simulation (menu-driven on-screen or batch-mode).
5. An optimized computer platform implementation that ensures fast and accurate results.
6. Unlimited model size.

A typical SIMULINK session starts by either defining a new model or recalling a previously defined model and then proceeds to a simulation of the performance of that model. In practice these two steps are often performed iteratively as the model designer creates and modifies a model to achieve the desired behavior [Ref. 12].

LIST OF REFERENCES

1. Pettit, Ray H., *ECM and ECCM Techniques for Digital Communication Systems*, Wadsworth, Inc., Belmont, (CA), 1982
2. Sklar, Bernard, *Digital Communications Fundamentals and Applications*, Prentice-Hall, Inc., (NJ), 1988
3. Haykin, Simon, *An Introduction to Analog and Digital Communications*, John Wiley & Sons, Inc., Canada, 1989
4. Tomasi, Wayne, *Electronic Communications Systems*, Prentice-Hall, Inc., (NJ), 1998
5. Schleher, D. Curtis., *Electronic Warfare in the Information Age*, Artech House, Inc., Norwood, MA, 1999
6. Balanis, Constantine A., *Antenna Theory*, John Wiley & Sons, Inc., Canada, 1997
7. Naval Air Warfare Center, *Electronic Warfare and Radar Systems Engineering Handbook*, Electronic Warfare Division, Pont Mugu, CA, 1997
8. Peterson, Roger L., Ziemer, Rodger E., Borth, David E., *Introduction to Spread Spectrum Communications*, Prentice-Hall, Inc., (NJ), 1995
9. Dixon, Robert C., *Spread Spectrum Systems with Commercial Applications*, John Wiley & Sons, Inc., Canada, 1994
10. Wicker, Stephen B., *Error Control Systems for Digital Communication and Storage*, Prentice-Hall, Inc., (NJ), 1995
11. Robertson, R. Clark, *EC 4560 Communications ECCM*, Naval Postgraduate School, Monterey, CA, 1999 (Unpublished)
12. Wang, Weizheng, *Communications Toolbox for Use with MATLAB*, The Math Works Inc., (MA), 1997

THIS PAGE INTENTIONALLY LEFT BLANK

BIBLIOGRAPHY

1. Proakis, John G., *Digital Communications*, McGraw-Hill, Inc., San Francisco, (CA), 1995
2. Jeruchim, Michel C., Balaban, Philip, Shanmugan, K. Sam, *Simulation of Communication Systems*, Plenum Press, New York, 1992
3. Dabney, James B., Harman, Thomas L., *Mastering Simulink*, Prentice-Hall, Inc., (NJ), 1998
4. Gardner, Floyd M., Baker, John D., *Simulation Techniques*, John Wiley & Sons, Inc., Canada, 1997
5. Freeman, Roger L., *Telecommunications Transmission Handbook*, John Wiley & Sons, Inc., Canada, 1998
6. Torrieri, Don J., *Principles of Secure Communication Systems*, Artech House, MA, 1992
7. Simon, Marvin K., Omura, Jim K., Scholtz, Robert A., Levitt, Barry K., *Spread Spectrum Communications Handbook*, McGraw-Hill, Inc., New York, 1994
8. Cook, Charles E., Ellersick, Fred W., Milstein, Laurence B., Schilling, Donald D., *Spread Spectrum Communications*, IEEE, Inc., New York, 1983
9. Collin, Robert E., *Antennas and Radiowave Propagation*, McGraw-Hill, Inc., New York, 1985
10. Stutzman, Warren L., Thiele, Gary A., *Antenna Theory and Design*, John Wiley & Sons, Inc., Canada, 1981
11. Kraus, John D., *Electromagnetics*, McGraw-Hill, Inc., New York, 1992
12. Vaseghi, Saeed V., *Advanced Signal Processing and Digital Noise Reduction*, Wiley and Teubner Partnership, New York, 1996

THIS PAGE INTENTIONALLY LEFT BLANK

INITIAL DISTRIBUTION LIST

	No. Copies
1. Defense Technical Information Center 8725 John J. Kingman Rd., Ste 0944 Ft. Belvoir, VA 22060-6218	2
2. Dudley Knox Library Naval Postgraduate School 411 Dyer Rd. Monterey, CA 93943-5101	2
3. Chairman, Code EC..... Department of Electrical and Computer Engineering Naval Postgraduate School Monterey, CA 93943-5121	1
4. Engineering and Technology Curricular Office, Code 34 Naval Postgraduate School Monterey, CA 93943-5109	1
5. Professor Rasler W. Smith, Code EC/SR..... Department of Electrical and Computer Engineering Naval Postgraduate School Monterey, CA 93943-5121	1
6. Professor Jovan Lebaric, Code EC/LE..... Department of Electrical and Computer Engineering Naval Postgraduate School Monterey, CA 93943-5121	1
7. Professor David V. Adamiak, Code EC/AD Information Warfare Academic Group Naval Postgraduate School Monterey, CA 93943-5121	1
8. Kara Kuvvetleri Komutanligi Kutuphanesi..... Yucetepe, Ankara, 06100 TURKEY	1
9. Kara Kuvvetleri Komutanligi MEBS Bsk.ligi Yucetepe, Ankara, 06100 TURKEY	1
10. Kara Harp Okulu Komutanligi Kutuphanesi..... Bakanliklar, Ankara, 06100 TURKEY	1

11.	Cem Sen	3
	Esat Caddesi 128/1	
	Kucukesat, Ankara, 06660 TURKEY	